The stochastic movements of individual streambed grains

by

J. Kevin Pierce

B.S. Physics, West Virginia University 2013

M.Sc. Physics, University of British Columbia 2016

A THESIS SUBMITTED IN PARTIAL FULFILLMENT
OF THE REQUIREMENTS FOR THE DEGREE OF

Doctor of Philosophy

in

THE FACULTY OF ARTS
(Department of Geography)

The University of British Columbia
(Vancouver)

June 2021

The following individuals certify that they have read, and recommend to the Faculty of Graduate and Postdoctoral Studies for acceptance, the thesis entitled:

The stochastic movements of individual streambed grains

submitted by **J. Kevin Pierce** in partial fulfillment of the requirements for the degree of **Doctor of Philosophy** in **Department of Geography**.

Examining Committee:

Marwan Hassan, Geography
Supervisor

Brett Eaton, Geography
Supervisory Committee Member

Rui Ferreira, University of Lisbon
Civil Engineering

Magnus Monolith, Other Department
External Examiner

Additional Supervisory Committee Members:

Person1
Supervisory Committee Member

Person 2
Supervisory Committee Member

Abstract

A central task within Earth science is to understand and predict the evolution of landscapes due to flowing water. As rainfall channelizes and flows downhill, it carves out basins and etches in networks of intersecting channels. In the highlands of these networks, water arranges boulders and gravels into an intricate array of patterns – steps, pools, bars, and riffles, which cooperate with vegetation both live and dead to set the stage for much of Earth's biota. In the lowlands, channels laden with old mountain sediments, weathered and abraded to fine particles, splay across floodplains and drift between configurations through millennia.

Sediment transport is a main driver of all fluvial dynamics. Channel evolution ultimately occurs because individual sediment grains move from one location to another. Yet in a majority of modelling studies, landscapes are represented as continua, where the locations of individual grains are averaged away, and sediment transport is represented as a steady stream of mass, rather than the intermittent movements of individual grains Useful as this continuum approach may be, many fluvial phenomena are not well-suited for it. Sediment transport rates are known to fluctuate widely through space and time, and these fluctuations are understood to initiate bedform development and control channel widths. The largest grains in small mountain channels are known to confer the most stability, while violating any assumption of being small compared to the scales of interest. To understand fluvial dynamics, we need the capability to model discrete grains, not just continua.

In this thesis, I present four or five years of my theoretical research into

the movements of individual sediment grains in river channels. This subfield of Earth science, with a focus on grain-scale process, has existed at least since Hans Albert Einstein in 1937, and within it, modellers have traditionally compromised on severe approximations to balance realism against mathematical difficulty. In this enterprise, perfectly flat beds which do not change shape, spherical grains, infinite movement velocities, and turbulence free flows have been typical assumptions to make progress, even though they have little basis in reality. The research presented here takes on more mathematical difficulty than before to introduce more realism, adding some bricks to the fortress, and introducing new methods to the field which should work well for other people to make more bricks later. I hope you find it useful! Happy reading.

Lay Summary

The lay or public summary explains the key goals and contributions of the research/scholarly work in terms that can be understood by the general public. It must not exceed 150 words in length.

Preface

Insert the sheet music to my life flows on in endless song.

Contents

List of Tables

List of Figures

Acknowledgments

Thanks Leo Golubovic, Mindy Saunders, Calisa and Jim Pierce, Kim and Kelsey Pierce, Johnathan Ramey, Linda Mendez, Tex Wood, Charles Wood, and all of the Appalachian intelligensia who paved my way. Tyler cannon. . .

The people whose benevolence spans generations: both those I know: Joe, Joyce, Ama, Ivory Nichols, and Parry Steele, and those I was unlucky to miss. Maragret Squire Avis and Oddessa Mathis. Joe, Joyce, Ama, and Parry Steele. My

Shawn Chartrand, Conor McDowell, Matteo Saletti, Will Booker, David Adams, Leo King, Tobias Mueller, Nisreen Ghazi,

Adam Payne, Adam Collins, Megat Denney, Andrew Rice, Evan Graber, Scott Ferris, Craig Tenney, and the rest of the WVU physics lounge family.

Andy Osadetz, Josh Plankeel,

My partner Mary for putting up with the late nights.

Mike church and olav slaymaker for the inspiring seminars.

marwan hassan for being one of the most emotionally intelligent people I've ever met.

Chapter 1

Sediment transport and landscape evolution

1.1 Geomorphology traditions

Geomorphology can be defined as the study of Earth's evolution by tectonics, weathering, and erosion (**?**). This science has long been characterized by observation and description (**???**). Only relatively recently did the science turn to quantitative methods (*Bagnold*, 1941; **?**; **?**; **?**), with researchers working to frame observations in terms of underlying processes and to describe them with mathematical models modified from physics (**???**).

This quantitative shift or incorporation of physics methods into geomorphology has been criticized as overly reductionist (**?**). Many of the problems addressed within physics involve closed systems with perfect order (**???**). These systems stand in contrast to the systems in geomorphology. Earth's surface is open and highly disordered. The surface receives fluxes of mass and energy across its boundaries by tectonics, climate, transpiration, and sunlight, and its component parts vary widely in their characteristics, activities, and compositions. With this complexity (**?**), we can conclude that a complete reduction of geomorphology to physics is likely impossible.

There are nevertheless lessons physics can exchange with geomorphology and sediment transport theory. This is the central theme of this thesis.

Before presenting original research, the first chapter summarizes key developments in quantitative geomorphology models which have resulted from this exchange. The section is organized along two classifications. First, I distinguish earlier works as "stochastic" or "deterministic". Stochastic models introduce randomness or noise as a means to crudely represent the complexity of natural systems (open boundaries, diversity in component parts) within idealized mathematical models of nature. Deterministic models involve Newtonian equations without noise to represent nature. Second, I distinguish earlier models as "discrete" or "continuous". These terms reflect whether the degrees of freedom of individual particles are retained in mathematical models, or whether they are averaged away. When grains are tracked, a model is discrete. When they are discussed as a flow, it is continuous. We can therefore discuss a "discrete and stochastic" model, or a "continuous and deterministic" model, and so on. With these distinctions in mind, we launch into a survey of the foundation upon which this thesis builds: physics-inspired, process-based models of sediment transport and landscape evolution.

1.2 Description of fluvial sediment transport

1.3 Models of bedload: Determinism and continuity

1.3.1 Exner's landscape evolution

Exner was probably the first to describe landscape evolution as a mathematical result of sediment transport (**?**), when he related the topographic elevation to the sediment flux via

$$\frac{\partial z}{\partial t}(\mathbf{x}, t) = -\nabla q(\mathbf{x}, t). \tag{1.1}$$

This equation links the temporal evolution of the land elevation z at a location $\mathbf{x} = (x, y)$ to spatial gradients in the sediment flux.

Within the Exner equation, the elevation z and sediment flux q are represented as continuous fields. This representation can be interpreted as an average over the detailed locations of individual grains, and it is expected to be an excellent approximation whenever the scales of interest are large compared to the size of the averaging window, which should be taken much larger than the size of the largest grains being modelled (*Coleman and Nikora*, 2009).

Yet there are many contexts on Earth's surface where the scale of interest is not much larger than the largest grains involved in the system. We can wonder, for example, in mountain channels, how large boulders contribute to the formation of steps (*Saletti and Hassan*, 2020; **?**), or other structures with sizes comparable to channel widths, like ribs or stone cells (*Hassan et al.*, 2007; *Venditti et al.*, 2017). In these cases, individual grains are comparable to the scales of interest, and the continuum approximation breaks down.

1.4 Bagnold's sediment flux

When the Exner equation applies, the question arises as to how one should relate the sediment flux within it to the fluid flow characteristics. One of the most influential approaches from physical arguments is due to Bagnold (*Bagnold*, 1956, 1966). Bagnold described sediment transport as a process which ultimately converts flow energy to heat. He assumed that the flow power P_f available to move sediment scaled as $P_f \propto \tau - \tau_c$, where τ is the average bed shear stress and τ_c is the threshold shear stress at which particles first begin to move. He reasoned that if the average downstream flux of particles is q, and particles move on average with velocity proportional to the fluid velocity near the bed, then the power P_g required to sustain particle motion scales as $P_g \propto q/\tau^{1/2}$. Balancing fluid propulsion against frictional dissipation ($P_f = P_g$) then provides Bagnold's sediment transport formula

$$q = k(\tau - \tau_c)\tau^{1/2}. \tag{1.2}$$

1.4.1 The combination: two-phase deterministic/continuum models

1.4.2 Challenges of the continuum approximation

The sediment flux fluctuates, and it depends on observation scale.

The bed is not continuous, but it is discrete. Discrete beds have not been described in the stochastic paradigm – only in the deterministic paradigm.

1.5 Discrete and deterministic

1.5.1 Saltation models: Van Rijn and Wiberg

1.5.2 Discrete element modelling

haff and other 2d approaches. early days. mcewan and heald

1.5.3 State of the art in discrete/deterministic

Coupled DEM/CFD

1.5.4 Challenges of the discrete and deterministic approach

simulations are very expensive at realistic scales

1.6 Discrete and stochastic

this is my baby

1.6.1 The stochastic alternative: Einstein's flux

Explain the idea of entrainment and deposition. Formulate the movement characteristics of individual particles in the stair-step approach. Find q= El. Summarize the major strengths and limitations.

1.6.2 Tsujimoto's landscape

Explain what tsujimoto essentially did to couple Einstein into Exner, giving the entrainment form of the exner equation. Cite Parker and Furbish who provided refinements of it. Describe the inherently nonlocal characteristics of sediment flux. Indicate the major strengths and weaknesses - key weakness being that, if the sediment flux is a fluctuating quantity, as formulated by Einstein, then

1.6.3 The details of entrainment

1.6.4 State of the art in the stochastic paradigm

Ancey's developments to describe the full probability distribution of the sediment flux.

Lisle and Lajenesse's efforts to include a finite movement velocity into einstein's 37 model.

Increased emphasis on the dynamical origins of grain kinematics, including ancey 2014 and fan 2014 and the representation of turbulence by white noise in a Langevin equation.

1.6.5 Limitations: Realism versus complexity

1.7 The point of the thesis

1.7.1 Open problems in the stochastic paradigm

1.7.2 Quantities of interest

Explain what the pdf of position is explain what the variance represents explain that the moments more generally are of interest explain that the sediment flux is key to landscape evolution. not just in mean value, but also in its fluctuations.

1.7.3 Tools of the trade

The Langevin equation

When particles are subjected to fluctuating forces, their Newtonian equation of motion can be written

In this equation, F is the deterministic or steady component of the forcing, while ξ is the fluctuating component. The classic example is due to Einstein, and

Master equations and probability flow

Idealized noises

1.7.4 Organization of the thesis

Four main problems. Ch 2 is about how to calculate the sediment flux and to understnad particle motion with fluctuating velocities. Ch3 is a sketch of how we can incorporate bed elevation changes into sediment transport modelling based on stochastic theories. Ch4 is the

1.8 Introduction: birth-death models for the probability distribution of bedload flux

In river science, a fundamental problem is the determination of the bedload flux, or the rate of downstream movement of bedload grains (*Ballio et al.*, 2014). Since bedload transport has strong feedback with stream morphology (*Church*, 2006; *Recking et al.*, 2016), its prediction is useful to a wide range of environmental considerations. These considerations span a wide range, from aquatic habitat restoration to energy production (*Kondolf et al.*, 2014; *Wohl et al.*, 2015). Unfortunately, existing approaches to compute the bedload flux are inadequate. Predictions regularly deviate by two orders of magnitude from measured values (*Barry et al.*, 2004; *Bathurst*, 2007; *Gomez and Church*, 1989; *Recking et al.*, 2012).

Predicting bedload fluxes is challenging because transport is not always

well correlated to average characterizations of flow and bed material. Local fluxes can range through orders of magnitude as details of turbulent fluctuations and bed organization vary, while average characterizations of flow and sediment remain constant (*Charru et al.*, 2004; *Hassan et al.*, 2007; *Sumer et al.*, 2003; *Venditti et al.*, 2017). The same turbulence and sediment organization details which correlate with the bedload flux also interact with it. Turbulent impulses induce sediment motion (*Amir et al.*, 2014; *Celik et al.*, 2014; *Shih et al.*, 2017; *Valyrakis et al.*, 2010), moving sediment affects turbulent characteristics (*Liu et al.*, 2016; *Santos et al.*, 2014; *Singh et al.*, 2010), and bedload fluxes modify the stability and arrangement of bed surface grains (*Charru et al.*, 2004; *Hassan et al.*, 2007; *KIRCHNER et al.*, 1990). The bedload flux is in a cyclical feedback with its controls: these controls are the details of turbulence and bed organization (*Jerolmack and Mohrig*, 2005).

As a result, bedload fluxes exhibit wide fluctuations, even as average characterizations of flow and bed organization remain steady (*Ancey and Heyman*, 2014). In the most controlled laboratory experiments, with steady flows driving uniform glass beads under conditions which do not favor bedform development, instantaneous fluxes are often as much as 200% mean values (*Ancey et al.*, 2008; *Böhm et al.*, 2004; *Heyman et al.*, 2014, 2016). In natural streams, with temporally or spatially varying grain size distributions (*Chen and Stone*, 2008; *Lisle and Madej*, 1992), unsteady flows (*Mao*, 2012; **?**), a variety of dynamic bed surface structures (*Hassan et al.*, 2007; *Venditti et al.*, 2017), variable sediment supply (*Elgueta*, 2018; *Madej et al.*, 2009), lateral adjustment (*Pitlick et al.*, 2013; *Redolfi et al.*, 2018), and migrating bedforms (*Dhont and Ancey*, 2018; *Gomez and Church*, 1989) all imparting additional sources of variabilility through their feedbacks with the flux, instantaneous fluxes can be even larger.

Apparently, bedload fluxes have statistical characteristics. Einstein was the first to recognize the statistical character of bedload transport (*Einstein*, 1937). He understood transport as a random switching between states of motion and rest (*Einstein*, 1950; *Zee and Zee*, 2017). He called the transition from rest to motion entrainment, and he characterized it with a prob-

ability which was linked to extreme events in fluid turbulence (*Einstein*, 1950; *Einstein and El-Samni*, 1949). He called the transition from motion to rest deposition, and he considered it an implicit function of the bedload flux (*Einstein*, 1950; *Zee and Zee*, 2017). By convolving over sequences of entrainment and deposition, employing some semi-emprical arguments, Einstein developed a formula for the average bedload flux (*Einstein*, 1950).

Many investigators have criticized and developed Einstein's ideas (*Ancey et al.*, 2006; *Armanini et al.*, 2015; *Lisle et al.*, 1998; *Paintal*, 1971; *Papanicolaou et al.*, 2002; *Shen and Cheong*, 1980; *Sun and Donahue*, 2000; *Yalin*, 1972). These revisions focus on the more ad hoc elements of Einstein's derivations, and they lend a more mechanistic basis, a firmer mathematical foundation, and more generality to the approach. Although all of these authors accepted the statistical character of bedload motion, none developed theories for a probability distribution for the bedload flux. This is desirable since its higher moments give unambiguous measurements of the magnitude of bedload fluctuations.

The extension of the Einstein approach to obtain a probability distribution of the bedload flux, with fluctuations stemming from the random character of entrainment and deposition, was first explored by *Lisle et al.* (1998); *Sun and Donahue* (2000), and it was further developed by *Ancey et al.* (2006), and the more recent work I will discuss extensively in this review. All of these authors revisited Einstein's ideas from a foundation in the stochastic mathematics which became formalized somewhat after Einstein's work (e.g. **?**), treating the transitions between motion and rest states as random events characterized by probabilities. This enabled them to apply the formalism of continuous time Markov processes to derive a probability distribution of the bedload flux, with a mean value which was an improved version of the *Einstein* (1950) formula, very similar to the revised formula of *Yalin* (1972), and a variance which provided an unambiguous prediction of the magnitude of bedload fluctuations.

Deterministic processes trace the evolution of some set of variables $\{x_1(t), x_2(t), \dots\}$ through time. Stochastic processes, in contrast, trace the evolution of a probability distribution for random variables $P_{X_1,X_2,\dots}(x_1, x_2, \dots; t)$ through

time. The Markov moniker refers to the amount of memory in the process. If the probability distribution of the variables of interest can be predicted in the future using only distribution functions from the present, the process is Markovian. Otherwise, if predicting the future requires knowledge of the entire history, the process is non-Markovian (**??**). Markov birth-death processes consider the probabilistic creation and annhilation of members of a population (**??**).

To model the bedload flux with such a process, the population considered is the number of moving particles within a control volume over the bed. This population is subject to creation by entrainment and annhilation by deposition (*Ancey et al.*, 2008, 2014, 2015; *Heyman et al.*, 2013; *Ma et al.*, 2014; *Turowski*, 2009). This approach is exciting because Markov birth-death processes are highly studied in physics, chemistry, and population ecology, so there are many extensions readily available (*Bailey*, 1968; *Field and Tough*, 2010; *Méndez et al.*, 2015; *Pielou*, 2008; *van den Broek*, 2012; **?**; **?**; **?**). At the same time, birth-death modeling of the bedload flux remains relatively undeveloped: birth-death models are all one-dimensional and designed for a single grain size.

In this article, I review the literature on Markov birth-death models of the bedload flux. In the review I assume some familiarity with discrete state continuous time Markov processes, which could be gleaned from reading the appropriate chapter in **?**. These theories are exciting because they describe the mean bedload flux and its fluctuations within a volume (*Ancey et al.*, 2006, 2008; *Turowski*, 2009), statistical properties of the flux at a point in space (*Heyman et al.*, 2013; *Ma et al.*, 2014), and the spatial and temporal correlations in the bedload flux within a reach of channel (*Ancey and Heyman*, 2014; *Ancey et al.*, 2015). All of these considerations are new, and they are unique within the river science literature in that they do not ignore the statistical character of bedload transport. They initiate a theoretical framework from which the feedbacks between the arrangement of bed particles, turbulence, and channel morphology which lead to bedload fluctuations can be more carefully studied and understood. In reverse, the capacity of bedload models to describe fluctuations provides an additional benchmark

against which to judge models, a task which is notably difficult (*Iverson*, 2003).

One of the first birth-death models of the bedload flux I will review is *Ancey et al.* (2006): these authors generalized *Einstein* (1950) using a birth-death framework to obtain a statistical distribution of the bedload flux within a control volume. They found the fluctuations predicted by the Einstein-like model were not large enough to describe experimental data. In order to match the wide fluctuations of experimental data, *Ancey et al.* (2008) reworked their earlier control volume model to include a collective entrainment effect. Collective entrainment is a mathematical term charaterizing the correlations between moving grains due to turbulence, collisions, or granular avalanche effects.

The *Ancey et al.* (2008) model has been generalized and applied in a handful of followup works. *Turowski* (2009) generalized it to include limited sediment availability. *Heyman et al.* (2013) and *Ma et al.* (2014) studied how the *Ancey et al.* (2008) model could be interpreted to describe the statistics of the bedload flux at a fixed point in space, rather than just a control volume like that considered by *Einstein* (1950). Control volumes are less desirable because transport is practically easier to measure at a point in space than it is within a control volume.

Ancey and Heyman (2014); *Ancey et al.* (2015) generalized the *Ancey et al.* (2008) model in order to understand spatial characteristics of bedload transport. They considered a reach of channel as an array of adjacent control volumes (cells), and they coupled the *Ancey et al.* (2008) model between adjacent cells. They mapped this generalized birth-death model for the bedload flux distributed over an array of control volumes onto an advection diffusion equation for the bedload flux. Some reprecussions of this model were further explored in context of experimental data by *Heyman et al.* (2014).

All of these works contain many simplifying assumptions, and many of these were carefully highlighted by their authors. These studies were selected for this review because, taken together, they define a research trajectory which can be extrapolated to suggest future research topics. To be sure,

there is a long road ahead before Markov models can accomodate all of the complexities of natural river channels, some of which I've mentioned. The goal of this review is to indicate this trajectory in order to motivate future research: this is pursued in sections 1.9 and **??**. I discuss some of the future research topics I believe the trajectory points out in section 1.10, and I develop a few of these ideas myself in **??**. Along the way, I have somewhat changed the mathematical treatment and the notation from some of the original papers in order to highlight the historical progression between each work, and to illustrate that these works all share the same theme.

1.9 Background: the foundational stochastic model of bedload transport

Einstein (1950) can be credited with the first attempt to understand the bedload flux as random quantity. Einstein understood the movement of individual bedload grains as a random succession of motion and rest intervals. He termed the transition from rest to motion entrainment, and characterized it by a probability related to fluid turbulence. When particles are set in motion, Einstein considered they moved in discrete jumps of the same average distance. We define the bedload flux as the volume of grains passing a stream cross section per unit time. It is a volume of grains per time per unit width of stream, so its units are area/time. Therefore, Einstein's mean flux formula is derived from summing the alternate start-stop motions of all bed particles which cross a surface in a time interval.

The conceptual picture Einstein considered is depicted in figure 1.1. All bed particles are identical and are considered to have the same average geometry when at rest on the bed, meaning their entrainment characteristics are identical. For continuity with the rest of the review, we consider sediment particles are spheres of radius a, although *Einstein* (1950) was more general. We can follow Einstein to compute the mean number of these particles crossing a flow cross-sectional surface S in an interval of time. This will construct the mean bedload flux $\langle q_s \rangle$. In subsequent sections, we consider q_s a random variable, and we will review approaches to derive its full proba-

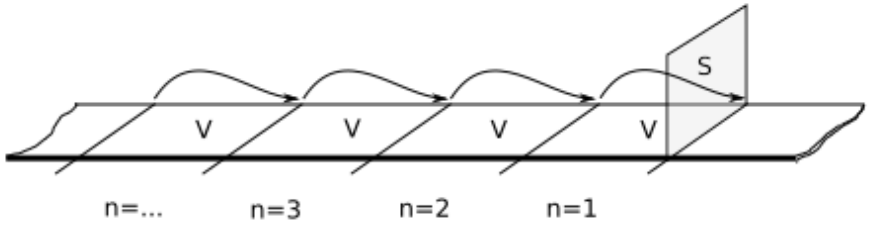

Figure 1.1: Einstein's conceptual picture (adapted from *Yalin* (1972)). Particles move in discrete jumps of length L from left to right through an array of adjacent control volumes. The bedload flux is the volume of bedload particles crossing the surface S per unit width and time.

bility distribution. From these contemporary models, an Einstein-like mean flux formula emerges from taking the mean of the probability distribution for q_s. Hence we use averaging brackets $\langle \cdot \rangle$ for the sake of continuity.

Einstein's derivation goes as follows: we partition the channel into a sequence of identical control volumes V. Each volume has dimensions L, w, and h ($V = lwh$). L is the downstream length of each control volume, and it is also the average jump distance of particles. w and h are the width and height of each control volume. Let P_n be the probability that any individual grain on the bed is entrained *at least* n times during the time interval T. That is, let P_n be the probability that an individual grain undergoes *at least* n jumps of length L in an interval T, meaning it travels a distance nL or more in T. Considering that each control volume contains N_V grains at rest within it, it follows that on average

$$N_V P_n. \tag{1.3}$$

grains are displaced *at least* a distance nL from a control volume within the time interval T.

Now we derive the mean flux. Note that the grains passing through a cross-sectional surface S (of area lw) in the time T could have come from

any upstream location. Therefore, the number of grains crossing S in T is

$$\sum_{n=1}^{\infty} N_V P_n. \tag{1.4}$$

This is the net arrival of grains in the interval T from all upstream control volumes. Multiplying by the particle volume ν_p and dividing by the timescale T and channel width w gives the mean bedload flux (volume per width per time):

$$\langle q_s \rangle = \frac{\nu_p N_V}{wT} \sum_{n=1}^{\infty} P_n = A \frac{a^2}{T} \sum_{n=1}^{\infty} P_n. \tag{1.5}$$

In the second equality, we have introduced $\nu_p = 4\pi a^3/3$, and two assumptions of Einstein. First, is the reasonable assumption that the number N_V of particles on the surface within V is proportional to the ratio of bed surface and particle areas: $N_V \propto Lw/a^2$, and second is the assumption that the travel distance L is proportional to particle size: $L \propto a$. The latter assumption is more difficult to justify (e.g. *Yalin*, 1972). A is a constant of proportionality.

Einstein implies the probability that an individual grain travels a distance nL or more in T is equivalent to the probability that an individual grain travels at least a distance L successively n times in T. Hence $P_n = P_1^n$ by the law of multiplication of probabilities, so that $\sum_{n=1}^{\infty} P_n = \sum_{n=1}^{\infty} P_1^n = P_1/(1 - P_1)$, using the geometric series (noting $P_1 < 1$ because it is a probability). Owing to this substitution, Einstein's mean bedload formula takes the form

$$\langle q_s \rangle = A \frac{a^2}{T} \frac{P_1}{1 - P_1}, \tag{1.6}$$

where A is a constant of proprotionality. The $P_1/(1 - P_1)$ structure of Einstein's formula is a distinctive characteristic. In order to use the apply the Einstein formula to predict bedload transport in natural streams or experiments, the timescale T and the probability P_1 that at least one grain entrains in T must be determined. Then the formula can be calibrated to a

given setting by adjusting the constant A.

In the original work, Einstein considered the timescale T proportional to the "time of the grain" formed by the grain's size a and its settling velocity w in still fluid: $T \propto a/w$. We will revisit this assumption shortly. Regarding the probability P_1, one of Einstein's most influential and enduring ideas within hydraulic engineering is his conception of the probability P_1 that at least one particle entrains in T. He considered that entrainment is driven by the fluctuating lift force imparted by the turbulent fluid, and it is resisted by the submerged weight of grains. Therefore, he formulated P_1 as an exceedance probability of the lift force over weight, so he wrote P_1 as an integral over the probability distribution of fluid shear stress. Einstein developed an alternative perspective on the incipient motion of particles that embraced turbulence and did not rely on the critical shear stress concept (e.g. *Kennedy*, 1995).

This formulation of entrainment probability in terms of the exceedance of random driving quantities over (possibly random) resisting quantities has been generalized and extended a great deal. *Paintal* (1971) made a significant extension by including random granular geometry of bed particles into the force balance. More recently, *Tregnaghi et al.* (2012) ammended the theory to include the impulse concept: the experimentally verified idea that force magnitude and duration are of equal importance for entrainment (e.g. *Celik et al.*, 2014; *Diplas et al.*, 2008). Refined theories of the entrainment probability, all fundamentally similar to the original ideas of *Einstein* (1950), have been carefully reviewed by *Dey and Ali* (2018); *Dey and Papanicolaou* (2008), and they are a subject of intensive ongoing research.

As noted by *Yalin* (1972), who wrote a careful review and revision of *Einstein* (1950), the Einstein theory for $\langle q_s \rangle$ is theoretically sound, at least to equation 1.6, and provided Einstein's probabilities P_n are interpreted in a careful way. I have mimiced Yalin to say P_n is the probability of *at least* n jumps in T. Had I said P_n was the probability of (only) n jumps in T, the relationship $P_n = P_1^n$ would not follow, so the Einstein flux would not develop the notable $P_1/(1 - P_1)$ form as in 1.6. Einstein was not as clear as he could have been on this distinction. Notably, the more general

birth-death theories which reproduce Einstein as a limiting case (e.g. *Ancey et al.*, 2006) use probability concepts relating to (only) one entrainment in a time interval. Therefore, to link back to Einstein from these contemporary theories, we need to follow *Yalin* (1972) to express the mean flux $\langle q_s \rangle$ in terms of the probabilities of (only) n entrainments in a time interval, which we can denote by a lower case letter p_n. These two probabilties, P_n (at least) and p_n (only), have probably been conflated often within the literature.

Yalin appealed to scaling arguments in order to refine Einstein's theory. He highlighted that Einstein's prescription of $T \propto a/w$, where w is the settling velocity, was not supported by any experimental evidence or theoretical argument. Yalin noted that within Einstein's theory, "T appears in connection to the study of detachment of individual grains due to turbulent fluctuations", from which he concluded that T should be actually be measured in terms of a period τ of turbulent fluctuations:

$$T = N_\tau \tau, \tag{1.7}$$

where N_τ is the dimensionless number of turbulent fluctuations in T (which is considered unknown but very large).

Yalin introduces a probability p of (only) one entrainment during an individual turbulent fluctuation. Since the number N_τ of turbulent fluctuations in T is very large, he considers this probability is very small, so that the probability of (only) n detachments in T can be computed with the Poisson distribution:

$$p_n = \frac{(N_\tau p)^n}{n!} e^{-N_\tau p}. \tag{1.8}$$

The probability P_n of *at least* n detachments in T can be expressed in terms of the probability p_n of (only) n detachments in T as

$$P_n = \sum_{i=n}^{\infty} p_i. \tag{1.9}$$

Owing to equations 1.7, 1.8, and 1.9, the mean bedload flux 1.5 becomes

$$\langle q_s \rangle = A\frac{a^2}{N_\tau \tau}\sum_{n=1}^{\infty}\sum_{i=n}^{\infty} p_i = A\frac{a^2}{N_\tau \tau}\sum_{n=1}^{\infty} np_n = A\frac{aL}{\tau}p. \tag{1.10}$$

The unknown number of turbulent fluctuations N_τ cancels. Hence, Yalin's ammended Einstein formula is proportional to p, rather than $P_1/(1-P_1)$ as in *Einstein* (1950). In Yalin's mind, the probability p is the probability of entrainment of only one grain in a small interval τ related to the period of turbulent fluctuations.

When Einstein's conceptual picture of bedload transport is revisited from a Markov process framework, the probability distribution $P(q_s)$ of the bedload rate can be derived from his assumptions (*Ancey et al.*, 2006). This distribution implies a mean bedload formula $\langle q_s \rangle = \sum q_s P(q_s)$ formally similar to Yalin's Einstein-like formula 1.10, and it provides additional information about the magnitude of bedload fluctuations, which are characterized without ambiguity by the variance $\langle \delta q_s^2 \rangle$, where $\delta q_s = q_s - \langle q_s \rangle$ is the deviation of the bedload flux from the mean. Jumping ahead a little, the fluctuations $\langle (\delta q_s)^2 \rangle$ derived in this way are not large enough to match experimental data (*Ancey et al.*, 2006), and this is because *Einstein* (1950), *Yalin* (1972), and *Ancey et al.* (2006) each assumed the transitions between rest and motion were independent between all particles.

Ancey et al. (2008) fixed this problem by describing bedload transport within a more general birth-death process framework (**?**). They included a collective interaction into the entrainment rates of bed particles in their model, and with this inclusion they derived bedload fluctuations of realistic magnitude. Their collective interaction biases entrainment, making it more likely when particles are already moving, a point we will discuss. It leads to clouds of active particles, and a wide tail on the bedload flux probability distribution: both of these features are in accord with experimental observations (*Ancey et al.*, 2006, 2008; *Drake et al.*, 1988). I'll start the review with *Ancey et al.* (2006), which is essentially *Einstein* (1950) revisited from the birth-death framework, lending it more generality by treating the bedload

flux as a probability distribution. The mean of this probability distribution reproduces equation 1.10, which is a satisfying historical coherence. Followups and refinements of the *Ancey et al.* (2006) work constitute the bulk of the review in section **??**.

1.10 Scope: identifying future research directions

1.10.1 recap

Einstein developed first stochastic theories describing the diffusion and flux of bedload. Ancey 2006, building on earlier work from Lisle 1998 and the many investigators who criticized and revised Einstein, formalized Einstein's assumptions over a foundation in Markov process theory, and extended his work by treating the bedload flux within a control volume as the cooperation of many independent two-state Markov processes: each bed particle within the control volume makes random transitions between motion and rest. Thus he derived a statistical distribution of the bedload rate which reproduces Einstein's result when the mean is taken. However, the magnitude of fluctuations predicted by this model are too small.

Ancey 2008 extended the Einstein theory by linking the transition rates between particles within the observation window with a collective entrainment term: they prescribed that the transition rate from rest to motion depends on the number of active particles. This is a simple way to include the effects of coherent turbulence and impact-based entrainment: it is an experimental observation that moving particles tend to come in waves (*Drake et al.*, 1988). The Ancey 2008 model was demonstrated capable of describing fluctuations, and all of its parameters have physical meanings, but notably there is no clear suggestion as to how collective and individual entrainment processes can be separated within experiments. Clearly, approaches to derive entrainment probabilities are focused on the individual entrainment rate (*Dey and Ali*, 2018), and there have been no developments with regard to computing the collective entrainment rate: there is no clear physical model of collective entrainment yet.

Turowski 2009 extended the Ancey work to take account of limited supply, in order to describe semi-alluvial channels where alluvial deposits lie on top of bedrock. He continued to work within the Einstein paradigm by describing the transport rate within a control volume, rather than by counting the number of particles leaving the control volume: although the Ancey 2008 work essentially outlines this possibiilty. The transport rate at a point should be considered as the number of emigration events in a unit time.

Heyman et al 2013 and Ma et al 2014 went on to consider the statistics of emigration: they tried to discern what could be learned about the transport rate at a fixed point from the control volume formalism of Ancey et al and Einstein before that. Heyman et al was concerned with the statistics of the waiting time between successive emigration events. The original Einstein (1937, 1950) assumptions generate an exponential waiting time ditsribution with a timescale related to the entrainment rate. However, Heyman et al (2013) showed that when collective entrainment effects were included there are two timescales: one fast timescale related to the individual entrainment rate, and one slower timescale related to collective entrainment effects. Thus, the distribution of waiting times between successive emigration events, which is a useful concept for alternative stochastic models of the bedload flux distribution (e.g. *Turowski*, 2010), is a more subtle object if collective entrainment occurs. These effects are accentuated at low transport rates, where the fast and slow timescales are more disparate. At high rates, the timescales become comparable and the waiting time between successive emigration events blends into an Einstein-like exponential.

All of these approaches considered bedload transport within a control volume or at a point, but indeed, a very large set of contemporary river science studies are concerned with the diffusion or spreading of bed material through a downstream reach of river (*Hassan et al.*, 2016). Bedload diffusion is not captured by a model at a single location: often, it has been described using an advection diffusion equation. These advection diffusion equations follow from considerations of mass balance within river channels, but they were not derived from any underlying microstructural model until (*Ancey and Heyman*, 2014). *Ancey and Heyman* (2014) extended the previous con-

trol volume model (*Ancey et al.*, 2008) to an array of control volumes, where emigration from the ith volume is immigration to the $i+1$th volume.

In an approach widely used in chemical physics (*Gardiner*, 1983) and ecology (*Bailey*, 1968), *Ancey et al.* (2015,?) derived an advection diffusion equation from their microstructural model in a limit as the size of each control volume goes to zero while the number becomes infinite. Thus, in their interpretation, bedload diffusion emerges in the continuum limit of coupled birth-death immigration-emigration models. They rederived the famous Exner equation of bedload diffusion.

Taken together, this research exhibits a coherent progression from the original work of Einstein to a more mathematically and physically based set of more general approaches. Within these approaches the bedload flux is understood as a random quantity. The mean bedload flux and the magnitude of its fluctuations are modelled in an unambiguous way (*Ancey et al.*, 2006, 2008) considering no limitations in sediment availability, and it was shown that collective effects are a necessary inclusion to properly describe fluctuations in bedload transport (*Ancey et al.*, 2008). An extension to a more realistic situation of finite supply was developed (*Turowski*, 2009), and the relationships between these control volume based models and the definition of bedload flux as particles crossing a plane perpendicular to the flow were developed (*Ballio et al.*, 2014; *Heyman et al.*, 2013; **?**).

These approaches did not address spatial correlations or variations in bedload fluxes, although the problem of bedload diffusing through a reach of channel is of contemporary significance (*Hassan et al.*, 2016). This extension was the most recent development in birth-death modelling of bedload (*Ancey and Heyman*, 2014; *Ancey et al.*, 2015). By extending the *Ancey et al.* (2008) model to an array of adjacent control volumes, an advection-diffusion equation describing the concentration of bedload in motion was developed, providing the first connection between a microscale stochastic model of bedload transport with a macroscopic advection-diffusion formulation. *Heyman et al.* (2014) examined the spatial correlations between local bedload fluxes expressed by the *Ancey and Heyman* (2014) model. This is the state of the art of bedload flux models.

1.10.2 Assumptions, calibraiton problems, and unclear aspects: A criticism of the birth-death approach

First, the various glaring assumptions of the birth-death approaches are highlighted.

1. Models only consider one particle size, while natural streams exhibit wide distributions of sizes and bedload transport expresses a wide set of effects related to particle size segregation (*Chen and Stone*, 2008; *Parker and Klingeman*, 1982; *Wilcock and Crowe*, 2003).

2. There is no clear means to discriminate collective and individual entrainment processes within experiments.

3. There is only a one-way feedback in these models: bedload is considered subordinate to the fluid flow, and the effect of bedload transport back onto the fluid flow is considered negligible. In fact, there are measurable influences of bedload transport on the fluid phase (); it's not yet clear whether a one-way coupled scheme such as this can actually describe natural streams across a realistic range of conditions.

4. Collective entrainment is somewhat of a catch-all term with the physical mechanisms which may contribute to it unresolved. These may include collective entrianment, the formation and disintegration of particle clusters, interactions between the motion of grains of idfferent size, turbulent structure, local avalanche behavior, and bed form migration.

5. there have been no theories developed to compute the collective entrainment rate from any simplified mechanical model, although there is a very large set of work concerned with calculating the individual entrainment rate from considerations of fluid turbulence and random granular arrangement (*Dey and Ali*, 2018; *Dey and Papanicolaou*, 2008; *Einstein*, 1950; *Einstein and El-Samni*, 1949; *Grass*, 1970; *Ong et al.*, 2008; *Paintal*, 1971; *Tregnaghi et al.*, 2012; *Wu and Yang*, 2004). Calculating the collective entrainment rate from underlying

principles appears on the surface very difficult. If it is considered to stem from collisions of moving grains with stationary grains, the collective entrainment probability will be related to the probability of collisions with the granular bed. If it is considered to stem from granular avalanches, where coherent turbulent structures initiate collections or clusters of grains into motion simultaneously, the collective entrainment probability will depend on the collective dynamics of the granular assembly – leading immediately into the murky physics of force balance within granular assemblies.

6. Einstein-like assume a clean division between rest and motion states, which is no doubt an idealization. Bedload transport makes a continuous transition from the idealized start-stop motions of Einstein-like models to a less idealized granular flow or creep, where all particles move together in a coorelated fluid-like flow (), meaning bedload models should only hold at relatively low mobility stages.

7. At the same time, the divison of motion into only two categories may be flawed. A wide collection of studies have highlighted different modes of motion. *Einstein* (1950) considered that bedload was particles moving "in a rolling, sliding, or saltating mode". What if rolling, sliding, and saltating modes of motion were treated independently? In an *Ancey et al.* (2006) model of independent particles switching between states, this would require a four-state model. There are too many transition probabilities within such a model probably to calibrate the model from experiments. Again, in order to consider such a scenario we would need more knowledge of underlying mechanics.

Incorporating multiple grain sizes in birth-death models is possible, in principle. As a first approximation, it is easy to introduce multiple grain sizes without including interactions between grain sizes in the entrainment and deposition probabilities for each size fraction. However, spatial and temporal heterogeniety in the bed surface characteristics are a hallmark of bedload transport of gravel mixtures (*Hassan et al.*, 2007). This leaves

models such as *Ancey et al.* (2008) somewhat without basis when multiple grain sizes are considered. The concept of **?** is essential to include when multiple grain sizes are considered: the bed surface state determines which grains can entrain (e.g. *Parker and Klingeman*, 1982; *Wilcock and Crowe*, 2003), and presumably which grains can deposit, as well. The entrainment and deposition rates of each size fraction will need to depend on the bed surface state, and fractional transport will set up spatial hetereogenieties in the bed surface state, so that an *Ancey and Heyman* (2014) type model, incorporating the possiblity of spatial hetereogeniety, should be mixed with a *Turowski* (2009) type model to incorporate the effect of the bed surface state on the entrainment and deposition rates of each size fraction. This extension will not be easy, and it will introduce many undetermined parameters: to pin down this transport model of multiple interacting size fractions will take a lot of work.

These stochastic models are admittedly difficult to calibrate. Their calibration requires a large dataset which is prohibitive to measure within natural streams. Therefore, their applicability in real streams remains limited until the inputs of stochastic models can be computed from physical theories based upon practically measurable quantities. This quest for relationships to compute the inputs of stochastic models from measurable quantities has been called "stochastic closure" for the analogous problem in turbulence (*Heyman et al.*, 2016). The difficult issues precluding the application of stochastic models to natural streams should not be downplayed: much more work is needed.

Chapter 2

Calculation of the sediment flux

2.1 Introduction

A relativity weak flow shearing a bed of sediment entrains individual particles into a state of motion controlled by turbulent forcing and intermittent collisions with other grains at rest on the bed, generating wide fluctuations in the sediment velocity (*Fathel et al.*, 2015; *Heyman et al.*, 2016). Bed load particles move downstream until they are disentrained when they happen to encounter sufficiently sheltered divots on the bed surface to interrupt their motions (*Charru et al.*, 2004; *Gordon et al.*, 1972). Eventually, the bed around them rearranges and destroys this shelter, or turbulent fluctuations overcome the shelter (**??**), particles are once again entrained, and the cycle repeats. Bed load transport is thus a kind of itinerant motion, characterized by alternation between fluctuating movements and rest. This process has proven itself extremely challenging to describe mathematically, given the technicality of the stochastic physics required (*Ancey*, 2020; **?**).

To date, descriptions of bed load transport have therefore simplified the problem in various ways to enable progress. The foundational work is due to Einstein, who considering bed load motions as instantaneous, so he could describe bed load transport as an alternating sequence of "steps" and

rests having random length and duration (*Einstein*, 1937), in a pioneering application of the continuous time random walk (*Montroll*, 1964). Einstein concluded that particles move downstream with a mean velocity $\langle u \rangle = k_E l$, where k_E is the rate at which an individual bed particle entrains into motion, and l is the mean length of each downstream step. Later, he applied these ideas to calculate the mean downstream flux of many particles (*Einstein*, 1950). Einstein reasoned that if the density of resting particles on the bed is ρ_b, the overall areal entrainment rate of particles can be written $E = \rho_b k_E$, so the mean downstream sediment flux can be expressed as $\langle q_s \rangle = \rho_b \langle u \rangle = El$.

Many researchers have since refined Einstein's approach to provide more realistic descriptions of individual particle motions than Einstein's instantaneous step model. One set of efforts has concentrated on particle motions only, calculating the downstream velocity distributions of moving particles using Langevin-type equations to describe turbulent flow and collision forces (*Ancey and Heyman*, 2014; *Fan et al.*, 2014; **?**). These models do not yet include transitions between motion and rest. Another set of efforts has concentrated on including both motion and rest phases while promoting Einstein's instantaneous steps into finite periods of motion (*Lajeunesse et al.*, 2018; *Lisle et al.*, 1998; *Pierce and Hassan*, 2020), but due to mathematical challenges, these models characterize particle motions by a constant velocity, rather than the fluctuating velocities that real sediment particles exhibit.

Researchers have also refined stochastic formulations of the sediment flux beyond the description of the mean flux provided by Einstein (*Furbish et al.*, 2012a). Experiments demonstrate that the sediment flux exhibits wide fluctuations due to (1) variations in the number of moving particles and (2) variations in the velocities of moving particles (*Ancey and Heyman*, 2014; *Ancey et al.*, 2008). As a result of these sediment tranport fluctuations, measurements of the mean sediment flux depend on the timescale over which they are collected (*Singh et al.*, 2009; **?**; **?**), giving a scale-dependent character to the mean sediment flux. To date, very few models have calculated the probability distribution of the bed load sediment flux, and among these, even fewer have described any observation-scale dependence of the sediment flux (**?**).

This survey reveals two major issues in need of research attention. First, we do not yet have the capability to describe individual sediment trajectories through motion and rest including velocity fluctuations in the motion state; and second, we need more understanding of how to connect individual particle trajectories through motion and rest to the overall downstream sediment flux probability distribution and the dependence of the moments of this distribution on the observation time. Here, we develop a new statistical physics-based formalism which addresses both of these problems by describing individual particle trajectories with a Langevin-type equation of motion. This stochastic equation includes alternation between motion and rest at random intervals, and the motion state includes stochastic forcing that ascribes fluctuating velocities to moving particles. Using the probability distribution of particle position generated by this model, we construct a formalism to derive analytically the probability distribution of the sediment flux, and this distribution includes an explicit observation-scale dependence. Below, we develop the new formalism in sec. 2.2, solve it in sec. 2.4, and we discuss the implications of our results and future research ideas in secs. 2.5 and 2.6.

2.2 Model development

We consider an infinite one-dimensional domain populated with sediment particles on the surface of a sedimentary bed. We consider that the flow is weak enough that interactions among moving grains are very rare, although interactions between moving particles and the bed may be common. The flow is in constrast strong enough so that particles are in motion. We label the downstream coordinate as x, so that the downstream velocity of a moving particle is $\dot{x}$, and we describe all sediment particles as independent from one another, but governed by the same underlying dynamical equations, meaning we neglect any influence of sediment size or shape or spatial variations in the overlying fluid flow.

2.2.1 Dynamical equation for bed load sediment transport

From these assumptions, our first target is to write an equation of motion for the individual sediment particle encompassing two features. First, particles should alternate between motion and rest. The transition rate from rest to motion is called entrainment and occurs with probability per unit time (or rate) k_E, while the transition from motion to rest is called deposition and occurs with rate k_D. Second, particles in motion should move with mean velocity V and some fluctuations around this velocity. The simplest equation of motion including these features is

$$\dot{x}(t) = [V + \sqrt{2D}\xi(t)]\eta(t). \tag{2.1}$$

Here $\xi(t)$ is a Gaussian white noise having zero mean and unit variance representing velocity fluctuations among moving particles, and $\eta(t)$ is a dichotomous noise which takes on values $\eta = 1$, representing motion, and $\eta = 0$, representing rest. Here, V is the mean particle velocity, and D is a diffusivity [units L^2/T] of moving particles. The transition rate from $\eta = 0$ to $\eta = 1$ is k_E, and the transition rate from $\eta = 1$ to $\eta = 0$ is k_D. We write $k = k_E + k_D$ as a shorthand.

2.2.2 Derivation of the master equation for $P(x, t)$

The solution of equation 5.3 for a given realization of the two noises $\eta(t)$ and $\xi(t)$ gives the trajectory of a single particle. Averaging over the ensemble of all such trajectories from different realizations of the noises will obtain the probability distribution $P(x, t)$ that a particle which started at position $x = 0$ at time $t = 0$ has travelled to position x by time t. This distribution, by construction, will generalize earlier models which did not include velocity fluctuations among moving particles (*Lajeunesse et al.*, 2018; *Lisle et al.*, 1998).

We form the desired probability distribution of position as $P(y, t) = \left\langle \delta(y - x(t)) \right\rangle_{\eta,\xi}$, where $x(t)$ is the formal solution of eq. 5.3 and the average is over both noises, but this symbolic equation is not yet useful as taking these averages directly is a challenging mathematical problem (*Hanggi*, 1978).

A simpler approach is to conduct the necessary averages in Fourier space. Integrating eq. 1, using its solution in the probability distribution, then Fourier transforming gives

$$\tilde{P}(g,t) = \Big\langle \Big\langle \exp\Big[-ig \int_0^t du[V + \sqrt{2D}\xi(u)]\eta(u) \Big] \Big\rangle_\eta \Big\rangle_\xi . \tag{2.2}$$

Taking time derivatives and conducting the averages using known characteristics of averages of exponentials of Gaussian white noise (*Gardiner*, 1983; **?**) and the Furutsu-Norikov procedure for time derivatives of averages involving dichotomous noise (**?**), in a method similar to (*Balakrishnan*, 1993), provides the Fourier-space master equation

$$\partial_t^2 \tilde{P}(g,t) = (igV - g^2 D - k)\partial_t \tilde{P} + k_E(igV - g^2 D)\tilde{P}, \tag{2.3}$$

and inverse Fourier transforming provides the master equation

$$(\partial_t^2 + V\partial_x\partial_t + k_E V\partial_x + k\partial_t - D\partial_x^2\partial_t - k_E D\partial_x^2)P(x,t) = 0. \tag{2.4}$$

This is a diffusion-like equation governing the probability distribution of position for individual particles as they transport downstream through a sequence of motions and rests, with the movement velocity being a random variable. One can see in particular that taking an the entrainment rate k_E very large, meaning that all particles are generally moving, implies an advection-diffusion equation $(\partial_t + V\partial_x - D\partial_x^2)P = 0$ for the position, characteristic of a particle moving downstream with Gaussian velocity fluctuations. Otherwise, with k_E of similar order as k_D, there is a finite probability that the particle is at rest, and the advection-diffusion process is often interrupted by deposition, giving rise to the additional terms in eq. 5.4.

2.3 Formalism for the downstream sediment flux

Now we express the probability distribution of the sediment flux using the probability distribution of particle position $P(x,t)$ provided as the solution of equation 5.4. We apply a modified version of the approach recently de-

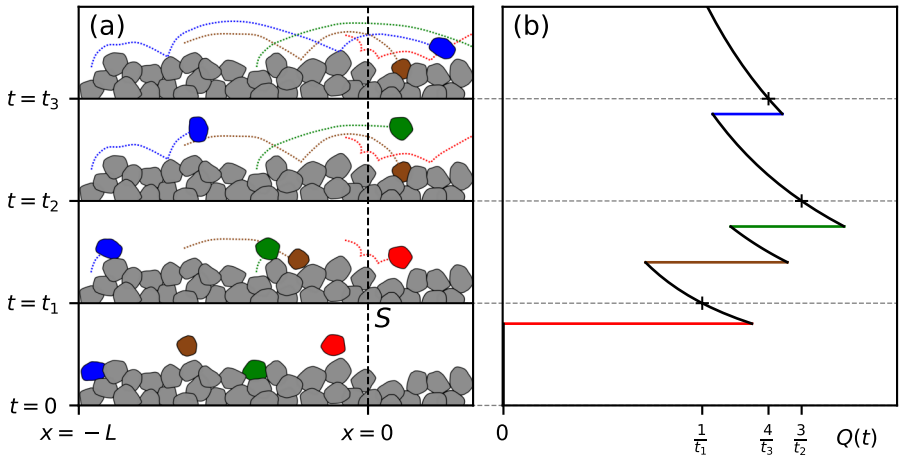

Figure 2.1: The left panel indicates the configuration for the flux. The particle trajectories within are calculated from equation 5.3, demonstrating alternation between rest and motion with fluctuating velocity. Particles begin their transport with positions $-L \leq x \leq 0$ at $t = 0$, and as depicted in the right panel, the flux is calculated as the number of particles $N_>(t)$ which lie to the right of $x = 0$ at the observation time t, divided by t: $Q(t) = t^{-1}N_>(t)$. We calculate the probability distribution of Q over all realizations of the trajectories and initial positions as $L \to \infty$

veloped by Banerjee and coworkers for (*Banerjee et al.*, 2020). The basic idea, as depicted in Figure 1, is that we distribute particles in all states of motion along a domain at random locations at $x < 0$, then we calculate using $P(x, t)$ the rate of particle arrival to $x > 0$ within the sampling time T.

The rate of particles crossing the surface in an observation time T is

$$Q(T) = \frac{1}{T}\sum_{i=1}^{N} \mathcal{I}_i(T). \tag{2.5}$$

In this equation, $\mathcal{I}_i(T)$ is an indicator function which is 1 whenever the ith

particle has passed our control surface and 0 otherwise. All particles which have not crossed the control surface (or which have crossed and then crossed back) contribute nothing to the flux. The probability distribution of the flux is then

$$P(Q|T) = \Big\langle \delta\Big(Q - \frac{1}{T}\sum_{i=1}^{N} \mathcal{I}_i(T)\Big)\Big\rangle. \tag{2.6}$$

The average is over the initial conditions of each particle and the ensemble of trajectories for each particle. Taking the Laplace transform over Q (i.e. forming the characteristic function) obtains

$$\tilde{P}(s|T) = \left\langle \int_0^\infty dQ e^{-sQ} \delta\Big(Q - \frac{1}{T}\sum_{i=1}^{N} \mathcal{I}_i(T)\Big)\right\rangle \tag{2.7}$$

$$= \Big\langle \exp\Big(\frac{s}{T}\sum_{i=1}^{N} \mathcal{I}_i(T)\Big)\Big\rangle \tag{2.8}$$

$$= \prod_{i=1}^{N} \Big\langle \exp\Big(-\frac{s}{T}\mathcal{I}_i(T)\Big)\Big\rangle \tag{2.9}$$

$$= \prod_{i=1}^{N} \Big[1 - \big(1 - e^{-s/T}\big)\big\langle \mathcal{I}_i(T)\big\rangle\Big] \tag{2.10}$$

This progression relies on the independence of averages for each particle (so the average of a product is the product of averages) and the fact that $\mathcal{I}_i(T)$ is either 1 or 0 ($e^{ax} = 1 - (1 - e^a)x$ if $x = 0, 1$). The average over initial conditions and possible trajectories for the ith particle can be written

$$\langle \mathcal{I}_i(t)\rangle = \frac{1}{L}\int_L^0 dx' \int_0^\infty dx \mathcal{P}(x, t|x') = \frac{1}{L}\int_0^L dx' \int_0^\infty dx \mathcal{P}(x, t|-x'), \tag{2.11}$$

where $\mathcal{P}(x, t|x')$ is the probability density that the particle is found at position x at time t given it was initially at x' at time 0. This is the part of the flux that depends on the particle dynamics (ie instantenous velocities and entrainment/deposition characteristics).

Inserting (7) into (6) and taking the limit as $L \to \infty$ and $N \to \infty$ while

the density of particles $\rho = N/L$ remains constant provides

$$\tilde{P}(s|T) = \lim_{N\to\infty} \Big(1 - \frac{1}{N}\big(1 - e^{-s/T}\big)\mu(T)\Big)^N = \exp\Big[-\big(1 - e^{-s/T}\big)\mu(T)\Big]. \tag{2.12}$$

where $\mu(T) = \rho \int_0^\infty dx \int_0^\infty dx' \mathcal{P}(x, T|x')$ is a rate constant which encodes the particle dynamics. This expression is the characteristic function of a Poisson distribution. Expanding in $e^{-s/T}$ and inverting the Laplace transform provides the distribution of the flux

$$P(Q|T) = \sum_{k=0}^{\infty} \frac{\mu(T)^k}{k!} e^{-\mu(T)} \delta(Q - \frac{k}{T}). \tag{2.13}$$

This equation implies that the mean flux is $\langle Q\rangle(T) = \int_0^\infty dQQP(Q|T) = \mu(T)/T$, and similarly the variance is $\sigma_Q^2(T) = \mu(T)/T^2$. The conclusion is that if the flux is considered as a time averaged number of particles crossing a control surface, the mean flux is always Poissonian no matter how particles move, provided they do not interact with one another.

2.4 Results

2.4.1 Derivation of the position probability distribution and its moments

$$P(x, 0) = \delta(x) \tag{2.14}$$

$$\partial_t P(x, 0) = -\frac{Vk_E}{k}\delta'(x) \tag{2.15}$$

These initial conditions come from the initial state

$$P(x, 0) = \lim_{t\to 0} \frac{k_E}{k}\delta(x - Vt) + \frac{k_D}{k}\delta(x). \tag{2.16}$$

$$\bar{\tilde{P}}(g, s) = \frac{s + k + Dg^2 - igVk_D/k}{s(s + k) + (Dg^2 - igV)(s + k_E)}. \tag{2.17}$$

$$\tilde{P}(x, s) = \frac{-D\partial_x^2 + Vk_D/k\partial_x + s + k}{VR(s + k_E)} \exp\Big[\frac{Vx}{2D} - \frac{V|x|}{2D}R\Big]. \tag{2.18}$$

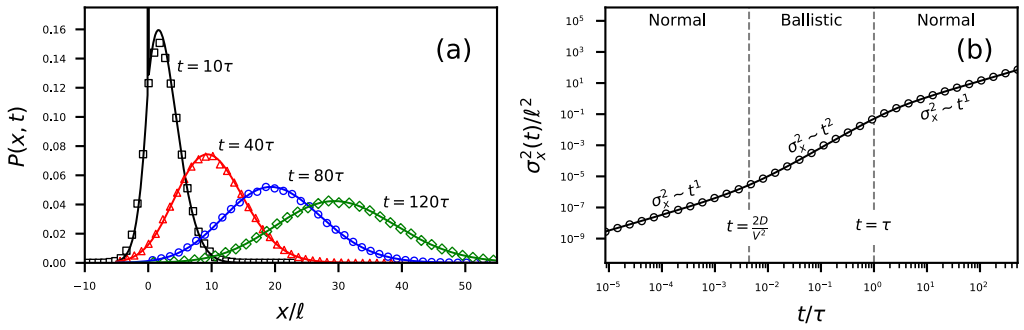

Figure 2.2: The left panel shows the probability distribution of position evolving through time. From the initial state, which is a mixture of moving and resting particles, the distribution splits at short times into contributions from Delta function-like stationary particles and Normal-like moving particles. The right panel demonstrates the resulting spreading characteristics of particles. This short-time splitting noted in the left panel gives rise to ballistic diffusion at short timescales, followed by normal diffusion, as exemplified by equation 4.8.

$$R = \sqrt{1 + \frac{4D}{V^2}\frac{s(s+k)}{s+k_E}} \tag{2.19}$$

$$P(x,t) = \left[-D\partial_x^2 + Vk_D/k\partial_x + k + \delta(t) + \partial_t\right] \int_0^t \mathcal{I}_0\left(2\sqrt{k_E k_D u(t-u)}\right) e^{-k_E(t-u)} \times \sqrt{\frac{1}{4\pi D u}} \exp\left[-k_D u - \frac{(x-Vu)^2}{4Du}\right] du \tag{2.20}$$

The mean is $\langle x \rangle = k_E V t/k$. The variance is

$$\sigma_x^2 = 2\left[\frac{k_E V^2 k_D}{k^3} + \frac{k_E D}{k}\right]\left(\frac{1}{k}e^{-kt} - \frac{1}{k} + t\right) \tag{2.21}$$

2.4.2 Calculation of the flux

$$\mu(t) = \rho \int_0^\infty dx_i \int_0^\infty dx P(x + x_i, t). \tag{2.22}$$

Taking the Laplace transform,

$$\tilde{\mu}(s) = \rho \int_0^\infty dx_i \int_0^\infty dx \tilde{P}(x + x_i, s). \tag{2.23}$$

$$\mu(t) = \rho \int_0^t \mathcal{I}_0\Big(2\sqrt{k_E k_D u(t-u)}\Big) e^{-k_E(t-u)-k_D u} \times \left[\sqrt{\frac{D}{\pi u}}\Big([\overleftarrow{\partial}_t + k]u - \frac{1}{2}\Big) e^{-V^2 u/4D} + \frac{V}{2}\Big([\overleftarrow{\partial}_t + k]u - \frac{k_D}{k}\Big) \operatorname{erfc}\left(-\sqrt{\frac{V^2 u}{4D}}\right)\right] du. \tag{2.24}$$

2.4.3 Connection to earlier work

2.5 Discussion

2.5.1 The role of stochasticity in landscape evolution

2.5.2 Methods to calculate the sediment flux

2.5.3 Outlook and future research

2.6 Conclusion

Chapter 3

Analysis of the bed elevation

The transport characteristics of coarse grains moving under a turbulent flow ultimately control a wide set processes within rivers, including the export of contaminants (*Macklin et al.*, 2006; *Malmon et al.*, 2005), the success of ecological restoration efforts (*Gaeuman et al.*, 2017), and the response of channel morphology to disturbances (*Hassan and Bradley*, 2017). Although the displacements of individual grains are certainly a mechanical consequence of forces imparted from the flow, bed, and other grains (*González et al.*, 2017; *Vowinckel et al.*, 2014; *Wiberg and Smith*, 1985), accurately characterizing these forces within natural channels is practically impossible, especially considering the intense variability these forces display (*Celik et al.*, 2010; *Dwivedi et al.*, 2011; *Schmeeckle et al.*, 2007). In response, investigators have developed a stochastic concept of bedload transport (*Einstein*, 1937), whereby the erosion and deposition of individual grains are modeled as the random results of undetermined forces (*Ancey et al.*, 2006; *Einstein*, 1950; *Paintal*, 1971).

Essentially two types of bedload transport model have been developed from this concept. The first type provides the probabilistic dynamics of a small population of tracer grains as they transport downstream (*Einstein*, 1937; *Hubbell and Sayre*, 1964; *Lajeunesse et al.*, 2018; *Martin et al.*, 2012; *Nakagawa and Tsujimoto 9 Kyoto*, 1977; *Wu et al.*, 2019a), while the second provides the statistics of the number of moving grains ("the particle

activity") within a control volume (*Ancey et al.*, 2006, 2008; *Einstein*, 1950; *Furbish et al.*, 2012b). In the first type, individual displacements are considered to result from alternate step-rest sequences, where step lengths and resting times are random variables following statistical distributions (*Einstein*, 1937). Differences between the random-walk motions of one grain and the next imply a spreading apart of tracer grains as they transport downstream: bedload tracers undergo diffusion.

Resting time distributions have been carefully studied in relation to these models because the predicted diffusion characteristics are critically dependent on whether the distribution has a light or heavy tail (*Bradley*, 2017; *Martin et al.*, 2012; *Weeks and Swinney*, 1998). Resting times have puzzled researchers because early experiments show exponential distributions (*Einstein*, 1937; *Hubbell and Sayre*, 1964; *Nakagawa and Tsujimoto 9 Kyoto*, 1977; *Yano*, 1969), while later experiments show heavy-tailed power-law distributions (*Bradley*, 2017; *Liu et al.*, 2019; *Martin et al.*, 2012; *Olinde and Johnson*, 2015; *Voepel et al.*, 2013; **?**). A predominant hypothesis is that power-law distributed resting times originate from buried grains (*Martin et al.*, 2014; *Voepel et al.*, 2013); this hypothesis permits surface grains to retain exponential resting times. Conceptually, when grains rest on the surface, material transported from upstream can deposit on top of them, preventing entrainment until its removal, driving up resting times and imparting a heavy tail to the distribution. To our knowledge, *Martin et al.* (2014) have provided the only direct support for this hypothesis by tracking grains through complete cycles of burial and exhumation using a narrow flume with glass walls. They observed heavy-tailed resting times of buried grains and described their results with a mathematical model similar to an earlier effort by *Voepel et al.* (2013). Both of these models treat bed elevation changes as a random walk and interpret resting times as return periods from above in the bed elevation time-series (*Redner and Dorfman*, 2002). Each describes resting time distributions from different experiments, but they rely on different random walk models, and their treatment of bed elevations as a process independent of sediment transport is questionable at first glance, since bedload transport is the source of bed elevation changes (*Wong et al.*,

2007), and neither model explicitly includes bedload transport. Models of sedimentary bed evolution incorporating sediment transport processes might enhance understanding of sediment resting times.

The second type of stochastic model prescribes rates (probabilities per unit time) to the erosion and deposition events of individual grains within a control volume to calculate the particle activity (*Einstein*, 1950). These approaches aim at a complete statistical characterization of the bedload flux (*Fathel et al.*, 2015; *Furbish et al.*, 2012b, 2017; *Heyman et al.*, 2016), including probability distributions (*Ancey et al.*, 2006, 2008), spatial and temporal characteristics of its fluctuations (*Ancey et al.*, 2008; *Dhont and Ancey*, 2018; *Heyman*, 2014; *Roseberry et al.*, 2012), and the dependence of these statistical characteristics on the length and time scales over which they are measured or calculated (*Ma et al.*, 2014; *Singh et al.*, 2009, 2012; **?**). A recent surge in research activity has generated rapid progress and spawned many new inquiries in this subject. For example, *Ancey et al.* (2006) demonstrated that a constant erosion rate as originally proposed by *Einstein* (1950) was insufficient to develop realistically large particle activity fluctuations, so they added a positive feedback between the particle activity and erosion rate they called "collective entrainment" (*Ancey et al.*, 2008; *Heyman et al.*, 2013, 2014; *Lee and Jerolmack*, 2018; *Ma et al.*, 2014). While they deemed this feedback necessary to model realistic activity fluctuations, the implications of this collective entrainment term on bed topography and particle activity changes has not been fully explored.

In this work, we present the first stochastic model coupling the erosion and deposition of individual bedload grains to local bed elevation changes. Our model extends the *Ancey et al.* (2008) model to describe the interplay between bedload flux and bed elevation fluctuations in a control volume. This development permits a systematic study of the repercussions of collective entrainment, and it frames bed elevation changes as a direct consequence of the sediment transport process. Our model has two key assumptions: (1) bedload erosion and deposition can be characterized by probabilities per unit time, or rates (*Ancey et al.*, 2008; *Einstein*, 1950); and (2) these rates are contingent on the local bed elevation, encoding the property that ero-

sion of sediment is emphasized from regions of exposure, while deposition is emphasized in regions of shelter (*Wong et al.*, 2007; **?**). We study statistical characteristics of bedload transport, bed elevation, and resting times of sediment undergoing burial using a mixture of numerical simulations and analytical approximations. We introduce the stochastic model in section 5.2, and we solve it in section 5.3.1 with a mixture of numerical and analytical techniques. We discern several new features of particle activity and bed elevation statistics that result from feedbacks between the erosion and deposition rates and the local bed elevation. We present these features in section 5.3. We conclude with the implications of our results and speculate on topics for future research in sections 5.4 and 5.5.

3.1 Stochastic model of bedload transport and bed elevations

We prescribe a volume of downstream length L containing some number n of moving particles in the flow and some number m of stationary particles composing the bed at time t, as depicted in figure 3.1. We define m relative to the mean number of grains within the control volume, so that it can be either positive or negative. n is always a positive integer including 0. For simplicity, we consider all particles as approximately spherical with the same diameter $2a$, so their mobility and packing characteristics are consistent. Following *Ancey et al.* (2008), we prescribe four events that can occur at any instant to modify the populations n and m, and we characterize these events using probabilities per unit time (rates). These events are (1) migration of a moving particle into the volume from upstream ($n \to n+1$), (2) the entrainment (erosion) of a stationary particle into motion within the volume ($m \to m-1$ and $n \to n+1$), (3) the deposition of a moving particle to rest within the volume ($m \to m+1$ and $n \to n-1$), and (4) the migration of a moving particle out of the volume to downstream ($n \to n-1$). The four events are depicted as arrows in figure 3.1. As the events occur at random intervals, they set up a joint stochastic evolution of the populations n and m characterized by a joint probability distribution $P(n, m, t)$ for the

number of particles in motion and rest in the volume at t. The populations

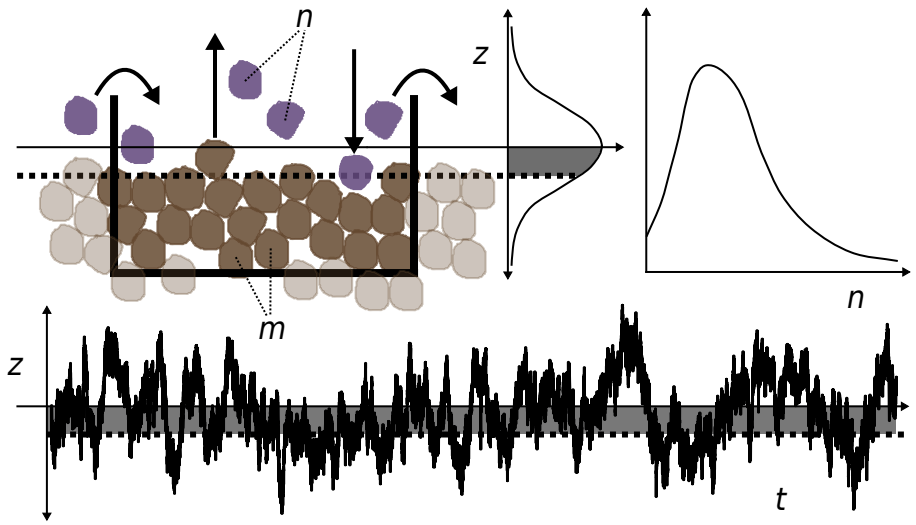

Figure 3.1: Definition sketch of a control volume containing n moving grains and m resting grains. Migration, entrainment, and deposition are represented by arrows, and the instantaneous bed elevation is depicted by dotted lines. The bed is displayed in a degraded state, where $m < 0$. The marginal distributions of n and m are indicated in the upper right panel, while the bottom panel is a realized time-series of bed elevations computed from m using (3.1).

n and m provide the bulk bedload flux q_s and the local bed elevation z. The mean bedload transport rate is given by $q_s = u_s\langle n\rangle/L$, where u_s is the characteristic velocity of moving bedload and $\langle n\rangle = \sum_{n,m} nP(n,m)$ is the mean number of grains in motion (*Ancey et al.*, 2008; *Charru et al.*, 2004; *Furbish et al.*, 2012b). The bed elevation is related to m through the packing geometry of the bed. To quantify this, we introduce a packing fraction ϕ of grains in the bed (*Bennett*, 1972), and for simplicity we consider the bed as two-dimensional (*Einstein*, 1950; *Paintal*, 1971). The deviation from the

mean bed elevation is then

$$z(m) = \frac{\pi a^2}{\phi L} m = z_1 m. \tag{3.1}$$

The constant $z_1 = \pi a^2/(\phi L)$ is an important scale of the problem. z_1 is the magnitude of bed elevation change in an average sense across the control volume associated with the addition or removal of a single grain.

Bed elevation changes modify the likelihood of entrainment and deposition in a negative feedback (*Wong et al.*, 2007; **?**); that is, aggradation increases the likelihood of entrainment, while degradation increases the likelihood of deposition. *Wong et al.* (2007) concluded that bed elevation changes induce an exponential variation in entrainment and deposition probabilities, while **?** concluded that the variation is linear. For simplicity, we incorporate the scaling of **?** and note its equivalence to the *Wong et al.* (2007) scaling when bed elevation changes are small. Because experimental distributions of bed elevations are often symmetrical, (*Martin et al.*, 2014; *Pender et al.*, 2001; *Wong et al.*, 2007; **?**), we expect the erosion and deposition feedbacks to have the same strength. That is, as bed elevation changes drive up (down) erosion rates, so they drive down (up) deposition rates to the same degree. Merging these ideas with those of *Ancey et al.* (2008), we write the four possible transitions with local bed elevation-dependent entrainment and deposition rates as

$$R_{MI}(n+1|n) = \nu \qquad \text{migration in,} \tag{3.2}$$

$$R_E(n+1, m-1|n, m) = (\lambda + \mu n)[1 + \kappa m], \qquad \text{entrainment,} \tag{3.3}$$

$$R_D(n-1, m+1|n, m) = \sigma n[1 - \kappa m], \qquad \text{deposition.} \tag{3.4}$$

$$R_{MO}(n-1|n) = \gamma n \qquad \text{migration out.} \tag{3.5}$$

In equations (3.3) and (3.4), κ is a coupling constant between bed elevations and the entrainment and deposition rates. ν is the rate of migration into the control volume, λ is the conventional entrainment rate, μ is the collective entrainment rate, σ is the deposition rate, and γ is the rate of migration out of the control volume. At $m = 0$, these equations reduce to those of

the *Ancey et al.* (2008) model. Away from this elevation, entrainment and deposition are alternatively suppressed and enhanced depending on the sign of m, constituting a feedback between bed elevation changes and erosion and deposition. We refer to κ as a coupling constant since it controls the strength of this feedback. We later demonstrate the relationship

$$\kappa \approx \left(\frac{z_1}{2l}\right)^2 \tag{3.6}$$

where l is a characteristic length scale of bed elevation change that we interpret as the active layer depth (*Correa et al.*, 2017; *Wong et al.*, 2007). All four rates are independent of the past history of the populations and depend only on the current populations (n, m). As a result, the model is Markovian (**??**), meaning time intervals between any two subsequent transitions are exponentially distributed (*Gillespie*, 2007).

We write the master equation for the probability flow using the forward Kolmogorov equation $\partial P(n,m;t)/\partial t = \sum_{n',m'}[R(n,m|n',m')P(n',m';t) - R(n',m'|n,m)P(n,m;t)]$ (*Ancey et al.*, 2008; **?**; **?**) as

$$\begin{aligned}\frac{\partial P}{\partial t}(n,m;t) = \nu P(n-1,m;t)+[\lambda(m+1)+\mu(n-1)][1+\kappa(m+1)]P(n-1,m+1;t)\\ + \sigma(n+1)[1-\kappa(m-1)]P(n+1,m-1;t) + \gamma(n+1)P(n+1,m;t)\\ - \{\nu+\lambda+\mu n(1+\kappa m)+\sigma n(1-\kappa m)+\gamma n\}P(n,m;t). \end{aligned} \tag{3.7}$$

The joint probability distribution $P(n,m;t)$ solving this equation fully characterizes the statistics of n and m – proxies for the bedload flux and local bed elevation. The average entrainment and deposition rates E and D over all bed elevations are $E = \lambda + \mu\langle n\rangle$ and $D = \sigma\langle n\rangle$. We anticipate that solutions of (5.4) will adjust from the initial conditions to a steady-state distribution $P_s(n,m)$ – independent of time – if the constant factors in the transition rates are representative of equilibrium conditions. Equilibrium requires $E = D$, meaning there is no net change in elevation, and $\nu = \gamma\langle n\rangle$, meaning mass is conserved in the control volume (inflow = outflow). This Master equation describes a two-species stochastic birth-death model (**?**) of a type well-known in population ecology (*Pielou*, 2008; *Swift*, 2002) and

chemical physics (*Gardiner*, 1983). In our context, the two populations are the moving and stationary grains in the volume.

3.2 Model solutions

Unfortunately, equation (5.4) does not appear to admit an analytical solution unless $\kappa = 0$ (but see *Swift* (2002) for the generating function method which fails in this case). The difficulty originates from the product terms between n and m representing the bed elevation dependence of collective entrainment and deposition rates. In response to this difficulty, we resort to numerical methods and analytical approximations, simulating equation (5.4) with the Gillespie algorithm (*Gillespie*, 1977, 2007; **?**) and solving it approximately with mean field and Fokker-Planck approaches (*Gardiner*, 1983; **?**). The simulation algorithm is described in 3.2.1, and analytical approximations are described in 3.2.2.

3.2.1 Numerical simulations

The Gillespie algorithm leverages the defining property of a Markov process: when transition rates are independent of history, time intervals between transitions are exponentially distributed (**?**). As a result, to step the Markov process through a single transition, one can draw a first random value from the exponential distribution of transition intervals to determine the time of the next transition, then draw a second random value to choose the type of transition that occurs using relative probabilities formed from equations (3.2-3.5). The transition is enacted by shifting t, n and m by the appropriate values to the

Table 3.1: Migration, entrainment, and deposition rates at $z(m) = 0$ from *Ancey et al.* (2008). Units are s^{-1} (probability/-time). In our model, bed elevation changes modulate these rates in accord with (3.2-3.5).

flow	ν	λ	μ	σ	γ
(a)	5.45	6.59	3.74	4.67	0.77
(g)	7.74	8.42	4.34	4.95	0.56
(i)	15.56	22.07	3.56	4.52	0.68
(l)	15.52	14.64	4.32	4.77	0.48

type of transition (that is, entrainment is $m \to m-1$ and $n \to n+1$, and so on). This procedure can be iterated to form an exact realization of the stochastic process (*Gillespie*, 2007). We provide additional background on the stochastic simulation method in the supplementary material and refer the reader to *Gillespie* (2007) for more detail.

Using this method, we simulated 4 transport conditions with 13 different values of l taken across a range from $l = a$ (a single radius) to $l = 10a$ (10 radii). These values include the range exhibited by the available experimental data on bed elevation timeseries (*Martin et al.*, 2014; *Singh et al.*, 2009; *Wong et al.*, 2007). For the migration, entrainment, and deposition parameters representing bedload transport at each flow condition $(\nu, \lambda, \mu, \sigma, \gamma)$, we used the values measured by *Ancey et al.* (2008) in a series of flume experiments: these are summarized in table 3.1. Flow conditions are labeled (a), (g), (i), and (l), roughly in order of increasing bedload flux (see *Ancey et al.* (2008) for more details). In all simulations, we take the packing fraction $\phi = 0.6$ – a typical value for a pile of spheres (e.g., *Bennett*, 1972), and we set $L = 22.5$cm and $a = 0.3$cm in accord with the *Ancey et al.* (2008) experiments. Each simulation was run for 250 hours of virtual time, a period selected to ensure neat convergence of particle activity and bed elevation statistics.

3.2.2 Approximate solutions

We approximately decouple the n and m dynamics in equation (5.4) using the inequality $l \gg z_1$ (equivalently $\kappa \ll 1$) which holds for large values of the active layer depth l. These inequalites mean many entrainment or deposition events are required for an appreciable change in the entrainment or deposition rates. We concentrate on steady state conditions $\partial P/\partial t = 0$ and introduce the exact decomposition $P(n, m) = A(n|m)M(m)$ to equation (5.4), with the new distributions normalized as $\sum_m M(m) = 1$ and

$\sum_n A(n|m) = 1$. This provides the steady state equation

$$\begin{aligned} 0 = \nu A(n-1|m)M(m) + [\lambda+\mu(n-1)][1+\kappa(m+1)]A(n-1|m+1)M(m+1) \\ +\sigma(n+1)[1-\kappa(m-1)]A(n+1,m-1)M(m-1) + \gamma(n+1)A(n+1|m)M(m) \\ -\{\nu + [\lambda+\mu n](1+\kappa m) + \sigma n(1-\kappa m) + \gamma n\}A(n,m)M(m). \quad (3.8) \end{aligned}$$

Summing this equation over n provides a still exact description of the distribution of bed elevations $M(m)$ in terms of the conditional mean particle activity $\langle n|m\rangle = \sum_n nA(n|m)$:

$$\begin{aligned} 0 = [\lambda + \mu\langle n|m+1\rangle][1+\kappa(m+1)]M(m+1) \\ +\sigma\langle n|m-1\rangle[1-\kappa(m-1)]M(m-1) \\ -\{[\lambda+\mu\langle n|m\rangle](1+\kappa m) + \sigma\langle n|m\rangle(1-\kappa m)\}M(m). \quad (3.9) \end{aligned}$$

Unforunately, these two equations are no easier to solve than the original master equation, since the coupling between n and m is not reduced in equation (3.8).

The simplest approximation to these equations holds that κ is so small that the dynamics of n are totally independent of m: $A(n|m) = A(n)$. Taking this limit in equation (3.8), summing over m, and using $\langle m\rangle = 0$ reproduces the *Ancey et al.* (2008) particle activity model. As shown by *Ancey et al.* (2008), this has solution

$$A(n) = \frac{\Gamma(r+n)}{\Gamma(r)n!}p^r(1-p)^n. \quad (3.10)$$

which is a negative binomial distribution for the particle activity with parameters $r = (\nu+\lambda)/\mu$ and $p = 1-\mu/(\sigma+\gamma)$. This result implies $\langle n|m\rangle = \langle n\rangle$, so with the definitions of E and D and the equilibrium condition $E = D$, equation (3.9) provides

$$0 \approx [1+\kappa(m+1)]M(m+1) + [1-\kappa(m-1)]M(m-1) - 2M(m). \quad (3.11)$$

This mean field equation matches the discrete Ornstein-Uhlenbeck model

of bed elevation changes developed by *Martin et al.* (2014). We summarize that the independent bed elevation and particle activity models of *Martin et al.* (2014) and *Ancey et al.* (2008) derive from the model we present in a mean field approximation when κ is insignificant.

In the supplementary information we show the Fokker-Planck approximation (*Gardiner*, 1983) formed by expanding $M(m \pm 1)$ to second order in m within equation (3.11) provides the solution $M(m) \propto \exp(-\kappa m^2)$: this is a normal distribution of bed elevations with variance $\sigma_m^2 \propto \frac{1}{2\kappa}$. As we will demonstrate in section 5.3, and as we have already suggested with equation (3.6), this is a poor approximation to the bed elevation variance. Nevertheless, this approximation does capture the Gaussian shape of the bed elevation distribution. The essential issue with this mean field approach is that the conditional mean particle activity $\langle n|m \rangle$ varies significantly with m in actuality, especially when collective entrainment contributes to the mean entrainment rate E. We will discuss these points subsequently when developing more refined approximations and presenting numerical results.

A more careful approximate solution to equation (3.9) can be obtained by prescribing a phenomenological equation for $\langle n|m \rangle$ into equation (3.9) in order to close the equation for m without solving equation (3.8). From numerical simulations we determine that

$$\langle n|m \rangle \approx \langle n \rangle \Big(1 - \frac{2\kappa m}{1 - \mu/\sigma}\Big) \tag{3.12}$$

captures the general features of the conditional mean particle activity. As we show in the supplementary information, introducing this closure equation to (3.9), making the Fokker-Planck approximation, and neglecting terms of $O(\kappa^2)$ provides

$$M(m) \approx M_0 e^{-2\kappa m^2}, \tag{3.13}$$

representing a Gaussian distribution with variance $\sigma_m^2 = \frac{1}{4\kappa}$ – smaller than the former mean field theory by a factor of two and in agreement with the result posited in equation (3.6). M_0 is a normalization constant. As we will demonstrate, this closure equation approach shows good coorespondence

with numerical solutions of equation (5.4), at least for the flow parameters in table 3.1.

3.3 Results

From the initial conditions, all simulations show a rapid attainment of steady-state stochastic dynamics of n and m which support a time-independent joint distribution $P(n, m)$. We show an elevation time-series in the bottom panel of figure 3.1. In order to describe the implications of coupling bedload transport to bed elevation changes, we present the numerical and analytical results for the probability distributions of bedload transport and bed elevations in section 3.3.1 and the statistical moments of these quantities in section 3.3.2. We isolate the effects of collective entrainment on bed elevation changes in section 3.3.3, and we present the resting times of sediment undergoing burial in section 3.3.4.

3.3.1 Probability distributions of bedload transport and bed elevations

We compute this joint distribution by counting occurrences of the states (n, m) in the simulated time series. From this joint distribution we compute marginal distributions $P(n)$ and $P(m)$ by summing over m and n respectively. A representative subset of these marginal distributions is displayed in figure 4.1 alongside the approximate results of equations (3.10) and (3.13). The mean field equation (3.10) for the particle activity n closely represents the numerical results, and while there are small differences between numerical and analytical results for the relative number m of resting particles, the numerical solutions approximately match equation (3.13), having Gaussian profiles consistent with our assumption of a symmetric scaling of erosion and deposition rates with bed elevation changes.

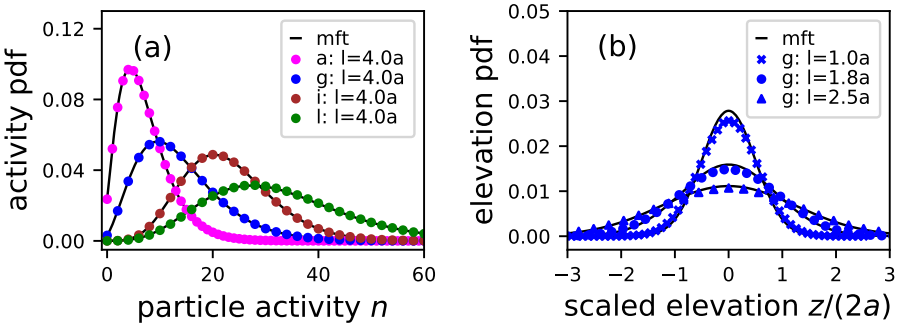

Figure 3.2: Panel (a) presents the probability distribution of particle activity n and panel (b) presents the probability distribution of the relative number of particles m for a representative subset of simulations. These distributions represent different flows from table 3.1, distinguished by color, and different values of the active layer depth l (equivalently the coupling constant κ), distinguished by the marker style. The mean field theories (mft) of equations (3.10) and (3.13) are displayed as solid black lines.

3.3.2 Statistical moments

We calculate the moments of n and m by summing over $P(n, m)$. The jth order unconditional moment of the particle activity n derives from

$$\langle n^j \rangle = \sum_n n^j P(n), \tag{3.14}$$

while the jth order moment of n held conditional on m is

$$\langle n^j | m \rangle = \sum_n n^j P(n, m). \tag{3.15}$$

We observe no dependence of the moments of m on the value of n. The mean elevation is always $\langle m \rangle = 0$ due to our initial assumption of symmetry in the entrainment and

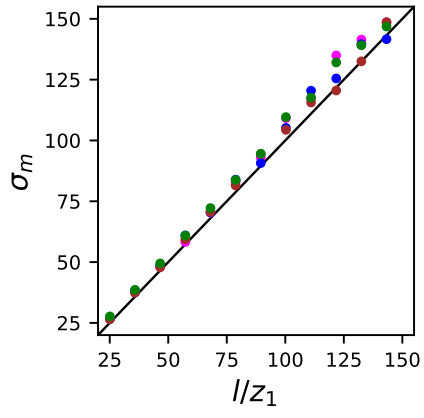

deposition rate scaling with m. Figure 4.2 demonstrates that the variance of bed elevations is approximately $\sigma_z^2 = z_1^2\sigma_m^2 = \frac{1}{4\kappa} = l^2$, agreeing with the approximation in equation (3.13); this result supports our earlier assertion that l is a characteristic length scale of bed elevation fluctuations. The close correspondence between the mean field approximation and the numerical simulations in figure (4.1a) suggests the unconditional moments of n correspond closely with the *Ancey et al.* (2008) result. We find them to be identical within numerical uncertainty.

The coupling between bed elevation changes and the erosion and deposition rates develop a strong dependence of the particle activity on m. Figure (3.4) displays the mean shift $[\langle n|m\rangle - \langle n\rangle]/\langle n\rangle$ and the variance shift $[\mathrm{var}(n|m) - \mathrm{var}(n)]/\mathrm{var}(n)$ of the particle activity due to departures of the bed elevation from its mean position. Figure (3.4a) demonstrates that the *Ancey et al.* (2008) flow conditions support departures of the mean particle activity by as much as 60% from the overall mean value when the bed is in a degraded state $z \approx -3l$, and the activity can be decreased by 20% when the bed is in an aggraded state. The closure model (3.12) used to derive the approximate bed elevation distribution (3.13) is plotted behind the conditional mean profiles in figure (3.4a), where it appears to be crude approximation, as it does not capture the asymmetry in this quantity. Nevertheless, figure 4.2 demonstrates the variance $1/(4\kappa)$ derived from this closure equation is representative of the numerical relationship. For the parameters of the *Ancey et al.* (2008) experiments, figure (3.4b) displays a variance shift with bed elevation changes that is less severe than the mean shift but is nevertheless appreciable, with bed elevations changing the magnitude of bedload activity fluctuations by as much as 20%. We summarize that bed elevation changes

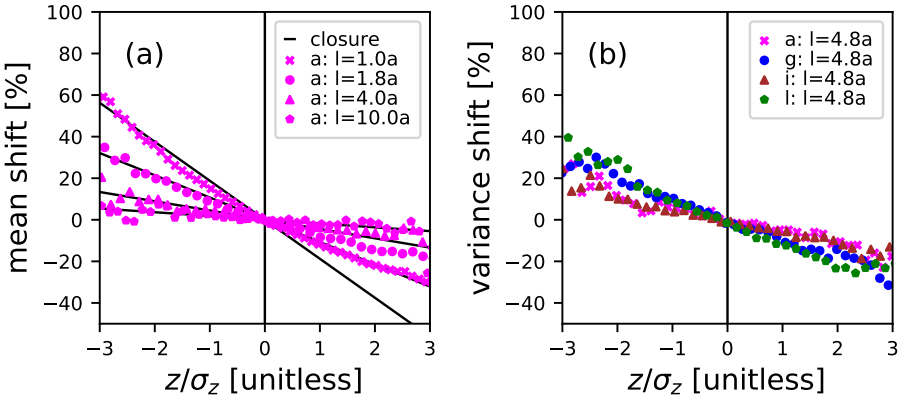

Figure 3.4: The shifts between particle activity moments conditioned on instantaneous elevations and their over-all mean values. Panel (a) indicates the mean particle activity shift versus the bed elevation measured in units of $\sigma_z = l$. This shift displays asymmetric dependence on m at the flow conditions of the *Ancey et al.* (2008) experiements, and departures of the bedload transport mean can be as much as 60% when the bed is in a severely degraded state with $z \approx -3l$. The closure equation (3.12) is plotted in panel (a) Panel (b) demonstrates a more symmetrical variance shift with some dependence on flow conditions displaying shifts of up to 20% with bed elevations. These results indicate that bedload statistics measurements on short timesclaes could be severely biased by departures from the mean bed elevation.

regulate the particle activity moments, with a moment suppression effect when the bed is aggraded, and a moment enhancement effect when the bed is degraded.

3.3.3 Collective entrainment and bedload activity fluctuations

Noting that bed elevations regulate the particle activity moments, we now study the influence of collective entrainment on this effect by modifying the relative proportion of the individual to collective contributions in the mean

entrainment rate $E = \lambda + \sigma\langle n \rangle$. Using the equilibrium condition $E = D$, we determine the fraction of entrainment due to the collective process is $f = \mu\langle n \rangle / E = \mu/\sigma$. Using this fraction, we can hold E constant and modify the prevalence of the collective entrainment process by setting $\lambda = E(1-f)$ and $\mu = \sigma f$. As we interpolate f between zero and one, the particle activity component of the master equation 5.4 interpolates from a purely Poissonian model (*Ancey et al.*, 2006) to a negative binomial model (*Ancey et al.*, 2008), isolating the imprint of collective entrainment on particle activity statistics over a dynamic sedimentary bed. Figure 3.5 depicts the modification of the

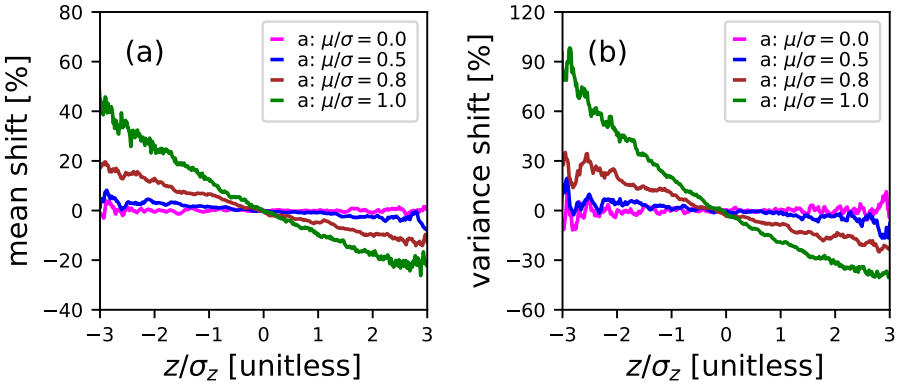

Figure 3.5: The shift of the mean particle activity in panel (a) and its fluctuations in panel (b) with departures of the bed elevation from its mean. All simulations are at flow condition (g) from table 3.1 except λ and μ are modified to shift the fraction $f = \mu/\sigma$ of the over-all entrainment rate E due to collective entrainment. Clearly, collective entrainment drives strong departures of the bedload statistics away from the mean field model (3.10) at large departures from the mean bed elevation. Panel (b) shows particle activity fluctuations suppressed by 90% when $z \approx -3l$ and collective entrainment is the dominant process. When collective entrainment is absent, meaning $\mu/\sigma = 0$, this moment regulation effect vanishes: it is a consequence of collective entrainment.

particle activity mean and variance as the importance of collective entrain-

ment is tuned (through λ and μ) with all other parameters fixed. When $f = 0$, the bed elevation ceases to influence the particle activity mean or variance, while larger fractions increasingly enable the moment regulation effect we introduced in section 3.3.2.

3.3.4 Resting times of sediment undergoing burial

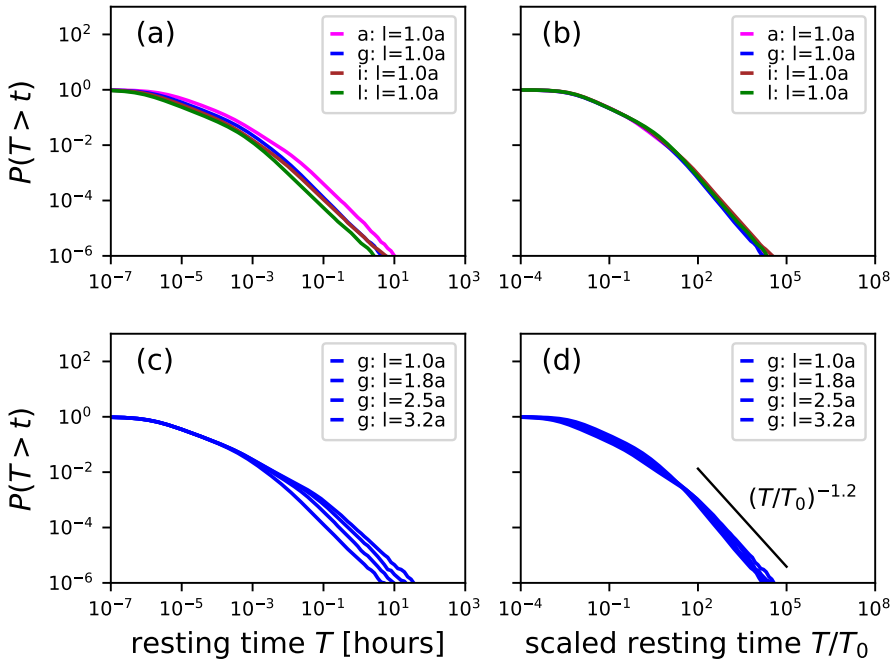

Figure 3.6: Resting time statistics scale differently with transport conditions and the bed elevation variance. Panel (a) shows differing flow conditions at a fixed l value, while panel (c) shows fixed flow conditions at differing l. When scaled by T_0 (3.17), both types of difference collapse in the tails of the distributions, as shown in panels (b) and (d). In panels (b) and (d), the black dotted lines indicate a power law decay of the collapsed tails having parameter $\alpha \approx 1.18$.

Resting times for sediment undergoing burial are obtained from analyz-

ing the return times from above in the time-series of m (e.g., *Redner and Dorfman*, 2002). Following *Voepel et al.* (2013) and *Martin et al.* (2014), we concentrate on a particular bed elevation m', and find all time intervals separating deposition events at $m = m'$ from erosion events at $m = m'+1$. These are the return times from above of the sedimentary bed conditional to the elevation m'. Binning these conditional return times (using logarithmically-spaced bins to reduce computational load) and counting the occurrences in each bin, we obtain an exceedance distribution of return times t_r held conditional to the elevation m': $P(T > t_r|m')$. Using the marginal probability distribution of bed elevations $P(m)$ (figure 4.1(b)), we derive the unconditional exceedance distribution of resting times as a sum over all elevations (*Martin et al.*, 2014; *Voepel et al.*, 2013; *Yang and Sayre*, 1971; **?**):

$$P(T > t_r) = \sum_{m'} P(m')P(T > t_r|m'). \tag{3.16}$$

A representative subset of these results are displayed in figure 3.6. Comparing panels 3.6(a) and 3.6(c) shows two separate variations with input parameters: first, the distributions vary with the flow conditions, and second, they vary with the standard deviation of bed elevations (l). However, as shown in panels 3.6(b) and 3.6(d), a characteristic timescale T_0 is found to collapse away both variations. We obtained this T_0 heuristically by considering the characteristic speed of bed elevation change. This is the mean number of grains leaving the bed per unit time is E, and the removal of a single grain changes the bed elevation by z_1 (3.1). Therefore, bed elevations change with a characteristic speed $v = z_1E$. Since the range of elevation deviations is l (figure 4.2), the time required for the bed to shift through this characteristic distance is l/v, or equivalently

$$T_0 = \frac{l}{z_1E}. \tag{3.17}$$

When scaling the resting time by this T_0, we obtain the collapse shown in figure 3.6. Using the log-likelihood estimation technique described by *Newman* (2005), we estimate the scaled resting time non-exceedance distri-

butions decay as a heavy tailed power law with parameter $\alpha = 1.18 \pm 0.32$ for all return times satisfying $T/T_0 > 10^3$. These distributions are sufficiently heavy tailed to violate the central limit theorem and drive anomalous super-diffusion of bedload, a result which supports the earlier conclusions of *Voepel et al.* (2013) and *Martin et al.* (2014).

3.4 Discussion

3.4.1 Context

Einstein developed the first stochastic models of bedload tracer diffusion (*Einstein*, 1937) and the bedload flux (*Einstein*, 1950), and his ideas can be viewed as the nexus of an entire paradigm of research that extends into the present day (e.g., *Ancey et al.*, 2008; *Hassan et al.*, 1991; *Hubbell and Sayre*, 1964; *Nakagawa and Tsujimoto 9 Kyoto*, 1977; *Wu et al.*, 2019a). These models aim to predict bedload transport characteristics from stochastic concepts of individual particle motions. With some exceptions (*Shi and Wang*, 2014; *Wu et al.*, 2019a,b; *Yang and Sayre*, 1971; **?**), existing descriptions are spatially one-dimensional, concentrating on the motion of grains in the downstream direction without including the vertical dimension wherein local bed elevation changes imply sediment burial (*Martin et al.*, 2014; *Voepel et al.*, 2013) and change the mobility of surface grains (*Yang and Sayre*, 1971; **?**).

3.4.2 Contributions

In this paper, we have built on earlier works (*Ancey et al.*, 2008; *Martin et al.*, 2014) to include the vertical dimension of bed elevation dynamics, study the interplay between bedload transport and bed elevation fluctuations, and investigate resting time distributions of sediment undergoing burial. To our knowledge, this model is the first description of bedload transport and bed elevations as a coupled stochastic population model based on individual grains. Numerical solutions and analytical approximations provided negative binomial distributions of bedload activity and normal distributions of

bed elevations. Although experiments under more natural conditions with segregation processes, migrating bedforms, or sediment supply perturbations have shown particle activity distributions with heavier tails (*Dhont and Ancey*, 2018; **?**) and non-Gaussian bed elevations (*Aberle and Nikora*, 2006; *Singh et al.*, 2012), our results reproduce the key features of the most controlled bed elevation (*Martin et al.*, 2014; *Wong et al.*, 2007) and bedload transport (*Ancey et al.*, 2008; *Heyman et al.*, 2016) experiments in the literature.

Our inclusion of coupling between the bed elevation and entrainment and deposition rates revealed a novel dependence of particle activity on bed elevation changes, highlighting a new consequence of the collective entrainment process (*Ancey et al.*, 2008; *Lee and Jerolmack*, 2018). This coupling develops a significant variation of the particle activity moments with deviations of the bed from its mean elevation. We isolated the role of collective entrainment in this bedload activity regulation, and pointed out that particle activity variations with bed elevations dissapear in the absence of collective entrainment. Finally, we obtained resting times for sediment undergoing burial within the sedimentary bed by analyzing return times from above in the bed elevation time-series. We found heavy-tailed power law resting times with tail parameters sufficient to drive anomalous diffusion of bedload at long timescales. The distribution tails were found to collapse across flow conditions using a timescale formed from the mean erosion rate and the active layer depth.

As our model builds on earlier works describing particle activity and bed elevation changes independently, it also reduces to these works in simplified limits when the coupling between the particle activity and bed elevation vanishes. With the mean field approach in section 3.2.2, we derived the *Martin et al.* (2014) Ornstein-Uhlenbeck model for bed elevations and the *Ancey et al.* (2008) birth-death model for the particle activity as simplified limits of our coupled model. While the mean field description of bed elevations over-predicts the bed elevation variance by approximately a factor of two, it does capture the Gaussian shape of the bed elevation distribution, and its conclusions on the tail characteristics of resting time distributions

for sediment undergoing burial are identical to ours within the numerical uncertainty: *Martin et al.* (2014) described a power-law distribution with tail parameter $\alpha \approx 1$ which falls neatly within our estimation $\alpha = 1.18 \pm 0.32$. In addition to our original contributions, we have corroborated the models of *Ancey et al.* (2008) and *Martin et al.* (2014) from an alternate perspective, showing their results to be mostly robust when accounting for bed elevation changes.

3.4.3 Next steps

The model we have presented computes statistical characteristics of the bedload particle activity and bed elevation within a control volume by assuming all particles on the bed surface have similar mobility characteristics while sediment transport and bed topography are in equilibrium. In actuality, particles span a range of sizes, and spatial organization occurs both in the forces imparted to particles by the flow (*Amir et al.*, 2014; *Shih et al.*, 2017) and in the mobility characteristics of particles on the bed surface (*Charru et al.*, 2004; *Hassan et al.*, 2007; *Nelson et al.*, 2014). Together, these factors may generate spatial correlations in particle activities that models concentrating on a single control volume will be unable to capture. Models chaining multiple control volumes together have shown spatial correlations in the particle activity as a result of collective entrainment (*Ancey et al.*, 2015; *Heyman et al.*, 2014), and similar approaches have also been applied to study correlations in turbulent flows (*Gardiner*, 1983). In light of this work, we consider the model we have presented as a preliminary step toward a multiple-cell model of particle activities and bed elevation changes with potential to express spatial correlations between longitudinal profile and particle activity statistics.

Like *Martin et al.* (2014), we obtained heavy-tailed power-law resting times for sediment undergoing burial by treating bed elevation changes as an unbounded random walk with a mean reverting tendency. This result suggests sediment burial can explain the heavy-tailed rests seen in field data (*Bradley*, 2017; *Olinde and Johnson*, 2015; **?**). Our resting time distribu-

tions show a divergent variance and possibily a divergent mean, since this occurs for $\alpha < 1$ (**?**) which is within range of our results. Divergent mean resting time distributions present a paradox, since they imply all particles should eventually be immobile, violating the equilibrium transport assumption. *Voepel et al.* (2013) demonstrated that a bounded random walk for bed elevations provides a power-law distribution that eventually transitions to a faster thin-tailed decay, allowing for power-law scaling like our result and *Martin et al.* (2014) without this divergent mean paradox. One resolution to this issue could come from a spatially distributed model with multiple cells. Neighboring locations might bound excessive local elevation changes through granular relaxations from gradients above the angle of repose. In this interpretation, divergent mean power law resting time distributions may be relics of single cell models for bed elevation changes. We should always expect a maximum depth to which the bed can degrade relative to neighboring locations; this could temper the power law tail without required the reflecting boundaries used by *Voepel et al.* (2013).

Finally, we studied probability distribution functions and first and second moments of the particle activity and bed elevation, making novel conclusions about coordination between the statistical characteristics of these quantites which deserve experimental testing. In the last decade, particle tracking experiments have emerged (*Fathel et al.*, 2015; *Heyman et al.*, 2016; *Lajeunesse et al.*, 2010; *Liu et al.*, 2019; *Martin et al.*, 2014; *Roseberry et al.*, 2012), that allow joint resolution of bed elevations and bedload transport. A suitably designed experiment could test our prediction that bed elevations regulate particle activity statistics, as essentially represented in figures 3.4 and 3.5. However, we have left many other statistical characteristics of bedload transport for future studies. For example, the dependence of bedload transport (*Singh et al.*, 2009; **?**) and bed elevation statistics (*Aberle and Nikora*, 2006; *Singh et al.*, 2009, 2012) on the spatial and temporal scales over which they are observed is an emerging research topic. Statistical quantities can either be monoscaling or multiscaling across the observation scale (**?**), and we currently lack physical understanding and general conclusions about the scale dependence of particle activity and bed elevation signals. The model we have

presented shows statistical monoscaling for both quantites (e.g. **?**), whereas other experiments indicate statistical multiscaling (*Aberle and Nikora*, 2006; *Singh et al.*, 2009, 2012). We consider this topic to go beyond the scope of the present work, and we have focused on statistical characteristics at the highest temporal resolutions, with no averaging over the observation scale.

3.5 Conclusion

We developed a stochastic model for particle activity and local bed elevations including feedbacks between elevation changes and the erosion and deposition rates. This model includes collective entrainment, whereby moving particles tend to destabilize stationary ones. We analyzed this model using a mixture of numerical and analytical methods and provided two key results:

1. Resting times for sediment undergoing burial lie on a heavy-tailed power law distributions with tail parameter $\alpha \approx 1.2$;

2. Collective entrainment generates a statistical regulation effect, whereby bed elevation changes modify the mean and variance of the particle activity by as much as 90%: this effect vanishes when collective entrainment is absent.

These results imply measurements of bedload transport statistics could be severely biased at observation timescales smaller than adjustments of the bed elevation timeseries when collective entrainment occurs. Next steps are to generalize our model to a multi-cell framework and to study spatial correlations in bed elevation and particle activity statistics.

Chapter 4

Inclusion of sediment burial

Many environmental problems including channel morphology (*Hassan and Bradley*, 2017), contaminant transport (*Macklin et al.*, 2006), and aquatic habitat restoration (*Gaeuman et al.*, 2017) rely on our ability to predict the diffusion characteristics of coarse sediment tracers in river channels. Diffusion is quantified by the time dependence of the positional variance σ_x^2 of a group of tracers. With the scaling $\sigma_x^2 \propto t$, the diffusion is said to be normal, since this is found in the classic problems (*Philip*, 1968). However, with the scaling $\sigma_x^2 \propto t^\gamma$ with $\gamma \neq 1$, the diffusion is said to be anomalous (*Sokolov*, 2012), with $\gamma > 1$ defining super-diffusion and $\gamma < 1$ defining sub-diffusion (*Metzler and Klafter*, 2000). *Einstein* (1937) developed one of the earliest models of bedload diffusion to describe a series of flume experiments (**?**). Interpreting individual bedload trajectories as a sequence of random steps and rests, Einstein originally concluded that a group of bedload tracers undergoes normal diffusion.

More recently, Nikora et al. realized coarse sediment tracers can show either normal or anomalous diffusion depending on the length of time they have been tracked (*Nikora et al.*, 2001, 2002). From numerical simulations and experimental data, Nikora et al. discerned "at least three" scaling ranges $\sigma_x^2 \propto t^\gamma$ as the observation time increased. They associated the first range with "local" timescales less than the interval between subsequent collisions of moving grains with the bed, the second with "intermediate" timescales less

than the interval between successive resting periods of grains, and the third with "global" timescales composed of many intermediate timescales. Nikora et al. proposed super-diffusion in the local range, anomalous or normal diffusion in the intermediate range, and sub-diffusion in the global range. They attributed these ranges to "differences in the physical processes which govern the local, intermediate, and global trajectories" of grains (*Nikora et al.*, 2001), and they called for a physically based model to explain the diffusion characteristics (*Nikora et al.*, 2002).

Experiments support the Nikora et al. conclusion of multiple scaling ranges (*Fathel et al.*, 2016; *Martin et al.*, 2012), but they do not provide consensus on the expected number of ranges or their scaling properties. This lack of consensus probably stems from resolution issues. For example, experiments have tracked only moving grains, resolving the local range (*Fathel et al.*, 2016; *Furbish et al.*, 2012a, 2017); grains resting on the bed surface between movements, resolving the intermediate range (*Einstein*, 1937; *Nakagawa and Tsujimoto 9 Kyoto*, 1977; *Yano*, 1969); grains either moving or resting on the bed surface, likely resolving local and intermediate ranges (*Martin et al.*, 2012); or grains resting on the surface after floods, likely resolving the global range (*Bradley*, 2017; *Phillips et al.*, 2013). At long timescales, a significant fraction of tracers bury under the bed surface (*Ferguson et al.*, 2002; *Haschenburger*, 2013; *Hassan et al.*, 1991, 2013; *Papangelakis and Hassan*, 2016), meaning burial dominates long term diffusion characteristics (*Bradley*, 2017; *Martin et al.*, 2014; *Voepel et al.*, 2013), possibly at global or even longer "geomorphic" timescales (*Hassan and Bradley*, 2017) than Nikora et al. originally considered. As a result, three diffusion ranges can be identified by patching together multiple datasets (*Nikora et al.*, 2002; *Zhang et al.*, 2012), but they are not resolved by any one dataset.

Newtonian bedload trajectory models also show multiple diffusion ranges, although they also do not provide consensus on the expected number of ranges or their scaling properties. The majority of these models predict two ranges of diffusion (local and intermediate) without predicting a global range. Among these, *Nikora et al.* (2001) used synthetic turbulence (*Kraichnan*, 1970) with a discrete element method for the granular phase (**?**); *Bia-*

lik et al. (2012) used synthetic turbulence with a random collision model (*Sekine and Kikkawa*, 1992); and *Fowler* (2016) used a Langevin equation with probabilistic rests. To our knowledge, only *Bialik et al.* (2015) have claimed to capture all three ranges from a Newtonian approach. They incorporated a second resting mechanism into their earlier model (*Bialik et al.*, 2012), implicitly suggesting that three diffusion ranges could result from two distinct timescales of sediment rest. However, Newtonian approaches have not evaluated the effect of sediment burial on tracer diffusion, probably due to the long simulation timescales required.

Random walk bedload diffusion models constructed in the spirit of *Einstein* (1937) provide an alternative to the Newtonian approach and can include a second timescale of rest by incorporating sediment burial. Einstein originally modeled bedload trajectories as instantaneous steps interrupted by durations of rest lying on statistical distributions (*Hassan et al.*, 1991), but this generates only one range of normal diffusion (*Einstein*, 1937; *Hubbell and Sayre*, 1964; *Nakagawa and Tsujimoto 9 Kyoto*, 1977). Recently, researchers have generalized Einstein's model in a few different ways to describe multiple diffusion ranges. *Lisle et al.* (1998) and **?** promoted Einstein's instantaneous steps to motion intervals with random durations and a constant velocity, providing two diffusion ranges – local and intermediate. *Wu et al.* (2019a) retained Einstein's instantaneous steps but included the possibility that grains can become permanently buried as they rest on the bed, also providing two diffusion ranges – intermediate and global. These earlier works suggest the minimal required components to model three bedload diffusion ranges: (1) exchange between motion and rest intervals and (2) the sediment burial process.

In this study, we incorporate these two components into Einstein's original approach to describe three diffusion ranges with a physically based model, as called for by *Nikora et al.* (2002). Einstein was a giant in river geophysics and fostered an entire paradigm of research leveraging and generalizing his stochastic methods (*Gordon et al.*, 1972; *Hubbell and Sayre*, 1964; *Nakagawa and Tsujimoto 9 Kyoto*, 1977; *Paintal*, 1971; *Yang and Sayre*, 1971; *Yano*, 1969). Einstein's model can be viewed as a pioneering

application of the continuous time random walk (CTRW) developed by *Montroll* (1964) in condensed matter physics to describe the diffusion of charge carriers in solids. To incorporate motion intervals and sediment burial, we utilize the multi-state CTRW developed by *Weiss* (1976, 1994) that extends the CTRW of *Montroll* (1964). Below, we develop and solve the model in section 5.2. Then, we discuss the predictions of our model, present its implications for local, intermediate, and global ranges of bedload diffusion, and suggest next steps for bedload diffusion research in sections 5.4 and 5.5.

4.1 Bedload trajectories as a multi-state random walk

4.1.1 Model assumptions

We construct a three-state random walk where the states are motion, surface rest, and burial, and we label these states as $i = 2$ (motion), $i = 1$ (rest), and $i = 0$ (burial). Our target is the probability distribution $p(x, t)$ to find a grain at position x and time t if we know it started with the initial distribution $p(x, 0) = \delta(x)$. We characterize times spent moving or resting on the surface by exponential distributions $\psi_2(t) = k_2 e^{-k_2 t}$ and $\psi_1(t) = k_1 e^{-k_1 t}$, since numerous experiments show thin-tailed distributions for these quantities (*Ancey et al.*, 2006; *Einstein*, 1937; *Fathel et al.*, 2015; *Martin et al.*, 2012; *Roseberry et al.*, 2012). We expect our conclusions will not be contingent on the specific distributions chosen, since all thin-tailed distributions provide similar diffusion characteristics in random walks (*Weeks and Swinney*, 1998; *Weiss*, 1994). We consider grains in motion to have characteristic velocity v (*Lisle et al.*, 1998; **?**), and we model burial as long lasting enough to be effectively permanent (*Wu et al.*, 2019a), with grains resting on the surface having a probability per unit time κ to become buried, meaning $\Phi(t) = e^{-\kappa t}$ represents the probability that a grain is not buried after resting for a time t, while $1 - \Phi(t)$ represents the probability that it is buried. We specify the initial conditions with probabilities θ_1 and θ_2 to be in rest and motion at $t = 0$, and we require $\theta_1 + \theta_2 = 1$ for normalization.

4.1.2 Governing equations

Using these assumptions, we derive the governing equations for the set of probabilities $\omega_{ij}(x,t)$ that a transition occurs from state i to state j at position x and time t using the statistical physics approach to multi-state random walks (*Schmidt et al.*, 2007; *Weeks and Swinney*, 1998; *Weiss*, 1994). Denoting by $g_{ij}(x,t)$ the probability for a particle to displace by x in a time t within the state i before it transitions to the state j, the transition probabilities $\omega_{ij}(x,t)$ sum over all possible paths to the state i from previous locations and times:

$$\omega_{ij}(x,t) = \theta_i g_{ij}(x,t) + \sum_{k=0}^{2} \int_0^x dx' \int_0^t dt' \omega_{ki}(x',t') g_{ij}(x-x', t-t'). \quad (4.1)$$

Defining another set of probabilities $G_i(x,t)$ that a particle displaces by a distance x in a time t within the state i and possibly remains within the state, we perform a similar sums over paths for the probabilities to be in the state i at x, t:

$$p_i(x,t) = \theta_i G_i(x,t) + \sum_{k=0}^{2} \int_0^x dx' \int_0^t dt' \omega_{ki}(x',t') G_i(x-x', t-t'). \quad (4.2)$$

Finally, the overall probability to be at position x at time t is

$$p(x,t) = \sum_{k=0}^{2} p_k(x,t) \quad (4.3)$$

This joint density is completely determined from the solutions of equations (4.1-4.2). We only need to specify the distributions g_{ij} and G_i.

4.1.3 Joint probability distribution

We construct these distributions from the assumptions described in section 4.1.1. Since particles resting on the bed surface bury in a time t with probability $\Phi(t)$, and resting times are distributed as $\psi_1(t)$, we obtain $g_{12}(x,t) = \delta(x) k_1 e^{-k_1 t} e^{-\kappa t}$ and $g_{10}(x,t) = \delta(x) k_1 e^{-k_1 t}(1 - e^{-\kappa t})$. Since motions have

velocity v for times distributed as $\psi_2(t)$, we have $g_{21}(x,t) = \delta(x-vt)k_2 e^{-k_2 t}$. Since burial is quasi-permanent, all other $g_{ij} = 0$. The G_i are constructed in the same way except using the cumulative probabilities $\int_t^\infty dt' \psi_i(t) = e^{-k_i t}$, since these characterize motions and rests that are ongoing (*Weiss*, 1994). We obtain $G_1(x,t) = \delta(x)e^{-k_1 t}$ and $G_2(x,t) = \delta(x-vt)e^{-k_2 t}$.

To solve equations (4.1-4.2) with these g_{ij} and G_i, we take Laplace transforms in space and time ($x, t \to \eta, s$) using a method similar to *Weeks and Swinney* (1998) to unravel the convolution structure of these equations, eventually obtaining

$$\tilde{p}(\eta, s) = \frac{1}{s} \frac{(s+\kappa+k')s + \theta_1(s+\kappa)\eta v + \kappa k_2}{(s+\kappa+k_1)\eta v + (s+\kappa+k')s + \kappa k_2}, \tag{4.4}$$

where $k' = k_1 + k_2$. Inverting this result using known Laplace transforms (*Arfken*, 1985; *Prudnikov et al.*, 1988) obtains

$$\begin{aligned} p(x,t) = \theta_1 \Big[1 - \frac{k_1}{\kappa+k_1}\Big(1 - e^{-(\kappa+k_1)t}\Big)\Big]\delta(x) \\ + \frac{1}{v} e^{-\Omega\tau - \xi}\Big(\theta_1\Big[k_1 \mathcal{I}_0\big(2\sqrt{\xi\tau}\big) + k_2\sqrt{\frac{\tau}{\xi}}\mathcal{I}_1\big(2\sqrt{\xi\tau}\big)\Big] \\ + \theta_2\Big[k_1\delta(\tau) + k_2\mathcal{I}_0\big(2\sqrt{\xi\tau}\big) + k_1\sqrt{\frac{\xi}{\tau}}\mathcal{I}_1\big(2\sqrt{\xi\tau}\big)\Big]\Big) \\ + \frac{1}{v}\frac{\kappa k_2}{\kappa+k_1} e^{-\kappa\xi/(\kappa+k_1)}\Big[(\theta_1/\Omega)\mathcal{Q}_2(\xi/\Omega, \Omega\tau) + \theta_2 \mathcal{Q}_1(\xi/\Omega, \Omega\tau)\Big] \end{aligned} \tag{4.5}$$

for the joint distribution that a tracer is found at position x at time t. This result generalizes the earlier results of *Lisle et al.* (1998) and *Einstein* (1937) to include sediment burial. In this equation, we used the shorthand notations $\xi = k_2 x/v$, $\tau = k_1(t - x/v)$, and $\Omega = (\kappa + k_1)/k_1$ (*Lisle et al.*, 1998). The $\mathcal{I}_\nu$ are modified Bessel functions of the first kind and the $\mathcal{Q}_\mu$ are generalized Marcum Q-functions defined by $\mathcal{Q}_\mu(x,y) = \int_0^y e^{-z-x}(z/x)^{(\mu-1)/2}\mathcal{I}_{\mu-1}(2\sqrt{xz})dz$ and originally devised for radar detection theory (*Marcum*, 1960; *Temme and Zwillinger*, 1997). The Marcum Q-functions derive from the burial process. Since we assumed resting grains

could bury with an exponential probability while the resting probability follows a modified Bessel distribution (*Einstein*, 1937; *Lisle et al.*, 1998), burial develops the Q-function convolution structure.

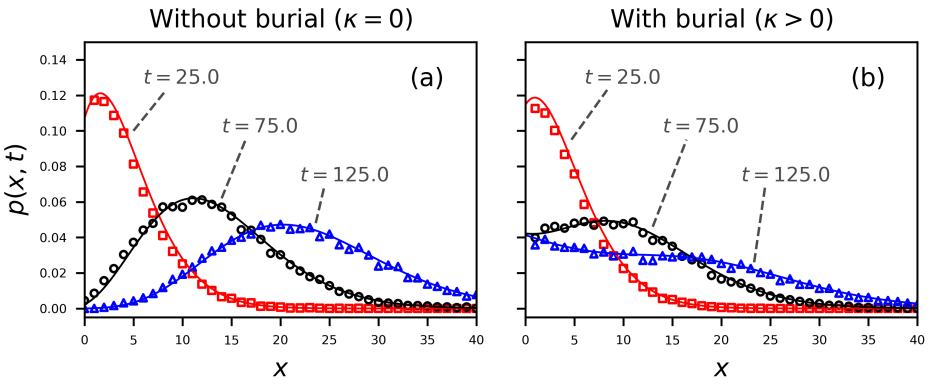

Figure 4.1: Joint distributions for a grain to be at position x at time t are displayed for the choice $k_1 = 0.1$, $k_2 = 1.0$, $v = 2.0$. Grains are considered initially at rest ($\theta_1 = 1$, $\theta_2 = 0$). The solid lines are the analytical distribution in equation (4.5), while the points are numerically simulated, showing the correctness of our derivations. Colors pertain to different times. Units are unspecified, since we aim to demonstrate the general characteristics of $p(x, t)$. Panel (a) shows the case $\kappa = 0$ – no burial. In this case, the joint distribution tends toward Gaussian at large times (*Einstein*, 1937; *Lisle et al.*, 1998). Panel (b) shows the case when grains have rate $\kappa = 0.01$ to become buried while resting. Because of burial, the joint distribution tends toward a more uniform distribution than Gaussian.

Figure 4.1 depicts the distribution (4.5) alongside simulations generated by a direct method based on evaluating the cumulative transition probabilities between states on a small timestep (*Barik et al.*, 2006). When grains do not become buried, as in panel (a) of figure 4.1, the distribution becomes Gaussian-like at relatively large observation times, exemplifying normal diffusion and satisfying the central limit theorem. When grains become buried, as in panel (b) of figure 4.1, the Q-function terms prevent the distribution from approaching a Gaussian at large timescales, exemplifying anomalous

diffusion (*Weeks and Swinney*, 1998) and violating the central limit theorem (*Metzler and Klafter*, 2000; *Schumer et al.*, 2009).

4.1.4 Positional variance

To obtain an analytical formula for tracers diffusing downstream while they gradually become buried, we derive the first two moments of position by taking derivatives with respect to η of the Laplace space distribution (4.4) using an approach similar to *Shlesinger* (1974) and *Weeks and Swinney* (1998), and we use these to calculate the positional variance $\sigma_x^2 = \langle x^2 \rangle - \langle x \rangle^2$. The first two moments are

$$\langle x(t) \rangle = A_1 e^{(b-a)t} + B_1 e^{-(a+b)t} + C_1, \tag{4.6}$$

$$\langle x^2(t) \rangle = A_2(t) e^{(b-a)t} + B_2(t) e^{-(a+b)t} + C_2, \tag{4.7}$$

so the variance is

$$\sigma_x^2(t) = A(t) e^{(b-a)t} + B(t) e^{-(a+b)t} + C(t). \tag{4.8}$$

In these equations, $a = (\kappa + k_1 + k_2)/2$ and $b = \sqrt{a^2 - \kappa k_2}$ are effective rates having dimensions of inverse time, while the A, B, and C factors are provided in table 4.1.

The positional variance (4.8) is plotted in figure 4.2 for conditions $\theta_1 = 1$ and $k_2 \gg k_1 \gg \kappa$. We interpret "$\gg$" to mean "of at least an order of magnitude greater". These conditions are most relevant to tracers in gravel-bed rivers, since they represent that grains are initially at rest (*Hassan et al.*, 1991; *Wu et al.*, 2019a), motions are typically much shorter than rests (*Einstein*, 1937; *Hubbell and Sayre*, 1964), and burial requires a much longer time than typical rests (*Ferguson and Hoey*, 2002; *Haschenburger*, 2013; *Hassan and Church*, 1994). Figure 4.2 demonstrates that under these conditions the variance (4.8) shows three diffusion ranges with approximate power law scaling ($\sigma_x^2 \propto t^\gamma$) that we identify as the local, intermediate, and global ranges proposed by Nikora et al., followed by a fourth range of no diffusion ($\sigma_x^2 = \text{const}$) stemming from the burial of all tracers. We suggest

Table 4.1: Abbreviations used in the expressions of the mean (4.6), second moment (4.7) and variance (4.8) of bedload tracers.

$$A_1 = \frac{v}{2b}\Big[\theta_2 + \frac{k_1 + \theta_2\kappa}{b-a}\Big]$$
$$B_1 = -\frac{v}{2b}\Big[\theta_2 - \frac{k_1 + \theta_2\kappa}{a+b}\Big]$$
$$C_1 = -\frac{v}{2b}\Big[\frac{k_1 + \theta_2\kappa}{b-a} + \frac{k_1 + \theta_2\kappa}{a+b}\Big]$$
$$A_2(t) = \frac{v^2}{2b^3}\Big[(bt-1)[k_1 + \theta_2(2\kappa + k_1 + b - a)] + \theta_2 b + \frac{(\kappa + k_1)(\theta_2\kappa + k_1)}{(b-a)^2}[(bt-1)(b-a) - b]\Big]$$
$$B_2(t) = \frac{v^2}{2b^3}\Big[(bt+1)[k_1 + \theta_2(2\kappa + k_1 - a - b)] + \theta_2 b - \frac{(\kappa + k_1)(\theta_2\kappa + k_1)}{(a+b)^2}[(bt+1)(a+b) + b]\Big]$$
$$C_2 = \frac{v^2}{2b^3}(\kappa + k_1)(\theta_2\kappa + k_1)\Big[\frac{2b-a}{(b-a)^2} + \frac{a+2b}{(a+b)^2}\Big]$$
$$A(t) = A_2(t) - 2A_1C_1 - A_1^2\exp[(b-a)t]$$
$$B(t) = B_2(t) - 2B_1C_1 - B_1^2\exp[-(a+b)t]$$
$$C(t) = C_2 - C_1^2 - 2A_1B_1\exp[-2at]$$

to call the fourth range geomorphic, since any further transport in this range can occur only if scour re-exposes buried grains to the flow (*Martin et al.*, 2014; *Voepel et al.*, 2013; *Wu et al.*, 2019b; **?**).

4.1.5 Diffusion exponents

Two limiting cases of equation (4.8) provide the scaling exponents γ of the diffusion $\sigma_x^2 \propto t^\gamma$ in each range. Limit (1) represents times so short a negligible amount of sediment burial has occurred, $t \ll 1/\kappa$, while limit (2) represents times so long motion intervals appear as instantaneous steps of mean length $l = v/k_2$, $1/k_2 \to 0$ while $v/k_2 =$ constant. Limit (1) provides local exponent $2 \leq \gamma \leq 3$ depending on the initial conditions θ_i, and intermediate exponent $\gamma = 1$. If grains start in motion or rest exclusively, meaning one $\theta_i = 0$, the local exponent is $\gamma = 3$, while if grains start in a mixture of motion and rest states, meaning neither θ_i is zero, the local exponent is $\gamma = 2$. Limit (2) provides global exponent $1 \leq \gamma \leq 3$ depending on the relative importance of κ and k_1. In the extreme $k_1/\kappa \ll 1$, we find $\gamma = 1$ in the global range, while in the opposite extreme $k_1/\kappa \to \infty$ we find

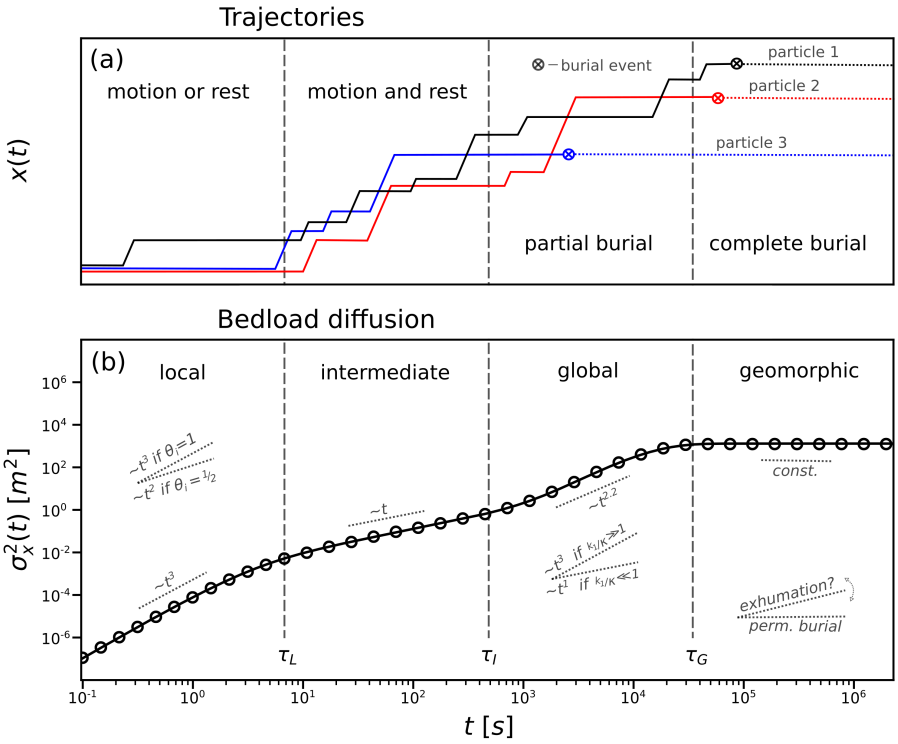

Figure 4.2: Panel (a) sketches conceptual trajectories of three grains, while panel (b) depicts the variance (4.8) with mean motion time 1.5 s, resting time 30.0 s, and movement velocity 0.1 m/s – values comparable to laboratory experiments transporting small (5 mm) gravels (*Lajeunesse et al.*, 2010; *Martin et al.*, 2012). The burial timescale is 7200.0s (two hours), and grains start from rest ($\theta_1 = 1$). The solid line is equation (4.8), and the points are numerically simulated. Panel (b) demonstrates four distinct scaling ranges of σ_x^2: local, intermediate, global, and geomorphic. The first three are diffusive. Three crossover times τ_L, τ_I, and τ_G divide the ranges. Within each range, a slope key demonstrates the scaling $\sigma_x^2 \propto t^\gamma$. Panel (a) demonstrates that different mixtures of motion, rest, and burial states generate the ranges. At local timescales, grains usually either rest or move; at intermediate timescales, they transition between rest and motion; at global timescales, they transition between rest, motion, and burial; and at geomorphic timescales, all grains bury. Additional slope keys in the local and global ranges of panel (b) illustrate the effect of initial conditions and rest/burial timescales on the diffusion, while the additional slope key within the geomorphic range demonstrates the expected scaling when burial is not permanent, as we discuss in section 5.4.

$\gamma = 3$. We summarize when $k_2 \gg k_1 \gg \kappa$ so all three diffusion ranges exist, equation (4.8) implies:

1. local range super-diffusion with $2 < \gamma < 3$ depending on whether grains start from purely motion or rest ($\gamma = 3$) or from a mixture of both states ($\gamma = 2$),

2. intermediate range normal diffusion $\gamma = 1$ independent of model parameters, and

3. global range super-diffusion $1 < \gamma < 3$ depending on whether burial happens relatively slowly ($\gamma \to 1$) or quickly ($\gamma \to 3$) compared to surface resting times.

Finally, the burial of all tracers generates a geomorphic range of no diffusion.

4.2 Discussion

4.2.1 Local and intermediate ranges with comparison to earlier work

We extended *Einstein* (1937) by including motion and burial processes in a multi-state random walk (*Weeks and Swinney*, 1998; *Weiss*, 1994) to demonstrate that a group of bedload tracers moving downstream while gradually becoming buried will generate a super-diffusive local range (*Fathel et al.*, 2016; *Martin et al.*, 2012; *Witz et al.*, 2019), a normal-diffusive intermediate range (*Nakagawa and Tsujimoto 9 Kyoto*, 1977; *Yano*, 1969), and a super-diffusive global range (*Bradley*, 2017; *Bradley et al.*, 2010), before the diffusion eventually terminates in a geomorphic range (*Hassan and Bradley*, 2017). *Nikora et al.* (2002) highlighted the need for such a physical description, although they suggested to use a two-state random walk between motion and rest states with heavy-tailed resting times, and they did not discuss sediment burial. However, other works have demonstrated that a two-state walk with heavy-tailed rests provides two diffusion ranges – not three (*Fowler*, 2016; *Weeks et al.*, 1996), and although heavy-tailed resting

times have been documented for surface particles (*Fraccarollo and Hassan*, 2019; *Liu et al.*, 2019), they are more often associated with buried particles (*Martin et al.*, 2012, 2014; *Olinde and Johnson*, 2015; *Shi and Wang*, 2014; *Voepel et al.*, 2013; **?**), while surface particles retain light-tailed resting times (*Ancey et al.*, 2006; *Einstein*, 1937; *Nakagawa and Tsujimoto 9 Kyoto*, 1977; *Yano*, 1969). Accordingly, we developed a random walk model of bedload trajectories with light-tailed surface resting times that incorporates sediment burial.

The local and intermediate range diffusion characteristics resulting from our model correspond closely to the original Nikora et al. concepts, while our global range has a different origin than Nikora et al. envisioned. *Nikora et al.* (2001) explained that local diffusion results from the non-fractal (smooth) characteristics of bedload trajectories between subsequent interactions with the bed, while intermediate diffusion results from the fractal (rough) characteristics of bedload trajectories after many interactions with the bed. Our model represents these conclusions: non-fractal (and super-diffusive) bedload trajectories exist on timescales short enough that each grain is either resting or moving, while fractal (and normal-diffusive) bedload trajectories exist on timescales when grains are actively switching between motion and rest states. We conclude that local and intermediate ranges stem from the interplay between motion and rest timescales, as demonstrated by earlier two-state random walk models (*Lajeunesse et al.*, 2018; *Lisle et al.*, 1998) and by all Newtonian models that develop sequences of motions and rests (*Bialik et al.*, 2012; *Nikora et al.*, 2001), even those including heavy-tailed rests (*Fowler*, 2016).

4.2.2 Global and geomorphic ranges with next steps for research

Nikora et al. explained that divergent resting times generate a sub-diffusive global range. However, studies have demonstrated that divergent resting times can generate super-diffusion in asymmetric random walks (*Weeks and Swinney*, 1998; *Weeks et al.*, 1996), and both experiments (*Bradley*, 2017; *Bradley et al.*, 2010) and models (*Shi and Wang*, 2014; *Wu et al.*, 2019a,b)

of bedload tracers undergoing burial have demonstrated global range super-diffusion. While our results also show global range super-diffusion, they do not necessarily refute the Nikora et al. conclusion of sub-diffusion at long timescales. We assumed sediment burial was a permanent condition which developed a non-diffusive geomorphic range. In actuality, burial is a temporary condition, because bed scour can exhume buried sediment back into transport (*Wu et al.*, 2019b), probably after heavy-tailed intervals (*Martin et al.*, 2014; *Voepel et al.*, 2013; **?**). We anticipate that a generalization of our model to include heavy-tailed timescales between burial and exhumation would develop four ranges of diffusion, where the long-time decay of the exhumation time distribution would dictate the geomorphic range diffusion characteristics as depicted in figure 4.2. If cumulative exhumation times decay faster than $T^{-1/2}$, as suggested by equilibrium transport models (*Martin et al.*, 2014; *Voepel et al.*, 2013; **?**) and laboratory experiments (*Martin et al.*, 2012, 2014), we expect a super-diffusive geomorphic range (*Weeks and Swinney*, 1998). However, if they decay slower than $T^{-1/2}$, as implicitly suggested by the data of *Olinde and Johnson* (2015), we expect a genuinely sub-diffusive geomorphic range (*Weeks and Swinney*, 1998), leaving Nikora et al. with the final word on long-time sub-diffusion.

The analytical solution of bedload diffusion in equation (4.8) reduces exactly to the analytical solutions of the *Lisle et al.* (1998) and *Lajeunesse et al.* (2018) models in the limit without burial ($\kappa \to 0$), the *Wu et al.* (2019a) model in the limit of instantaneous steps ($k_2 \to \infty$ and $l = v/k_2$), and the original *Einstein* (1937) model in the limit of instantaneous steps without burial. These reductions demonstrate that the majority of recent bedload diffusion models, whether developed from Exner-type equations (*Pelosi and Parker*, 2014; *Shi and Wang*, 2014; *Wu et al.*, 2019a) or advection-diffusion equations (*Lajeunesse et al.*, 2018; *Lisle et al.*, 1998), can be viewed equivalently as continuous-time random walks applied to individual bedload trajectories. Within random walk theory, sophisticated descriptions of transport with variable velocities (*Masoliver and Weiss*, 1994; *Zaburdaev et al.*, 2008), correlated motions (*Escaff et al.*, 2018; *Vicsek and Zafeiris*, 2012), and anomalous diffusion (*Fa*, 2014; *Masoliver*, 2016; *Metzler et al.*, 2014)

have been developed. Meanwhile, in bedload transport research, variable velocities (*Furbish et al.*, 2012a; *Heyman et al.*, 2016; *Lajeunesse et al.*, 2010), correlated motions (*Heyman et al.*, 2014; *Lee and Jerolmack*, 2018; *Saletti and Hassan*, 2020), and anomalous diffusion (*Bradley*, 2017; *Fathel et al.*, 2016; *Schumer et al.*, 2009) constitute open research issues. We believe further developing the linkage between existing bedload models and random walk concepts could rapidly progress our understanding.

4.3 Conclusion

We developed a random walk model to describe sediment tracers transporting through a river channel as they gradually become buried, providing a physical description of the local, intermediate, and global diffusion ranges identified by *Nikora et al.* (2002). Pushing their ideas somewhat further, we proposed a geomorphic range to describe diffusion characteristics at timescales larger than the global range when burial and exhumation both moderate downstream transport. At base level, our model demonstrates that (1) durations of sediment motions, (2) durations of sediment rest, and (3) the sediment burial process are sufficient to develop three diffusion ranges that terminate when all tracers become buried. A next step is to incorporate exhumation to better understand the geomorphic range. Ultimately, we emphasize that the multi-state random walk formalism used in this paper implicitly underlies most existing bedload diffusion models and provides a powerful tool for researchers targeting landscape-scale understanding from statistical concepts of the underlying grain-scale dynamics.

Chapter 5

Collisional model of sediment velocity distributions

5.1 Introduction

Bulk bed load transport rates show wide and frequent fluctuations which originate from coupling between the fluid and granular phases. Due to these fluctuations, measured transport rates often show extremely slow convergence through time, and predicted rates often deviate from measured values by several orders of magnitude. These challenges limit numerous ecological and engineering applications that rely on sediment transport predictions. In recent decades, stochastic formulations of the bed load flux have become increasingly popular for their potential to predict the mean transport rates required by applications while also predicting fluctuations, quantifying the dependence of measurements on the observation scale, and linking bulk transport characteristics to the "microscopic" dynamics of individual grains. Recent indications that sediment transport fluctuations might explain long-standing and unsolved problems in alluvial channel stability, such as channel width maintenance (**??**) and bedform initiation (*Ancey and Heyman*, 2014; *Bohorquez and Ancey*, 2016) provide additional motivation for these stochastic formulations. Many stochastic approaches express downstream transport rates as a sum over the instantaneous streamwise velocities of all particles

in motion within a control volume. In these approaches, the instantaneous velocity distribution of sediment particles therefore becomes an object of crucial importance. Unfortunately, current understanding of this distribution remains limited, and no mechanistic models have yet been presented that describe the full range of experimental observations. Here, we take some steps toward rectifying these shortcomings.

High-speed video experiments have measured different streamwise particle velocity distributions without providing much understanding as to why one distribution or another appears. One set of studies has shown exponential particle velocity distributions (*Charru et al.*, 2004; *Fathel et al.*, 2016, 2015; *Lajeunesse et al.*, 2010; *Roseberry et al.*, 2012; *Seizilles et al.*, 2014). These experiments involve uniformly-sized small sands or glass beads ($0.05 - 2$mm) having typical Stokes numbers $St \sim 1 - 10$. Their flow conditions are generally sub-critical ($Fr < 1$) and turbulent ($Re > 5000$) but not always: flows in *Lajeunesse et al.* (2010) were super-critical ($Fr > 1$), and flows in *Charru et al.* (2004) and **?** were viscous. A second set of studies have shown Gaussian particle velocity distributions (*Ancey and Heyman*, 2014; *Heyman et al.*, 2016; *Martin et al.*, 2012). In these experiments, particles are typically larger ($2 - 8$mm) uniformly-sized gravels or glass beads having higher Stokes numbers ($St \sim 10 - 500$). In all Gaussian cases, flows are turbulent ($Re > 5000$) and super-critical ($Fr > 1$). Two other experiments display velocity distributions that are intermediate between exponential and Gaussian and appear more like a Gamma distribution (*Houssais and Lajeunesse*, 2012; *Liu et al.*, 2019). The *Houssais and Lajeunesse* (2012) experiments involved a binomal distribution of glass beads with diameters 0.7mm and 2.2mm in turbulent and supercritical flow conditions. They resolved the velocity distributions for larger grains only. The *Liu et al.* (2019) experiments used uniformly-graded sand having median diameter 1.1mm. Flows were again turbulent and subcritical. From this experimental record, we can summarize that the shape of the velocity distribution does not consistentely relate to whether a flow is super or sub-critical (Fr), whether sediment grains are natural (sand, gravel) or synthetic (beads), or whether the flow is laminar or turbulent (Re). However, the typical Stokes numbers

of particles do seem to increase monotonically from exponential velocity experiments (where $St \sim 1$), to intermediate (Gamma-like) experiments (where $St \sim 10$), and eventually to Gaussian experiments (where $St \sim 10^2$.) Apparently, the shape of streamwise bed load velocity distributions depends on the particle size.

Existing models of streamwise bed load velocities can be divided into computational and statistical physics categories. Computational models numerically integrate some approximate coupled dynamics for individual grains and the fluid, generally modelling particles as spheres interacting through repulsive forces, and the flow using direct simulation of the Navier-Stokes equations or some related approximation (such as large eddy simulation or the St-Venant equations). When streamwise particle velocities have been analyzed in such simulations, they show exponential tails (*Furbish and Schmeeckle*, 2013; *González et al.*, 2017) that agree with only a subset of the experimental data. Statistical physics models have incorporated stochastic driving and resisting terms into the Newtonian dynamics of individual grains to develop a Langevin-like description of bed load particle motions. For the downstream velocity $u(t)$, *Fan et al.* (2014) wrote $\dot{u} = F - \gamma \mathrm{sgn} u + \xi(t)$ where F represents the steady component of the fluid forcing, the term involving γ is a quasi-static (Coulomb-type) friction term representing momentum dissipation by particle-bed collisions, and $\xi(t)$ is a Gaussian white noise representing variability in these forces. This model provides exponential velocity distributions which agree with one subset of experiments. *Ancey and Heyman* (2014) took a similar approach that includes different forces, solving $\dot{u} = \gamma(\overline{u} - u) + \xi(t)$. Here the term involving γ is similar to a Stokes drag, except it involves the mean sediment velocity $\overline{u}$, not the fluid velocity as for a "real" Stokes drag. $\xi(t)$ is again a Gaussian white noise representing fluctuations, and the model provides Gaussian velocity distributions that agree with another subset of experiments. While these models build insight into grain-scale sediment transport mechanics and provide powerful techniques with which to approach the problem, they have not yet provided a comprehensive explanation for the range of streamwise velocity distributions resolved in experiments.

Here, motivated by the realization that experimental particle velocity distributions vary systematically with the grain size, as summarized above, we hypothesize that the shape of the streamwise velocity distribution is controlled by the momentum dissipation characteristics of particle-bed collisions. It is well-known that the elasticity of granular collisions within viscous fluids depends on the particle size. In addition, the velocity distributions of granular gases are known to develop increasingly heavier tails than the Gaussian (Boltzmann) form of elastic gases as the inelastiscity of particle-particle collisions is increased. Taking inspiration from this established knowledge, we develop below a model for sediment grains in transport as they undergo inelastic particle-bed collisions. Our intentions are to test the hypothesis that particle-bed collision characteristics explain the range of experimentally-observed streamwise bed load particle velocity distributions, and to introduce more realistic forces into earlier statistical physics descriptions of individual bed load particle dynamics. We develop the model and explain our assumptions in section 5.2, then we present the analytical solution and major results in 5.3. We finally discuss the implications of these results, summarize our findings, and suggest ideas for further research in sections 5.4 and 5.5.

5.2 Model

Figure **??** indicates the configuration we have in mind. Nearly spherical and cohesionless particles of diameter d and mass m moving as bed load down a slope inclined at an angle θ in a steady turbulent shear flow. The flow is just strong enough to drive grains into rarefied transport of a kind typical in gravel-bed rivers: particles saltate along the bed in sequences of collisions between events of erosion and deposition; moving particles collide often with stationary particles, but rarely with other moving particles. Particles respond to turbulent drag forces $F_D(t)$ and episodic particle-bed collision forces. In contrast to the computational physics approach, we do not aim to characterize the exact timeseries of the forces on an individual particle. Instead, we model the ensemble of possible force timeseries

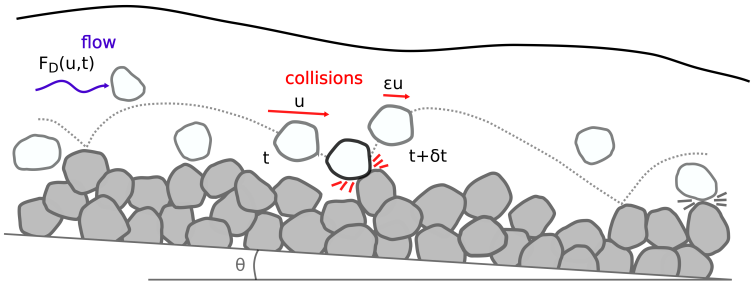

Figure 5.1: Definition sketch of rarefied sediment transport with turbulent fluid drag and particle-bed collision forces. During saltation, pre-collisional streamwise velocities u are transformed to postcollisional velocities $\varepsilon u < u$.

that particles could conceivably experience. Each possibility implies a different velocity timeseries $u(t)$ in the downstream direction. Our objective is to calculate the probability distribution $P(u)$ of this downstream velocity by averaging over the ensemble of forces. We include the most realistic article-bed collision and fluid forces we can while still allowing for analytical solutions.

Collision forces dissipate streamwise momentum, partly by converting it to vertical, lateral, or rotational momentum, and partly by deforming particles and generating heat (**?**). The microscopic details of particle-particle collisions have been thoroughly studied (*Brach*, 1989; *Lorenz et al.*, 1997; *Montaine et al.*, 2011). Here, we introduce a restitution-like coefficient ε as indicated in figure **??**. This ranges from $\varepsilon = 0$ for completely inelastic collisions to $\varepsilon = 1$ for completely elastic collisions. If the streamwise velocity just prior to a collision is u, just after the collision it becomes εu. Since this quantity combines effects of particle shape and collision geometry and should vary from one collision to the next, we consider that the fraction of streamwise momentum dissipated per collision ε lies on a statistical distribution $\rho(\varepsilon)$. Similar ideas are available in the granular physics literature

(**?**). Further assuming that the number of collisions per unit time is ν and that the time intervals between subsequent particle-bed collisions are exponentially distributed (*Gordon et al.*, 1972), we write the collision force in the downstream direction as

$$F_C(u,t) = -mu \sum_{k=1}^{N_\nu(t)} (1-\varepsilon_k)\delta(t-\tau_k). \tag{5.1}$$

Here, $N_\nu(t)$ is the number of collisions in time t, the τ_k ($k = 1, 2, \dots$) are times at which collisions occur, and the ε_k are elasticity coefficients characterizing the amount by which each collision slows the particle down. This collision force is a sequence of random impulses which are proportional to the pre-collisional streamwise momentum. This collision model should be adequate when the contact times between moving and resting particles are small compared to the times between collisions. These conditions are always satisfied for the idealized saltation-type motion depicted in figure **??**.

Fluid forces on a coarse particle in a viscous flow depend on the Reynolds number $\mathrm{Re}_p = dV/\nu$ defined by the particle size d, slip velocity V between particle and fluid, and kinematic viscosity ν. These forces have been calculated analytically from the Navier-Stokes equations for vanishing Re_p and include acceleration, history, and velocity-dependent drag terms (*Hjelmfelt and Mockros*, 1966; *Maxey and Riley*, 1983; **?**). At realistic Re_p analytical results are limited, so it is standard practice to turn instead to empirical corrections on the small Re_p formulas (*Schmeeckle et al.*, 2007; **?**). A dominant contribution to the downstream drag force F_D on nearly spherical particles at large Re_p can be written $F_D = \frac{\pi}{8}\rho_f d^2 C_D(\mathrm{Re}_p)|V|V$, where ρ_f is the fluid density, d is the particle diameter, $C_D(\mathrm{Re}_p)$ is an empirical drag coefficient, and $V = U - u$ is the slip velocity between the fluid (U) and particle (u) velocities (*Coleman*, 1967; *Dwivedi et al.*, 2012; *Schmeeckle et al.*, 2007). In the present model we set $C_D = \frac{24}{\mathrm{Re}_p}(1 + 0.194\mathrm{Re}_p^{0.631})$ (*Clift et al.*, 1978; *González et al.*, 2017) and we do not involve acceleration and history terms for simplicity, although we acknowledge their potential importance for coarse sediment transport (*Armenio and Fiorotto*, 2001; **?**; **?**).

Drag forces have been argued to fluctuate rapidly compared to the inertial response times of coarse sediment grains (*Fan et al.*, 2014). The magnitude of drag fluctuations has been observed to follow a Gaussian distribution (*Celik et al.*, 2014; *Dwivedi et al.*, 2010; *Hofland and Battjes*, 2006; *Schmeeckle et al.*, 2007). Using these ideas, we make two key simplifications of the drag force above. First, we split the drag F_D into quasi-steady and fluctuating components (*Michaelides*, 1997), and second, we represent drag fluctuations as a Gaussian white noise characterized by a particle diffusivity D (*Ancey and Heyman*, 2014; *Fan et al.*, 2014). Defining $\bar{V}$ as a representative slip velocity which we specify more carefully later, $\bar{C}_D$ as the empirical drag coefficient evaluated at this slip velocity, and $\xi(t)$ as a Gaussian white noise of mean 0 and variance 1 (*Gardiner*, 1983), we express the fluid forces as

$$F_D(t) = \frac{\pi}{8}\rho_f d^2 \bar{C}_D \bar{V}^2 + \sqrt{2D}\eta(t). \tag{5.2}$$

In this drag force **??** and the collision force 5.1, the turbulent fluctuations $\xi(t)$, collision times τ_k, and dissipation coefficients ε_k, can take any values consistent with their distribution and correlation functions. This set of possiblities defines a statistical ensemble.

5.2.1 Langevin equation

With the above forces, we express the Langevin equation $m\dot{u}(t) = F_D(t) + F_C(t)$ for the sediment dynamics as

$$m\dot{u}(t) = \Gamma + \sqrt{2D}\eta(t) - mu(t)\xi_{\nu,\varepsilon}(t). \tag{5.3}$$

This equation replaces the steady friction terms of earlier stocahstic bed load models with an episodic term which provides a more realistic representation of particle-bed collisions during saltation. It represents a jump-diffusion process (*Daly and Porporato*, 2006) with multiplicative Poisson noise (*Denisov et al.*, 2009; *Dubkov et al.*, 2016). Collisions introduce "jumps" in velocity while turbulent generates "diffusion". The collision term is "multiplicative" in the sense that u multiplies the Poisson noise. Equations like 5.3 have

long been studied in the stochastic physics literature (*Hanggi*, 1978; **?**), but solving such equations remains extremely challenging (*Daly and Porporato*, 2010; *Dubkov and Kharcheva*, 2019; *Luczka et al.*, 1995; *Mau et al.*, 2014). One issue is that multiplicative white noises imply the prescription dilemma of stochastic calculus (*Gardiner*, 1983; **?**), meaning 5.3 is not defined without further specifying an integration rule (**?**). Here, the Ito interpretation (lower endpoint integration rule) is the physical choice since the energy dissipated by collisions depends strictly on pre-collisional velocities, not post-collisional. Given this integration rule, the remaining issues are to obtain the integro-differential equation characterizing the ensemble of velocities defined by 5.3, and then to solve this equation for the velocity distribution $P(u)$.

5.2.2 Chapman-Komogorov equation and particle-bed collision integral

We derive the equation governing the streamwise velocity distribution $P(u,t)$ from a simple limiting argument in appendix **??**, finding

$$\nu^{-1}\partial_t P(u,t) = -\tilde{\Gamma}\partial_u P(u,t) + \tilde{D}\partial_u^2 P(u,t) + \mathcal{I}_c(u,t). \tag{5.4}$$

In this equation, we introduced the scaled parameters $\tilde{\Gamma} = \Gamma/(\nu m)$ and $\tilde{D} = D/(\nu m)$. The term

$$\mathcal{I}_c(u,t) = -P(u,t) + \int_0^1 \frac{d\varepsilon}{\varepsilon} P\big(\frac{u}{\varepsilon},t\big)\rho(\varepsilon) \tag{5.5}$$

is a "collision integral" term representing particle-bed collisions. Equation 5.4 is a nonlocal extension of the Fokker-Planck equation used in earlier bed load models (*Ancey and Heyman*, 2014; *Fan et al.*, 2014). Such equations combining are known as Chapman-Komogorov equations (*Gardiner*, 1983). Nonlocality is introduced by the collision integral 5.5 which transfers probability from higher pre-collisional velocities u/ε to lower post-collisional velocities u. This term is analogous to the collision integral of the Boltzmann equation in kinetic theory and granular gases (**??**). Physically, it corresponds to binary collisions between particles having different masses

and random resitution coefficients **?** in the limit that the mass of one particle (here, the particle resting on the bed) goes to infinity. Mathematically, it represents the probability distribution of the product between ε and u (c.f. *Feller*, 1967).

Owing to its nonlocality, equation 5.4 does not admit analytical solutions as is, so we make one further approximation. We assume the distribution of dissipation coefficients $\rho(\varepsilon)$ is sharply peaked at some most common (mode) value ε'. This allows for a Kramers-Moyal type expansion of the particle-bed collision integral (*Gardiner*, 1983). Expanding all terms in the integrand except $\rho(\varepsilon)$ provides

$$\mathcal{I}_c(u,t) = -P(u,t) + \frac{1}{\varepsilon'}P\big(\frac{u}{\varepsilon'},t\big) + \sum_{k=1}^{\infty}\frac{\alpha_k}{k!}(\varepsilon-\varepsilon')^k\Big[\frac{1}{\varepsilon}P\big(\frac{u}{\varepsilon}\big)\Big]^{(k)}\Big|_{\varepsilon=\varepsilon'}, \quad (5.6)$$

where the $\alpha_k = \int_0^1 d\varepsilon\rho(\varepsilon)(\varepsilon-\varepsilon')^k$ are the central moments of ε around the mode elasticity ε' and the superscript (k) denotes the kth derivative. In what follows, we drop all but the first two terms to obtain the leading order contribution of particle-bed collisions to the velocity distribution. Higher orders could always be included later by perturbation theory. We solve the resulting approximate equation in steady-state, when $\partial P(u,t)/\partial t = 0$. Scaling the time in Equation 5.4, we can see this solution will be a good approximation to the time-dependent problem when particle motions generally survive multiple collisions.

5.3 Results

5.3.1 Derivation of the velocity distribution

Hereafter we drop the prime on the most common streamwise restitution coefficient ε'. With the truncation to two terms, equation 5.4 gives

$$0 = -\tilde{\Gamma}\partial_u P(u) + \tilde{D}\partial_u^2 P(u) - P(u) + \frac{1}{\varepsilon}P\big(\frac{u}{\varepsilon}\big), \quad (5.7)$$

which is now a non-local ordinary differential equation. Such equations have seen some attention in the mathematics literature, where they are called pantograph equations (**???**) for their relationship to a current collection device used on electric trains (*Ockendon and Tayler*, 1971). In the appendix we solve equation 5.7 using Laplace transforms, providing

$$P(u) = \frac{\theta(-u)}{K_+} \sum_{l=0}^{\infty} \frac{\varepsilon^{-l} e^{\lambda_+ \varepsilon^{-l} u}}{\prod_{m=1}^{l} (-\tilde{D}\lambda_+^2 \varepsilon^{-2m} + \tilde{\Gamma}\lambda_+ \varepsilon^{-m} + 1)} + \frac{\theta(u)}{K_-} \sum_{l=0}^{\infty} \frac{\varepsilon^{-l} e^{\lambda_- \varepsilon^{-l} u}}{\prod_{m=1}^{l} (-d\lambda_-^2 \varepsilon^{-2m} + \gamma\lambda_- \varepsilon^{-m} + 1)}. \quad (5.8)$$

The factors $\lambda_\pm$ are defined in the appendix; they are proportional to $\tilde{\Gamma}/\tilde{D}$. The normalization factors are $K_\pm$ are

$$K_\pm = d(\lambda_+ - \lambda_-) \prod_{l=1}^{\infty} (-d\lambda_\pm^2 \varepsilon^{2l} + \gamma\lambda_\pm \varepsilon^l + 1). \quad (5.9)$$

Although this velocity distribution appears quite complicated, one can verify that this is a normalized probability distribution which has very simple limiting behaviors as the most common dissipation coefficient ε approaches fully elastic ($\varepsilon = 1$) and inelastic ($\varepsilon = 0$) values.

It is rather simple to derive the moments of this probability distribution by multiplying 5.7 by u, integrating, and then solving the resulting moment evolution equations (c.f. **?**). The first moment is

$$\langle u \rangle = \frac{\Gamma}{\nu(1-\varepsilon)} = \frac{\gamma}{1-\varepsilon}, \quad (5.10)$$

which is scales weakly with the mean fluid drag and sharply with the rate and typical elasticity of collisions. The second moment is

$$\langle u^2 \rangle = 2\frac{d + \gamma\langle u \rangle}{1-\varepsilon^2}, \quad (5.11)$$

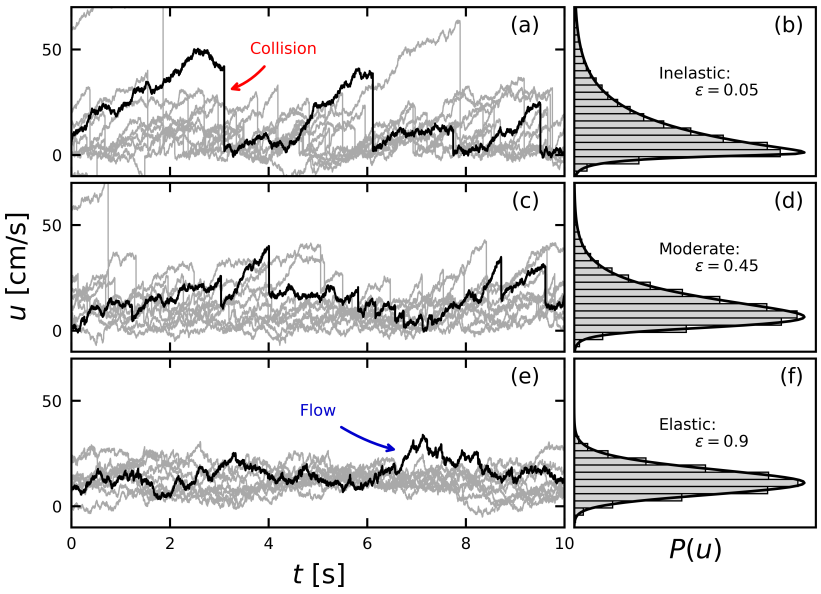

Figure 5.2: Left panels show velocity realizations as gray traces. Velocities are calculated from Monte Carlo simulations. Individual realizations are singled out as black traces. Particle-bed collisions imply sudden downward-velocity jumps. Flow forces generate fluctuating positive accelerations between collisions. Right panels show simulated histograms of particle velocities and exact solutions from equation 5.8.

leading to the velocity variance ($\sigma_u^2 = \langle u^2 \rangle - \langle u \rangle^2$)

$$\sigma_u = \sqrt{\frac{2d + \gamma^2}{1 - \varepsilon^2}}. \tag{5.12}$$

This equation demonstrates that velocity fluctuations originate from both the steady and fluctuating components of the flow forces, yet the variance is linear in these factors and is therefore relatively insensitive to them. In contrast, velocity fluctuations depend sharply on the parameters representing particle-bed collisions.

Figure 5.2 depicts velocity characteristics for different realizations of the fluid and collisional forces. We can see an apparent transition from

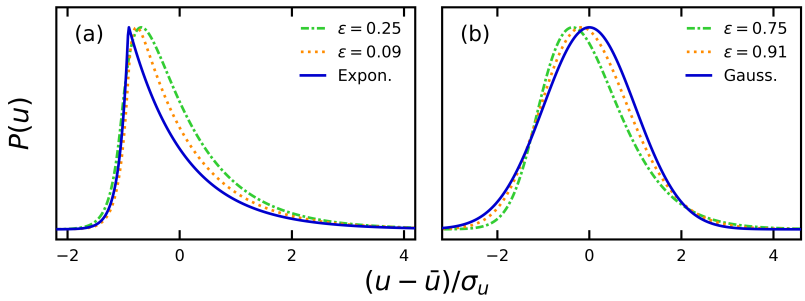

Figure 5.3: The particle velocity distribution approaches an exponential distribution in (a) as particle-bed collisions become extremely elastic ($\varepsilon \to 1$), and it approaches a Gaussian in (b) as they become extremely inelastic ($\varepsilon \to 0$). On the abscissa, the mean sediment velocity is standardized by its mean $\bar{u}$ and standard deviation σ_u.

exponential-like to Gaussian-like velocity distributions as typical collisions vary from more inelastic ($\varepsilon \to 0$) to more elastic ($\varepsilon \to 1$). In between, the full distribution 5.8 resembles a Gamma distribution, although it is not a Gamma distribution.

5.3.2 Exponential and Gaussian regimes

In fact, the apparent transition in figure 5.2 can be made rigorous: despite its complex appearance, simple Gaussian and exponential distributions appear as rigorous mathematical limits of equation 5.8. When particle-bed collisions are completely inelastic, 5.8 becomes an exponential distribution, and when they are completely elastic, 5.8 becomes Gaussian. Figure 5.3 demonstrates more closely the approach of the distribution toward these limits.

The exponential limit of 5.8 as $\varepsilon \to 0$ is rather easy to see. Taking $\varepsilon \to 0$ in 5.8, all terms in the series except for that with $l = 0$ become exponentially small, leaving behind the same two-sided exponential distribution derived by *Fan et al.* (2014) up to notational differences:

$$P(u) = \frac{d}{\sqrt{\gamma^2 + 4d}} e^{\frac{\gamma u}{2d} - \frac{\sqrt{\gamma^2+4d}|u|}{2d}}. \tag{5.13}$$

a/d	$M=4$	$M=8$	Callan
0.1	1.56905	1.56	1.56904
0.3	1.50484	1.504	1.50484
0.55	1.39128	1.391	1.39131
0.7	1.32281	10.322	1.32288
0.913	1.34479	100.351	1.35185

Table 5.1: Values of kd at which trapped modes occur when $\rho(\theta) = a$.

Thus, for bed load transport conditions with typically very inelastic particle-bed collisions, we can expect exponential-like velocities and large deviations from a Gaussian behavior.

The Gaussian limit as $\varepsilon \to 1$ of 5.8 is more difficult to evaluate. The challenge is that the statistical moments 4.6 and **??** diverge at the same time as the denominator factors of the distribution 5.8. In appendix **??** we return instead to the original equation 5.7 to evaluate this elastic limit, obtaining

$$P(u) = \frac{1}{\sqrt{2\pi\sigma_u^2}} e^{-\frac{(u-\bar{u})^2}{2\sigma_u^2}}. \tag{5.14}$$

This result is identical to the velocity distribution derived by *Ancey and Heyman* (2014), up to notation.

5.3.3 Comparison with experimental data

Now we compare the analytical distribution 5.8 with the available experimental data. Upfront, we point out that the distribution above has free parameters and this is only a proof of concept that the velocity distribution is capable of fitting the available experimental data; it is not a proof that this is the underlying mechanism for these data blahblahblah that was a good writing day.

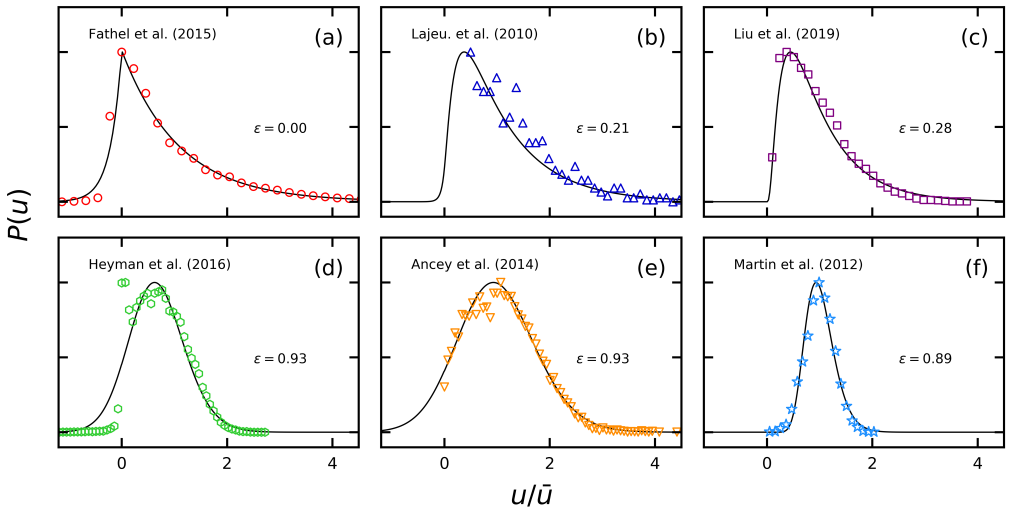

Figure 5.4: The features of the four possible modes corresponding to
(a) periodic
and (b) half-periodic solutions.

5.4 Discussion

We developed a Langevin description of bed load sediment transport which includes episodic collisions between particles and the bed. The model relates the shape of the instantaneous streamwise particle velocity distribution to the elasticity of particle-bed collisions, generalizes earlier approaches available in the literature which did not treat episodic collisions (*Ancey and Heyman*, 2014; *Fan et al.*, 2014), and provides a new physical explanation for the different streamwise sediment velocity distributions resolved in experiments. Although in reality, the turbulent forces on moving sediment particles vary in a complex spatio-temporal way, we have approximated the fluid forces on bed load particles as spatially uniform Gaussian white noise. Even though the non-Gaussian aspects of fluid turbulence certainly do impact sediment entrainment (*Celik et al.*, 2014; **?**), this flow model appears more or less justified since sediment transport experiments provide similar velocity distributions regardless of whether the flow is viscous or turbulent (*Charru et al.*, 2004; *Lajeunesse et al.*, 2010), and since particle relaxation

times are relatively long compared to the timescales of turbulent fluctuations (). We modelled particle-bed collision forces as a sequence of instantaneous impulses where the intervals between successive collisions were characterized as exponential random variables. The effect of each collision on the streamwise particle velocities was parameterized by a restitution-like coefficient. Although such approximate descriptions of particle-particle collisions are common in the theory of granular gases, the setting here is somewhat different than grains in air. Because particles within a viscous flow interact at a distance, we should expect the collision model will become poor when the time between subsequent collisions becomes small. Therefore, although the model seems appropriate for saltation, it could become questionable for the "reptation" transport mode when the times between subsequent particle-bed collisions are short. Of course, more realistic flow and collision forces could always be incorporated into Langevin equations for bed load transport. Unfortunately, numerical methods would likely be required to interpret the resulting equations, in contrast to the analytical approaches applied here.

Sediment transport experiments reveal correlations between particle size and the shape of the bed load velocity distribution. Experiments with smaller particles tend to give exponential distributions, and those with larger particles give Gaussian distributions. In fluid dynamics, the dissipation characteristics of particle-particle collisions in viscous flows are known to depend on the particle size and approach velocity through the Stokes number. In kinetic theory, it is known that gases of ideal elastic particles generate Gaussian (Boltzmann) velocity distributions, while gases of inelastic particles generate non-Gaussian distributions. Taken together, these ideas suggest that we might relate the shape of the particle velocity distribution to particle size. We can estimate typical Stokes numbers of colliding bed load particles in experiments as ..., using with the flow shear velocity and mean streamwise sediment velocity to calculate V. Estimating in this way, transport experiments with exponential velocities have $St \sim 1 - 10$, those with neither exponential nor Gaussian velocities have $St \sim 10 - 100$, and those with Gaussian velocities have $St > 100$. In experiments relating restitution coefficient to Stokes number for idealized collisions, restitution coefficients

vary sharply from 0 to 1 as St ranges from 1 to 500 *Joseph et al.* (2001); *Yang and Hunt* (2006); **?**. Although collision geometry and grain shape certainly complicate the narrative, these values of St are consistent with our model conclusion that the shape of the particle velocity depends on the elasticity of collisions.

In real channels, grain sizes often span a wide range. A major implication of the dependence of the shape of the particle velocity distribution on grain size is that different grain sizes in a mixture will impart distinct fluctuation signatures to the overall bulk transport rate. Even in the absence of sorting effects and differential mobility, smaller grains can be expected to carry more control over the largest fluctuations in the overall transport rate, since their velocity distributions have wider tails.

For example, in a mixture of small and large grains, neglecting any sorting effects whereby the mobility of small grains is contingent on the mobility of the large grains, small grains will have exponential velocities with relatively wide fluctuations, while large grains will have Gaussian velocities with relatively narrow fluctuations. Considering the over-all flux then as the number of moving particles times their velocities, transport fluctuations

aeolean transport extension maybe particle size distributions - interesting implications connection to computational physics approach connection to the stochastic description of the flux

5.5 Conclusion

We have demonstrated that particle-bed collisions control the shape of the particle velocity distribution.

.1 Derivation of Master Equation

To derive the master equation from 5.3, we temporarily consider the Gaussian white noise (GWN) $\xi(t)$ as a Poisson jump process having rate r and jumps $\sqrt{2d}h$ with h distributed as $f(h)$. We will later take a GWN limit on this noise. With this assumption, integrating 5.3 over a small time interval

δt considering the Ito interpretation for the collision term provides

$$u(t+\delta t) = \begin{cases} u(t) + \gamma\delta t & \text{with probability } 1 - r\delta t - \nu\delta t \\ u(t) + \sqrt{2d}h & \text{with probability } r\delta t \\ \varepsilon u(t) & \text{with probability } \nu\delta t \end{cases} \tag{15}$$

Considering the probability $P(u, t+\delta)$ as sum over possible paths from $P(u,t)$ develops

$$P(u,t+\delta t) = (1 - r\delta t - \nu\delta t)\int_{-\infty}^{\infty} dw\delta(u - w - \gamma\delta t)P(w,t) \tag{16}$$

$$+r\delta t\int_{-\infty}^{\infty} dw\int_{-\infty}^{\infty} dhf(h)\delta(u - w - \sqrt{2d}h)P(w,t) \tag{17}$$

$$+\nu\delta t\int_{-\infty}^{\infty} dw\int_{0}^{1} d\varepsilon\rho(\varepsilon)\delta(u - w\varepsilon)P(w,t). \tag{18}$$

Evaluating all integrals over δ-functions provides

$$P(u,t+\delta t) = (1 - r\delta t - \nu\delta t)P(u - \gamma\delta t, t) \tag{19}$$

$$+r\delta t\int_{-\infty}^{\infty} dhf(h)P(u + \sqrt{2d}h) \tag{20}$$

$$+\nu\delta t\int_{0}^{1} \frac{d\varepsilon}{\varepsilon}\rho(\varepsilon)P\big(\frac{u}{\varepsilon}\big). \tag{21}$$

Finally, we take $\delta t \to 0$ and limit the Poisson noise involving $\sqrt{2d}$ to a Gaussian white noise by taking $r \to \infty$ as $h \to 0$ such that $h^2 r = 1$ **?**. This process finally obtains the master equation (5.4).

.2 Derivation of Steady-state solution

Defining $\tilde{P}(s) = \int_{-\infty}^{\infty} due^{ius}P(u)$ as the Fourier transform (FT) of $P(u)$ and taking the FT of **??** develops the recursion relation

$$\tilde{P}(s) = \frac{\tilde{P}(s\varepsilon)}{q(s)}. \tag{22}$$

where

$$q(z) = dz^2 - i\gamma z + 1. \tag{23}$$

Recursing $N+1$ times provides

$$\tilde{P}(s) = \frac{\tilde{P}(s\varepsilon^{N+1})}{q(s\varepsilon^0)q(s\varepsilon^1)\dots q(s\varepsilon^N)}. \tag{24}$$

The polynomials $q(z)$ can always be factored as $q(z) = d(z - i\lambda_-)(z - i\lambda_+)$ where

$$\lambda_\pm = \frac{\gamma}{2d}\Big[1 \pm \sqrt{1 + 4d/\gamma^2}\Big]. \tag{25}$$

Using these factors to expand $\tilde{P}(s)$ in partial fractions provides

$$\tilde{P}(s) = \tilde{P}(s\varepsilon^{N+1}) \sum_{l=0}^{N} \Big[\frac{R_l^-}{s\varepsilon^l - i\lambda_-} + \frac{R_l^+}{s\varepsilon^l - i\lambda_+}\Big] \tag{26}$$

where the coefficients $R_l^\pm$ are the residues of the product $[q(s\varepsilon^0)\dots q(s\varepsilon^N)]^{-1}$:

$$R_l^\pm = \frac{s\varepsilon^l - i\lambda_\pm}{q(s\varepsilon^0)\dots q(s\varepsilon^N)}\Big|_{s=i\lambda_\pm\varepsilon^{-l}}. \tag{27}$$

The Fourier transform (24) has a beautiful feature as $N \to \infty$: since $0 < \varepsilon < 1$, the prefactor $\tilde{P}(s\varepsilon^{N+1})$ becomes the normalization condition $\tilde{P}(0) = 1$ for the probability distribution $P(u)$ in the limit. Taking this limit and evaluating the residues provides

$$\begin{aligned}\tilde{P}(s) = {} & \frac{1}{d(\lambda_+ - \lambda_-)\prod_{m=1}^{\infty} q(i\lambda_-\varepsilon^m)} \sum_{l=0}^{\infty} \frac{i}{(s\varepsilon^l - i\lambda_-)\prod_{m=1}^{l} q(i\lambda_-\varepsilon^{-m})} \\ & + \frac{1}{d(\lambda_+ - \lambda_-)\prod_{m=1}^{\infty} q(i\lambda_+\varepsilon^m)} \sum_{l=0}^{\infty} \frac{-i}{(s\varepsilon^l - i\lambda_+)\prod_{m=1}^{l} q(i\lambda_+\varepsilon^{-m})}\end{aligned} \tag{28}$$

Finally, inverting the Fourier transforms term by term with contour integration and incorporating (23) provides the steady-state solution (5.8).

.3 Calculation of the moments

Taking (5.4), multiplying by u^k, integrating over all space, and taking account of normalization of $P(u)$ provides a recursion relation for the moments:

$$0 = Dk(k-1)\langle u^{k-2}\rangle + \Gamma k\langle u^{k-1}\rangle + \nu(\varepsilon^k - 1)\langle u^k\rangle. \tag{29}$$

$k = 1$ provides the mean

$$\langle u\rangle = \frac{\Gamma}{\nu(1-\varepsilon)} = \frac{\gamma}{1-\varepsilon} \tag{30}$$

while $k = 2$ provides the second moment

$$\langle u^2\rangle = 2\frac{d + \gamma\langle u\rangle}{1-\varepsilon^2}, \tag{31}$$

leading to the velocity variance

$$\sigma_u = \sqrt{\frac{2d+\gamma^2}{1-\varepsilon^2}}. \tag{32}$$

.4 Weak and strong collision limits

Now we demonstrate that weak collisions imply a Gaussian-like distribution for sediment velocities. The limit is challenging since the steady-state distribution 5.8 and the moments above all diverge as $\varepsilon \to 1$. Following **?**, this suggests normalizing the distribution $P(u)$ using

$$z = \frac{u - \bar{u}}{\sigma_u} \tag{33}$$

and

$$Q(z) = \sigma_u P(u) \tag{34}$$

to seek a differential equation for $Q(z)$ with manageable behavior as $\varepsilon \to 1$. Incorporating this transformation into (5.4) provides a "normalized" Master

equation

$$(1-\varepsilon^2)\frac{d}{2d+\gamma}Q''(z)-\frac{\gamma\sqrt{1-\varepsilon^2}}{\sqrt{2d+\gamma^2}}Q'(z)-Q(z)+\frac{1}{\varepsilon}Q\Big(z+\Big[\frac{1-\varepsilon}{\varepsilon}z+\frac{\gamma\sqrt{1-\varepsilon^2}}{\varepsilon\sqrt{2d+\gamma^2}}\Big]\Big)=0 \tag{35}$$

This equation remains exact and is only a change of variables from (5.4). Now we approximate the equation for $\varepsilon \to 1$ by expanding the final term to second order around $z = 0$ before setting $\varepsilon = 1$, obtaining

$$Q''(z) + zQ'(z) + Q(z) = 0, \tag{36}$$

which is the classic Ornstein-Uhlenbeck Fokker-Planck equation whose solution is the standard normal distribution for $Q(z)$. This solution provides 5.14 when transformed back to the original variables $P(u)$ and u.

Appendix A

Summary and future work

A.1 Key contributions

A.1.1 Probability distribution of the sediment flux

A.1.2 Inclusion of velocity fluctuations into Einstein's model of individual particle trajectories

A.1.3 Quantification of the control of bed elevation fluctuations on sediment transport fluctuations

A.1.4 Understanding of how sediment burial affects the downstream spreading of sediment tracer particles

A.2 Models and the real world

A.3 Closure: Complexity vs Realism

Bibliography

Aberle, J., and V. Nikora, Statistical properties of armored gravel bed surfaces, *Water Resources Research*, *42*, 1–11, 2006. → pages 52, 54, 55

Amir, M., V. I. Nikora, and M. T. Stewart, Pressure forces on sediment particles in turbulent open-channel flow: A laboratory study, *Journal of Fluid Mechanics*, *757*, 458–497, 2014. → pages 7, 53

Ancey, C., Bedload transport: a walk between randomness and determinism. Part 1. The state of the art, *Journal of Hydraulic Research*, *58*, 1–17, 2020. → page 23

Ancey, C., and J. Heyman, A microstructural approach to bed load transport: Mean behaviour and fluctuations of particle transport rates, *Journal of Fluid Mechanics*, *744*, 129–168, 2014. → pages 7, 9, 10, 18, 19, 22, 24, 70, 71, 72, 76, 77, 82, 83

Ancey, C., T. Böhm, M. Jodeau, and P. Frey, Statistical description of sediment transport experiments, *Physical Review E - Statistical, Nonlinear, and Soft Matter Physics*, *74*, 1–14, 2006. → pages 8, 9, 10, 15, 16, 17, 19, 21, 33, 34, 35, 48, 59, 67

Ancey, C., A. C. Davison, T. Böhm, M. Jodeau, and P. Frey, Entrainment and motion of coarse particles in a shallow water stream down a steep slope, *Journal of Fluid Mechanics*, *595*, 83–114, 2008. → pages xii, xv, 7, 9, 10, 16, 19, 22, 24, 34, 35, 36, 37, 38, 39, 40, 41, 42, 43, 46, 47, 48, 51, 52, 53

Ancey, C., P. Bohorquez, and E. Bardou, Sediment transport in mountain streams, *Tech. rep.*, 2014. → page 9

Ancey, C., P. Bohorquez, and J. Heyman, Stochastic interpretation of the advection-diffusion, *Journal of Geophysical Research : Earth Surface*, *120*, 325–345, 2015. → pages 9, 10, 19, 53

Arfken, G., *Mathematical methods for physicists*, Academic Press, Inc., 1985. → page 61

Armanini, A., V. Cavedon, and M. Righetti, A probabilistic/deterministic approach for the prediction of the sediment transport rate, *Advances in Water Resources*, *81*, 10–18, 2015. → page 8

Armenio, V., and V. Fiorotto, The importance of the forces acting on particles in turbulent flows, *Physics of Fluids*, *13*, 2437–2440, 2001. → page 75

Bagnold, *Physics of Blown Sand*, 1941. → page 1

Bagnold, R. A., The flow of cohesionless grains in fluids, *Philosophical Transactions of the Royal Society of London. Series A, Mathematical and Physical Sciences*, *249*, 235–297, 1956.

Bagnold, R. A., An Approach to the Sediment Transport Problem from General Physics, *Tech. Rep. 4*, U.S. Geological Survey, Washington, DC, 1966.

Bailey, N. T., Stochastic birth, death and migration processes for spatially distribured populations., *Biometrika*, *55*, 189–198, 1968. → pages 9, 19

Balakrishnan, V., On a simple derivation of master equations for diffusion processes driven by white noise and dichotomic Markov noise, *Pramana*, *40*, 259–265, 1993. → page 27

Ballio, F., V. Nikora, and S. E. Coleman, On the definition of solid discharge in hydro-environment research and applications, *Journal of Hydraulic Research*, *52*, 173–184, 2014. → pages 6, 19

Banerjee, T., S. N. Majumdar, A. Rosso, and G. Schehr, Current fluctuations in noninteracting run-and-tumble particles in one dimension, *Physical Review E*, *101*, 1–16, 2020. → page 28

Barik, D., P. K. Ghosh, and D. S. Ray, Langevin dynamics with dichotomous noise; Direct simulation and applications, *Journal of Statistical Mechanics: Theory and Experiment*, 2006. → page 62

Barry, J. J., J. M. Buffington, and J. G. King, A general power equation for predicting bed load transport rates in gravel bed rivers, *Water Resources Research*, *40*, 1–22, 2004. → page 6

Bathurst, J. C., Effect of coarse surface layer on bed-load transport, *Journal of Hydraulic Engineering*, *133*, 1192–1205, 2007. → page 6

Bennett, C. H., Serially deposited amorphous aggregates of hard spheres, *Journal of Applied Physics*, *43*, 2727–2734, 1972. → pages 37, 41

Bialik, R. J., V. I. Nikora, and P. M. Rowiński, 3D Lagrangian modelling of saltating particles diffusion in turbulent water flow, *Acta Geophysica*, *60*, 1639–1660, 2012. → pages 57, 58, 67

Bialik, R. J., V. I. Nikora, M. Karpiński, and P. M. Rowiński, Diffusion of bedload particles in open-channel flows: distribution of travel times and second-order statistics of particle trajectories, *Environmental Fluid Mechanics*, *15*, 1281–1292, 2015. → page 58

Böhm, T., C. Ancey, P. Frey, J. L. Reboud, and C. Ducottet, Fluctuations of the solid discharge of gravity-driven particle flows in a turbulent stream, *Physical Review E - Statistical Physics, Plasmas, Fluids, and Related Interdisciplinary Topics*, *69*, 13, 2004. → page 7

Bohorquez, P., and C. Ancey, Particle diffusion in non-equilibrium bedload transport simulations, *Applied Mathematical Modelling*, *40*, 7474–7492, 2016. → page 70

Brach, R. M., Rigid body collisions, *American Society of Mechanical Engineers (Paper)*, *56*, 133–138, 1989. → page 74

Bradley, D. N., Direct Observation of Heavy-Tailed Storage Times of Bed Load Tracer Particles Causing Anomalous Superdiffusion, *Geophysical Research Letters*, *44*, 12,227–12,235, 2017. → pages 34, 53, 57, 66, 67, 69

Bradley, D. N., G. E. Tucker, and D. A. Benson, Fractional dispersion in a sand bed river, *Journal of Geophysical Research*, *115*, F00A09, 2010. → pages 66, 67

Celik, A. O., P. Diplas, C. L. Dancey, and M. Valyrakis, Impulse and particle dislodgement under turbulent flow conditions, *Physics of Fluids*, *22*, 1–13, 2010. → page 33

Celik, A. O., P. Diplas, and C. L. Dancey, Instantaneous pressure measurements on a spherical grain under threshold flow conditions, *Journal of Fluid Mechanics*, *741*, 60–97, 2014. → pages 7, 14, 76, 83

Charru, F., H. Mouilleron, and O. Eiff, Erosion and deposition of particles on a bed sheared by a viscous flow, *Journal of Fluid Mechanics*, *519*, 55–80, 2004. → pages 7, 23, 37, 53, 71, 83

Chen, L., and M. C. Stone, Influence of bed material size heterogeneity on bedload transport uncertainty, *Water Resources Research*, *44*, 1–11, 2008. → pages 7, 20

Church, M., Bed material transport and the morphology of alluvial river channels, *Annual Review of Earth and Planetary Sciences*, *34*, 325–354, 2006. → page 6

Clift, R., J. R. Grace, and M. E. Weber, Bubbles, Drops, and Particles, 1978. → page 75

Coleman, N. L., A theoretical and experimental study of drag and lift forces acting on a sphere resting on a hypothetical streambed, in *International Association for Hydraulic Research Congress*, pp. 185–192, Littleton, CO, 1967. → page 75

Coleman, S. E., and V. I. Nikora, Exner equation: A continuum approximation of a discrete granular system, *Water Resources Research*, *45*, 1–8, 2009. → page 3

Correa, A., D. Windhorst, D. Tetzlaff, P. Crespo, R. Célleri, J. Feyen, and L. Breuer, Accelerating advances in continental domain hydrologic modeling, *Water Resources Research*, *53*, 5998–6017, 2017. → page 39

Daly, E., and A. Porporato, Probabilistic dynamics of some jump-diffusion systems, *Physical Review E - Statistical, Nonlinear, and Soft Matter Physics*, *73*, 1–7, 2006. → page 76

Daly, E., and A. Porporato, Effect of different jump distributions on the dynamics of jump processes, *Physical Review E - Statistical, Nonlinear, and Soft Matter Physics*, *81*, 1–10, 2010. → page 77

Denisov, S. I., W. Horsthemke, and P. Hänggi, Generalized Fokker-Planck equation: Derivation and exact solutions, *European Physical Journal B*, *68*, 567–575, 2009. → page 76

Dey, S., and S. Z. Ali, Review Article: Advances in modeling of bed particle entrainment sheared by turbulent flow, *Physics of Fluids*, *30*, 2018. → pages 14, 17, 20

Dey, S., and A. Papanicolaou, Sediment threshold under stream flow: A state-of-the-art review, *KSCE Journal of Civil Engineering*, *12*, 45–60, 2008. → pages 14, 20

Dhont, B., and C. Ancey, Are Bedload Transport Pulses in Gravel Bed Rivers Created by Bar Migration or Sediment Waves?, *Geophysical Research Letters*, *45*, 5501–5508, 2018. → pages 7, 35, 52

Diplas, P., C. L. Dancey, A. O. Celik, M. Valyrakis, K. Greer, and T. Akar, The role of impulse on the initiation of particle movement under turbulent flow conditions, *Science*, *322*, 717–720, 2008. → page 14

Drake, T. G., R. L. Shreve, W. E. Dietrich, P. J. Whiting, and L. B. Leopold, Bedload transport of fine gravel observed by motion-picture photography, *Journal of Fluid Mechanics*, *192*, 193–217, 1988. → pages 16, 17

Dubkov, A. A., and A. A. Kharcheva, Steady-state probability characteristics of Verhulst and Hongler models with multiplicative white Poisson noise, *European Physical Journal B*, *92*, 1–6, 2019. → page 77

Dubkov, A. A., O. V. Rudenko, and S. N. Gurbatov, Probability characteristics of nonlinear dynamical systems driven by δ -pulse noise, *Physical Review E*, *93*, 1–7, 2016. → page 76

Dwivedi, A., B. Melville, and A. Y. Shamseldin, Hydrodynamic forces generated on a spherical sediment particle during entrainment, *Journal of Hydraulic Engineering*, *136*, 756–769, 2010. → page 76

Dwivedi, A., B. W. Melville, A. Y. Shamseldin, and T. K. Guha, Analysis of hydrodynamic lift on a bed sediment particle, *Journal of Geophysical Research: Earth Surface*, *116*, 2011. → page 33

Dwivedi, A., B. Melville, A. J. Raudkivi, A. Y. Shamseldin, and Y. M. Chiew, Role of turbulence and particle exposure on entrainment of large spherical particles in flows with low relative submergence, *Journal of Hydraulic Engineering*, *138*, 1022–1030, 2012. → page 75

Einstein, H. A., Bed load transport as a probability problem, Ph.D. thesis, ETH Zurich, 1937. → pages xvi, 7, 24, 33, 34, 51, 56, 57, 58, 59, 61, 62, 63, 66, 67, 68

Einstein, H. A., *The bedload function for sediment transportation in open channel flows*, technical ed., Soil Conservation Service, Washington, DC, 1950. → pages 7, 8, 10, 11, 14, 16, 20, 21, 24, 33, 34, 35, 37, 51

Einstein, H. A., and E. S. A. El-Samni, Hydrodynamic forces on a rough wall, *Reviews of Modern Physics*, *21*, 520–524, 1949. → pages 8, 20

Elgueta, M. A., Effects of episodic sediment supply on channel adjustment of an experimental gravel bed, Phd, University of British Columbia, 2018. → page 7

Escaff, D., R. Toral, C. Van Den Broeck, and K. Lindenberg, A continuous-time persistent random walk model for flocking, *Chaos*, *28*, 1–11, 2018. → page 68

Fa, K. S., Uncoupled continuous-time random walk model: Analytical and numerical solutions, *Physical Review E - Statistical, Nonlinear, and Soft Matter Physics*, *89*, 1–9, 2014. → page 68

Fan, N., D. Zhong, B. Wu, E. Foufoula-Georgiou, and M. Guala, A mechanistic-stochastic formulation of bed load particle motions: From individual particle forces to the Fokker-Planck equation under low transport rates, *Journal of Geophysical Research: Earth Surface*, *119*, 464–482, 2014. → pages 24, 72, 76, 77, 81, 83

Fathel, S., D. Furbish, and M. Schmeeckle, Parsing anomalous versus normal diffusive behavior of bedload sediment particles, *Earth Surface Processes and Landforms*, *41*, 1797–1803, 2016. → pages 57, 66, 69, 71

Fathel, S. L., D. J. Furbish, and M. W. Schmeeckle, Experimental evidence of statistical ensemble behavior in bed load sediment transport, *Journal of Geophysical Research F: Earth Surface*, *120*, 2298–2317, 2015. → pages 23, 35, 54, 59, 71

Feller, W., *An Introduction to Probability Theory and its Applications*, 3rd ed., Wiley, 1967. → page 78

Ferguson, R. I., and T. B. Hoey, Long-term slowdown of river tracer pebbles: Generic models and implications for interpreting short-term tracer studies, *Water Resources Research*, *38*, 17–1–17–11, 2002. → page 63

Ferguson, R. I., D. J. Bloomer, T. B. Hoey, and A. Werritty, Mobility of river tracer pebbles over different timescales, *Water Resources Research*, *38*, 3–1–3–8, 2002. → page 57

Field, T. R., and R. J. Tough, Coupled dynamics of populations supported by discrete sites and their continuum limit, *Proceedings of the Royal Society A: Mathematical, Physical and Engineering Sciences*, *466*, 2561–2586, 2010. → page 9

Fowler, K. J. A., Simulating runoff under changing climatic conditions, *Water Resources Research*, *52*, 1–24, 2016. → pages 58, 66, 67

Fraccarollo, L., and M. A. Hassan, Einstein conjecture and resting-Time statisticsÂ inÂ the bed-load transport of monodispersedÂ particles, *Journal of Fluid Mechanics*, *876*, 1077–1089, 2019. → page 67

Furbish, D. J., and M. W. Schmeeckle, A probabilistic derivation of the exponential-like distribution of bed load particle velocities, *Water Resources Research*, *49*, 1537–1551, 2013. → page 72

Furbish, D. J., A. E. Ball, and M. W. Schmeeckle, A probabilistic description of the bed load sediment flux: 4. Fickian diffusion at low transport rates, *Journal of Geophysical Research: Earth Surface*, *117*, 1–13, 2012a. → pages 24, 57, 69

Furbish, D. J., P. K. Haff, J. C. Roseberry, and M. W. Schmeeckle, A probabilistic description of the bed load sediment flux: 1. Theory, *Journal of Geophysical Research: Earth Surface*, *117*, 2012b. → pages 34, 35, 37

Furbish, D. J., S. L. Fathel, and M. W. Schmeeckle, Particle motions and bedload theory: The entrainment forms of the flux and the exner equation, in *Gravel-Bed Rivers: Process and Disasters*, edited by D. Tsutsumi and J. B. Laronne, 1 ed., chap. 4, pp. 97–120, John Wiley & Sons Ltd., 2017. → pages 35, 57

Gaeuman, D., R. Stewart, B. Schmandt, and C. Pryor, Geomorphic response to gravel augmentation and high-flow dam release in the Trinity River, California, *Earth Surface Processes and Landforms*, *42*, 2523–2540, 2017. → pages 33, 56

Gardiner, C. W., *Handbook of stochastic methods for physics, chemistry and the natural sciences*, Springer-Verlag, 1983. → pages 19, 27, 40, 43, 53, 76, 77, 78

Gillespie, D. T., Exact stochastic simulation of coupled chemical reactions, *Journal of Physical Chemistry*, *81*, 2340–2361, 1977. → page 40

Gillespie, D. T., Stochastic simulation of chemical kinetics, *Annual Review of Physical Chemistry*, *58*, 35–55, 2007. → pages 39, 40, 41

Gomez, B., and M. Church, An assessment of bed load sediment transport formulae for gravel bed rivers, *Water Resources Research*, *25*, 1161–1186, 1989. → pages 6, 7

González, C., D. H. Richter, D. Bolster, S. Bateman, J. Calantoni, and C. Escauriaza, Characterization of bedload intermittency near the threshold of motion using a Lagrangian sediment transport model, *Environmental Fluid Mechanics*, *17*, 111–137, 2017. → pages 33, 72, 75

Gordon, R., J. B. Carmichael, and F. J. Isackson, Saltation of plastic balls in a 'one-dimensional' flume, *Water Resources Research*, *8*, 444–459, 1972. → pages 23, 58, 75

Grass, A., Initial Instability of Fine Bed Sand, *Journal of the Hydraulics Division*, *96*, 619–632, 1970. → page 20

Hanggi, P., Correlation Functions and Masterequations of Generalized (Non-Markovian) Langevin Equations, *Z. Physik B*, *31*, 407–416, 1978. → pages 26, 77

Haschenburger, J. K., Tracing river gravels: Insights into dispersion from a long-term field experiment, *Geomorphology*, *200*, 121–131, 2013. → pages 57, 63

Hassan, M. A. ., and D. N. Bradley, Geomorphic controls on tracer particle dispersion in gravel-bed rivers, in *Gravel-Bed Rivers: Process and Disasters*, edited by D. Tsutsumi and J. B. Laronne, 1st ed., pp. 159–184, John Wiley & Sons Ltd., 2017. → pages 33, 56, 57, 66

Hassan, M. A., and M. Church, Vertical mixing of coarse particles in gravel bed rivers: A kinematic model, *Water Resources Research*, *30*, 1173–1185, 1994. → page 63

Hassan, M. A., M. Church, and A. P. Schick, Distance of movement of coarse particles in gravel bed streams, *Water Resources Research*, *27*, 503–511, 1991. → pages 51, 57, 58, 63

Hassan, M. A., B. J. Smith, D. L. Hogan, D. S. Luzi, A. E. Zimmermann, and B. C. Eaton, 18 Sediment storage and transport in coarse bed streams: scale considerations, in *Developments in Earth Surface Processes*, edited by H. Habersack, H. Piegay, and M. Rinaldi, vol. 11, chap. 18, pp. 473–496, Elsevier B.V, 2007. → pages 3, 7, 21, 53

Hassan, M. A., H. Voepel, R. Schumer, G. Parker, and L. Fraccarollo, Displacement characteristics of coarse fluvial bed sediment, *Journal of Geophysical Research: Earth Surface*, *118*, 155–165, 2013. → page 57

Hassan, M. A., S. Bird, D. Reid, and D. Hogan, Simulated wood budgets in two mountain streams, *Geomorphology*, *259*, 119–133, 2016. → pages 18, 19

Heyman, J., A study of the spatio-temporal behaviour of bed load transport rate fluctuations, *PhD Dissertation*, *6256*, 116, 2014. → page 35

Heyman, J., F. Mettra, H. B. Ma, and C. Ancey, Statistics of bedload transport over steep slopes: Separation of time scales and collective motion, *Geophysical Research Letters*, *40*, 128–133, 2013. → pages 9, 10, 19, 35

Heyman, J., H. B. Ma, F. Mettra, and C. Ancey, Spatial correlations in bed load transport : Evidence, importance, and modeling, *Journal of Geophysical Research: Earth Surface*, *119*, 1751–1767, 2014. → pages 7, 10, 19, 35, 53, 69

Heyman, J., P. Bohorquez, and C. Ancey, Entrainment, motion, and deposition of coarse particles transported by water over a sloping mobile bed, *Journal of Geophysical Research: Earth Surface*, *121*, 1931–1952, 2016. → pages 7, 22, 23, 35, 52, 54, 69, 71

Hjelmfelt, A. T., and L. F. Mockros, Motion of discrete particles in a turbulent fluid, *Applied Scientific Research*, *16*, 149–161, 1966. → page 75

Hofland, B., and J. A. Battjes, Probability density function of instantaneous drag forces and shear stresses on a bed, *Journal of Hydraulic Engineering*, *132*, 1169–1175, 2006. → page 76

Houssais, M., and E. Lajeunesse, Bedload transport of a bimodal sediment bed, *Journal of Geophysical Research F: Earth Surface*, *117*, 1–13, 2012. → page 71

Hubbell, D., and W. Sayre, Sand Transport Studies with Radioactive Tracers, *Journal of the Hydraulics Division*, *90*, 39–68, 1964. → pages 33, 34, 51, 58, 63

Iverson, R. M., How should mathematical models of geomorphic processes be judged?, in *Geophysical Monograph Series*, edited by P. R. Wilcock and R. M. Iverson, vol. 135, pp. 83–94, American Geophysical Union, 2003. → page 10

Jerolmack, D., and D. Mohrig, Interactions between bed forms: Topography, turbulence, and transport, *Journal of Geophysical Research: Earth Surface*, *110*, 2005. → page 7

Joseph, G. G., R. Zenit, M. L. Hunt, and A. M. Rosenwinkel, Particle-wall collisions in a viscous fluid, *Journal of Fluid Mechanics*, *433*, 329–346, 2001. → page 85

Kennedy, J. F., The Albert shields story, *Journal of Hydraulic Engineering*, *121*, 766–772, 1995. → page 14

KIRCHNER, J. W., W. E. DIETRICH, F. ISEYA, and H. IKEDA, The variability of critical shear stress, friction angle, and grain protrusion in water-worked sediments, *Sedimentology*, *37*, 647–672, 1990. → page 7

Kondolf, G. M., et al., Sustainable sediment management in reservoirs and regulated rivers: Experiences from five continents, *Earth's Future*, *2*, 256–280, 2014. → page 6

Kraichnan, R. H., Diffusion by a random velocity field, *Physics of Fluids*, *13*, 22–31, 1970. → page 57

Lajeunesse, E., L. Malverti, and F. Charru, Bed load transport in turbulent flow at the grain scale: Experiments and modeling, *Journal of Geophysical Research: Earth Surface*, *115*, 2010. → pages xvii, 54, 65, 69, 71, 83

Lajeunesse, E., O. Devauchelle, and F. James, Advection and dispersion of bed load tracers, *Earth Surface Dynamics*, *6*, 389–399, 2018. → pages 24, 26, 33, 67, 68

Lee, D. B., and D. Jerolmack, Determining the scales of collective entrainment in collision-driven bed load, *Earth Surface Dynamics*, *6*, 1089–1099, 2018. → pages 35, 52, 69

Lisle, I. G., C. W. Rose, W. L. Hogarth, P. B. Hairsine, G. C. Sander, and J. Y. Parlange, Stochastic sediment transport in soil erosion, *Journal of Hydrology*, *204*, 217–230, 1998. → pages xvi, 8, 24, 26, 58, 59, 61, 62, 67, 68

Lisle, T. E., and M. a. Madej, Spatial Variation in Armouring in a Channel with High Sediment Supply, *Dynamics of Gravel-bed Rivers*, pp. 277–293, 1992. → page 7

Liu, D., X. Liu, X. Fu, and G. Wang, Quantification of the bed load effects on turbulent open-channel flows, *Journal of Geophysical Research : Earth Surface*, *121*, 767–789, 2016. → page 7

Liu, M. X., A. Pelosi, and M. Guala, A Statistical Description of Particle Motion and Rest Regimes in Open-Channel Flows Under Low Bedload Transport, *Journal of Geophysical Research: Earth Surface*, *124*, 2666–2688, 2019. → pages 34, 54, 67, 71

Lorenz, A., C. Tuozzolo, and M. Y. Louge, Measurements of impact properties of small, nearly spherical particles, *Experimental Mechanics*, *37*, 292–298, 1997. → page 74

Luczka, J., R. Bartussek, and P. Hanggi, White-noise-induced transport in periodic structures., *Epl*, *31*, 431–436, 1995. → page 77

Ma, H., J. Heyman, X. Fu, F. Mettra, C. Ancey, and G. Parker, Bed load transport over a broad range of timescales: Determination of three regimes of fluctuations, *Journal of Geophysical Research: Earth Surface*, *119*, 2653–2673, 2014. → pages 9, 10, 35

Macklin, M. G., P. A. Brewer, K. A. Hudson-Edwards, G. Bird, T. J. Coulthard, I. A. Dennis, P. J. Lechler, J. R. Miller, and J. N. Turner, A geomorphological approach to the management of rivers contaminated by metal mining, *Geomorphology*, *79*, 423–447, 2006. → pages 33, 56

Madej, M. A., D. G. Sutherland, T. E. Lisle, and B. Pryor, Channel responses to varying sediment input: A flume experiment modeled after Redwood Creek, California, *Geomorphology*, *103*, 507–519, 2009. → page 7

Malmon, D. V., S. L. Reneau, T. Dunne, D. Katzman, and P. G. Drakos, Influence of sediment storage on downstream delivery of contaminated sediment, *Water Resources Research*, *41*, 1–17, 2005. → page 33

Mao, L., The effect of hydrographs on bed load transport and bed sediment spatial arrangement, *Journal of Geophysical Research: Earth Surface*, *117*, 1–16, 2012. → page 7

Marcum, J. I., A Statistical Theory of Target Detection By Pulsed Radar, *IRE Transactions on Information Theory*, *6*, 59–267, 1960. → page 61

Martin, R. L., D. J. Jerolmack, and R. Schumer, The physical basis for anomalous diffusion in bed load transport, *Journal of Geophysical Research: Earth Surface*, *117*, 1–18, 2012. → pages xvii, 33, 34, 57, 59, 65, 66, 67, 68, 71

Martin, R. L., P. K. Purohit, and D. J. Jerolmack, Sedimentary bed evolution as a mean-reverting random walk: Implications for tracer statistics, *Geophysical Research Letters*, *41*, 6152–6159, 2014. → pages 34, 38, 41, 43, 50, 51, 52, 53, 54, 57, 64, 67, 68

Masoliver, J., Fractional telegrapher's equation from fractional persistent random walks, *Physical Review E*, *93*, 1–10, 2016. → page 68

Masoliver, J., and G. H. Weiss, Telegrapher's equations with variable propagation speeds, *Physical Review E*, *49*, 3852–3854, 1994. → page 68

Mau, Y., X. Feng, and A. Porporato, Multiplicative jump processes and applications to leaching of salt and contaminants in the soil, *Physical Review E - Statistical, Nonlinear, and Soft Matter Physics*, *90*, 1–8, 2014. → page 77

Maxey, M. R., and J. J. Riley, Equation of motion for a small rigid sphere in a nonuniform flow, *Physics of Fluids*, *26*, 883–889, 1983. → page 75

Méndez, V., M. Assaf, D. Campos, and W. Horsthemke, Stochastic dynamics and logistic population growth, *Physical Review E - Statistical, Nonlinear, and Soft Matter Physics*, *91*, 2015. → page 9

Metzler, R., and J. Klafter, The random walk's guide to anomalous diffusion: A fractional dynamics approach, *Physics Report*, *339*, 1–77, 2000. → pages 56, 63

Metzler, R., J. H. Jeon, A. G. Cherstvy, and E. Barkai, Anomalous diffusion models and their properties: Non-stationarity, non-ergodicity, and ageing at the centenary of single particle tracking, *Physical Chemistry Chemical Physics*, *16*, 24,128–24,164, 2014. → page 68

Michaelides, E. E., Review—the transient equation of motion for particles, bubbles, and droplets, *Journal of Fluids Engineering, Transactions of the ASME*, *119*, 233–247, 1997. → page 76

Montaine, M., M. Heckel, C. Kruelle, T. Schwager, and T. Pöschel, Coefficient of restitution as a fluctuating quantity, *Physical Review E - Statistical, Nonlinear, and Soft Matter Physics*, *84*, 1–5, 2011. → page 74

Montroll, E. W., Random walks on lattices, *Journal of Mathematical Physics*, *6*, 193–220, 1964. → pages 24, 59

Nakagawa, H., and T. Tsujimoto 9 Kyoto, On probabilistic characteristics of motion of individual sediment particles on stream beds., in *Hydraulic Problems Solved by Stochastic Methods: Second International IAHR Symposium on Stochastic Hydraulics*, pp. 293–320, Water Resources Publications, Lund, Sweden, 1977. → pages 33, 34, 51, 57, 58, 66, 67

Nelson, P. A., D. Bellugi, and W. E. Dietrich, Delineation of river bed-surface patches by clustering high-resolution spatial grain size data, *Geomorphology*, *205*, 102–119, 2014. → page 53

Newman, M. E., Power laws, Pareto distributions and Zipf's law, *Contemporary Physics*, *46*, 323–351, 2005. → page 50

Nikora, V., J. Heald, D. Goring, and I. McEwan, Diffusion of saltating particles in unidirectional water flow over a rough granular bed, *Journal of Physics A: Mathematical and General*, *34*, 2001. → pages 56, 57, 67

Nikora, V., H. Habersack, T. Huber, and I. McEwan, On bed particle diffusion in gravel bed flows under weak bed load transport, *Water Resources Research*, *38*, 17–1–17–9, 2002. → pages 56, 57, 58, 66, 69

Ockendon, J. R., and A. B. Tayler, The dynamics of a current collection system for an electric locomotive, *Proceedings of the Royal Society of London. A. Mathematical and Physical Sciences*, *322*, 447–468, 1971. → page 79

Olinde, L., and J. P. L. Johnson, Using RFID and accelerometer-embedded tracers to measure probabilities of bed load transport, step lengths, and rest times in a mountain stream, *Water Resources Research*, *51*, 7525–7589, 2015. → pages 34, 53, 67, 68

Ong, H. G., J. W. Cheah, L. Chen, H. Tangtang, Y. Xu, B. Li, H. Zhang, L. J. Li, and J. Wang, Charge injection at carbon nanotube- SiO2 interface, *Applied Physics Letters*, *93*, 232–235, 2008. → page 20

Paintal, A. S., A stochastic model of bed load transport, *Journal of Hydraulic Research*, *9*, 527–554, 1971. → pages 8, 14, 20, 33, 37, 58

Papangelakis, E., and M. A. Hassan, The role of channel morphology on the mobility and dispersion of bed sediment in a small gravel-bed stream, *Earth Surface Processes and Landforms*, *41*, 2191–2206, 2016. → page 57

Papanicolaou, A. N., P. Diplas, N. Evaggelopoulos, and S. Fotopoulos, Stochastic incipient motion criterion for spheres under various bed packing conditions, *Journal of Hydraulic Engineering*, *128*, 369–380, 2002. → page 8

Parker, G., and P. C. Klingeman, On why gravel bed streams are paved, *Water Resources Research*, *18*, 1409–1423, 1982. → pages 20, 22

Pelosi, A., and G. Parker, Morphodynamics of river bed variation with variable bedload step length, *Earth Surface Dynamics*, *2*, 243–253, 2014. → page 68

Pender, G., T. B. Hoey, C. Fuller, and I. K. McEwan, Selective bedload transport during the degradation of a well sorted graded sediment bed, *Journal of Hydraulic Research*, *39*, 269–277, 2001. → page 38

Philip, J. R., Diffusion by continuous movements, *Physics of Fluids*, *11*, 38–42, 1968. → page 56

Phillips, C. B., R. L. Martin, and D. J. Jerolmack, Impulse framework for unsteady flows reveals superdiffusive bed load transport, *Geophysical Research Letters*, *40*, 1328–1333, 2013. → page 57

Pielou, E. C., *Mathematical Ecology*, 1 ed., John Wiley & Sons Ltd., New York, NY, 2008. → pages 9, 39

Pierce, J. K., and M. A. Hassan, Back to Einstein: Burial-Induced Three-Range Diffusion in Fluvial Sediment Transport, *Geophysical Research Letters*, *47*, 2020. → page 24

Pitlick, J., J. Marr, and J. Pizzuto, Width adjustment in experimental gravel-bed channels in response to overbank flows, *Journal of Geophysical Research: Earth Surface*, *118*, 553–570, 2013. → page 7

Prudnikov, A. P., Y. A. Brychkov, O. I. Marichev, and R. H. Romer, *Integrals and Series*, Gordon and Breach, New York, 1988. → page 61

Recking, A., F. Liébault, C. Peteuil, and T. Jolimet, Testing bedload transport equations with consideration of time scales, *Earth Surface Processes and Landforms*, *37*, 774–789, 2012. → page 6

Recking, A., G. Piton, D. Vazquez-Tarrio, and G. Parker, Quantifying the Morphological Print of Bedload Transport, *Earth Surface Processes and Landforms*, *41*, 809–822, 2016. → page 6

Redner, S., and J. R. Dorfman, *A Guide to First-Passage Processes*, vol. 70, Cambridge University Press, Cambridge, 2002. → pages 34, 50

Redolfi, M., W. Bertoldi, M. Tubino, and M. Welber, Bed Load Variability and Morphology of Gravel Bed Rivers Subject to Unsteady Flow: A Laboratory Investigation, *Water Resources Research*, *54*, 842–862, 2018. → page 7

Roseberry, J. C., M. W. Schmeeckle, and D. J. Furbish, A probabilistic description of the bed load sediment flux: 2. Particle activity and motions, *Journal of Geophysical Research: Earth Surface*, *117*, 2012. → pages 35, 54, 59, 71

Saletti, M., and M. A. Hassan, Width variations control the development of grain structuring in steep step-pool dominated streams: insight from flume experiments, *Earth Surface Processes and Landforms*, *45*, 1430–1440, 2020. → pages 3, 69

Santos, B. O., M. J. Franca, and R. M. Ferreira, Coherent structures in open channel flows with bed load transport over an hydraulically rough bed, in *Proceedings of the International Conference on Fluvial Hydraulics, RIVER FLOW 2014*, EPFL-CONF-202022, pp. 883–890, 2014. → page 7

Schmeeckle, M. W., J. M. Nelson, and R. L. Shreve, Forces on stationary particles in near-bed turbulent flows, *Journal of Geophysical Research: Earth Surface*, *112*, 1–21, 2007. → pages 33, 75, 76

Schmidt, M. G., F. Sagués, and I. M. Sokolov, Mesoscopic description of reactions for anomalous diffusion: A case study, *Journal of Physics Condensed Matter*, *19*, 2007. → page 60

Schumer, R., M. M. Meerschaert, and B. Baeumer, Fractional advection-dispersion equations for modeling transport at the Earth surface, *Journal of Geophysical Research: Earth Surface*, *114*, 1–15, 2009. → pages 63, 69

Seizilles, G., E. Lajeunesse, O. Devauchelle, and M. Bak, Cross-stream diffusion in bedload transport, *Physics of Fluids*, *26*, 2014. → page 71

Sekine, M., and H. Kikkawa, Mechanics of saltating grains. II, *Journal of Hydraulic Engineering*, *118*, 536–558, 1992. → page 58

Shen, H. W., and H. F. Cheong, Stochastic Sediment Bed Load Models, in *Application of Stochastic Processes in Sediment Transport*, edited by H. Shen and C. Fatt, p. 21, Water Resources Publications, Littleton, CO, 1980. → page 8

Shi, Z., and G. Wang, Hydrological response to multiple large distant earthquakes in the Mile well, China, *Journal of Geophysical Research F: Earth Surface*, *119*, 2448–2459, 2014. → pages 51, 67, 68

Shih, W. R., P. Diplas, A. O. Celik, and C. Dancey, Accounting for the role of turbulent flow on particle dislodgement via a coupled quadrant analysis of velocity and pressure sequences, *Advances in Water Resources*, *101*, 37–48, 2017. → pages 7, 53

Shlesinger, M. F., Asymptotic solutions of continuous-time random walks, *Journal of Statistical Physics*, *10*, 421–434, 1974. → page 63

Singh, A., K. Fienberg, D. J. Jerolmack, J. Marr, and E. Foufoula-Georgiou, Experimental evidence for statistical scaling and intermittency in sediment transport rates, *Journal of Geophysical Research: Earth Surface*, *114*, 1–16, 2009. → pages 24, 35, 41, 54, 55

Singh, A., F. Porté-Agel, and E. Foufoula-georgiou, On the influence of gravel bed dynamics on velocity power spectra, *Water Resources Research*, *46*, 1–10, 2010. → page 7

Singh, A., E. Foufoula-Georgiou, F. Porté-Agel, and P. R. Wilcock, Coupled dynamics of the co-evolution of gravel bed topography, flow turbulence and sediment transport in an experimental channel, *Journal of Geophysical Research F: Earth Surface*, *117*, 1–20, 2012. → pages 35, 52, 54, 55

Sokolov, I. M., Models of anomalous diffusion in crowded environments, *Soft Matter*, *8*, 9043–9052, 2012. → page 56

Sumer, B. M., L. H. Chua, N. S. Cheng, and J. Fredsøe, Influence of turbulence on bed load sediment transport, *Journal of Hydraulic Engineering*, *129*, 585–596, 2003. → page 7

Sun, Z., and J. Donahue, Statistically derived bedload formula for any fraction of nonuniform sediment, *Journal of Hydraulic Engineering*, *126*, 105–111, 2000. → page 8

Swift, R. J., A Stochastic Predator-Prey Model, *Bulletin of the Irish Mathematical Society*, *48*, 57–63, 2002. → pages 39, 40

Temme, N. M., and D. Zwillinger, *Special Functions: An Introduction to the Classical Functions of Mathematical Physics*, vol. 65, John Wiley & Sons Ltd., 1997. → page 61

Tregnaghi, M., A. Bottacin-Busolin, A. Marion, and S. Tait, Stochastic determination of entrainment risk in uniformly sized sediment beds at low transport stages: 1. Theory, *Journal of Geophysical Research: Earth Surface*, *117*, 1–15, 2012. → pages 14, 20

Turowski, J. M., Stochastic modeling of the cover effect and bedrock erosion, *Water Resources Research*, *45*, 1–13, 2009. → pages 9, 10, 19, 22

Turowski, J. M., Probability distributions of bed load transport rates: A new derivation and comparison with field data, *Water Resources Research*, *46*, 2010. → page 18

Valyrakis, M., P. Diplas, C. L. Dancey, K. Greer, and A. O. Celik, Role of instantaneous force magnitude and duration on particle entrainment, *Journal of Geophysical Research: Earth Surface*, *115*, 2010. → page 7

van den Broek, J., Non-homogeneous stochastic birth and death processes, Ph.D. thesis, Utrecht, 2012. → page 9

Venditti, J. G., P. A. Nelson, R. W. Bradley, D. Haught, and A. B. Gitto, Bedforms, structures, patches, and sediment supply in gravel-bed rivers, *Gravel-Bed Rivers: Process and Disasters*, pp. 439–466, 2017. → pages 3, 7

Vicsek, T., and A. Zafeiris, Collective motion, *Physics Reports*, *517*, 71–140, 2012. → page 68

Voepel, H., R. Schumer, and M. A. Hassan, Sediment residence time distributions: Theory and application from bed elevation measurements, *Journal of Geophysical Research: Earth Surface*, *118*, 2557–2567, 2013. → pages 34, 50, 51, 54, 57, 64, 67, 68

Vowinckel, B., T. Kempe, and J. Fröhlich, Fluid-particle interaction in turbulent open channel flow with fully-resolved mobile beds, *Advances in Water Resources*, *72*, 32–44, 2014. → page 33

Weeks, E. R., and H. L. Swinney, Anomalous diffusion resulting from strongly asymmetric random walks, *Physical Review E - Statistical Physics, Plasmas, Fluids, and Related Interdisciplinary Topics*, *57*, 4915–4920, 1998. → pages 34, 59, 60, 61, 63, 66, 67, 68

Weeks, E. R., J. S. Urbach, and H. L. Swinney, Anomalous diffusion in asymmetric random walks with a quasi-geostrophic flow example, *Physica D: Nonlinear Phenomena*, *97*, 291–310, 1996. → pages 66, 67

Weiss, G. H., The two-state random walk, *Journal of Statistical Physics*, *15*, 157–165, 1976. → page 59

Weiss, G. H., *Aspects and Applications of the Random Walk.*, North Holland, Amsterdam, 1994. → pages 59, 60, 61, 66

Wiberg, P. L., and J. D. Smith, A theoretical model for saltating grains in water., *Journal of Geophysical Research*, *90*, 7341–7354, 1985. → page 33

Wilcock, P. R., and J. C. Crowe, Surface-based transport model for mixed-size sediment, *Journal of Hydraulic Engineering*, *129*, 120–128, 2003. → pages 20, 22

Witz, M. J., S. Cameron, and V. Nikora, Bed particle dynamics at entrainment, *Journal of Hydraulic Research*, *57*, 464–474, 2019. → page 66

Wohl, E., B. P. Bledsoe, R. B. Jacobson, N. L. Poff, S. L. Rathburn, D. M. Walters, and A. C. Wilcox, The natural sediment regime in rivers: Broadening the foundation for ecosystem management, *BioScience*, *65*, 358–371, 2015. → page 6

Wong, M., G. Parker, P. DeVries, T. M. Brown, and S. J. Burges, Experiments on dispersion of tracer stones under lower-regime plane-bed equilibrium bed load transport, *Water Resources Research*, *43*, 1–23, 2007. → pages 34, 36, 38, 39, 41, 52

Wu, F. C., and K. H. Yang, Entrainment probabilities of mixed-size sediment incorporating near-bed coherent flow structures, *Journal of Hydraulic Engineering*, *130*, 1187–1197, 2004. → page 20

Wu, Z., E. Foufoula-Georgiou, G. Parker, A. Singh, X. Fu, and G. Wang, Analytical Solution for Anomalous Diffusion of Bedload Tracers Gradually Undergoing Burial, *Journal of Geophysical Research: Earth Surface*, *124*, 21–37, 2019a. → pages 33, 51, 58, 59, 63, 67, 68

Wu, Z., A. Singh, X. Fu, and G. Wang, Transient Anomalous Diffusion and Advective Slowdown of Bedload Tracers by Particle Burial and Exhumation, *Water Resources Research*, *55*, 7964–7982, 2019b. → pages 51, 64, 67, 68

Yalin, M. S., *Mechanics of Sediment Transport.*, (1972), Pergamon Press, 1972. → pages xiii, 8, 12, 13, 14, 15, 16

Yang, C. T., and W. Sayre, Stochastic Model for Sand Dispersion, *Journal of the Hydraulics Division*, *97*, 265–288, 1971. → pages 50, 51, 58

Yang, F. L., and M. L. Hunt, Dynamics of particle-particle collisions in a viscous liquid, 2006. → page 85

Yano, K., Tracer Studies on the Movement of Sand and Gravel, in *Proceedings of the 12th Congress IAHR, Vol 2.*, pp. 121–129, Kyoto, Japan, 1969. → pages 34, 57, 58, 66, 67

Zaburdaev, V., M. Schmiedeberg, and H. Stark, Random walks with random velocities, *Physical Review E - Statistical, Nonlinear, and Soft Matter Physics*, *78*, 1–5, 2008. → page 68

Zee, C. H., and R. Zee, Formulas for the transportation of bed load, *Journal of Hydraulic Engineering*, *143*, 1–11, 2017. → pages 7, 8

Zhang, Y., M. M. Meerschaert, and A. I. Packman, Linking fluvial bed sediment transport across scales, *Geophysical Research Letters*, *39*, 1–6, 2012. → page 57

Appendix A

Mathematical Compendia